J Toxicol Pathol 2016; 29 (3 Suppl): 49S–103S

Nonproliferative and Proliferative Lesions of the Rat and Mouse Skeletal Tissues (Bones, Joints, and Teeth)

Stacey Fossey[1], John Vahle[2], Philip Long[3], Scott Schelling[4#], Heinrich Ernst[5], Rogely Waite Boyce[6], Jacquelin Jolette[7], Brad Bolon[8], Alison Bendele[9], Matthias Rinke[10], Laura Healy[11], Wanda High[12], Daniel Robert Roth[13], Michael Boyle[6], and Joel Leininger[14*]

[1]*AbbVie Inc., North Chicago, IL, USA*
[2]*Lilly Research Laboratories, Indianapolis, IN, USA*
[3]*Vet Path Services, Inc., Mason, OH, USA*
[4]*Pfizer Inc., Andover, MA, USA*
[5]*Fraunhofer Institute, Hannover, Germany*
[6]*Amgen Inc., Thousand Oaks, CA, USA*
[7]*Charles River Laboratories, Senneville, Canada*
[8]*GEMpath Inc., Longmont, CO, USA*
[9]*Bolder BioPath, Inc., Boulder, CO, USA*
[10]*Bayer Pharma AG, Wuppertal, Germany*
[11]*LNH Tox Path Consulting, LLC, Kalamazoo, MI, USA*
[12]*WB High Preclin Path/Tox Consulting, LLC, Rochester, NY, USA*
[13]*Swissmedic, Bern, Switzerland*
[14]*JRL Consulting, LLC, Chapel Hill, NC, USA*
**Chair of the Skeletal Tissues INHAND Committee*
[#]*Dr. Schelling retired April 2015.*

The INHAND (International Harmonization of Nomenclature and Diagnostic Criteria for Lesions in Rats and Mice) Project (www.toxpath.org/inhand.asp) is an initiative of the Societies of Toxicological Pathology from Europe (ESTP), Great Britain (BSTP), Japan (JSTP) and North America (STP) to develop an internationally accepted nomenclature for proliferative and nonproliferative lesions in laboratory animals. The purpose of this publication is to provide a standardized nomenclature for classifying microscopic lesions observed in the skeletal tissues and teeth of laboratory rats and mice, with color photomicrographs illustrating examples of many common lesions. The standardized nomenclature presented in this document is also available on the internet (http://www.goreni.org/). Sources of material were databases from government, academic and industrial laboratories throughout the world. (DOI: 10.1293/tox.2016-I002; J Toxicol Pathol 2016; 29: 49S–103S)

Keywords: diagnostic pathology, nomenclature, diagnostic criteria, skeletal system, bone, joint, tooth

Introduction

The INHAND Project (International Harmonization of Nomenclature and Diagnostic Criteria for Lesions in Rats and Mice, www.toxpath.org/inhand.asp) is a joint initiative of the Societies of Toxicologic Pathology from Europe (ESTP), Great Britain (BSTP), Japan (JSTP) and North America (STP) to develop an internationally-accepted nomenclature for nonproliferative and proliferative lesions in rodents. The purpose of this publication is to provide a standardized nomenclature for classifying lesions in the skeletal system (bones, joints, and teeth) of laboratory rodents. The set of descriptive terms in this document is also available at the goRENI website (http://www.goreni.org/).

Terms of systemic nonproliferative lesions that occur across organ systems and are not specific to the skeletal system are not included in this monograph. Similarly, systemic neoplasms that may impact skeletal tissues, such as lymphoma or histiocytic sarcoma, are described in separate documents under the hematopoietic system and are not discussed in this document. The nomenclature recommended here is generally descriptive rather than diagnostic. A few terms (e.g., fibro-osseous lesion, degenerative joint disease) are more collective than descriptive, communicating a spectrum of changes in morphology

Address correspondence to: Stacey Fossey, AbbVie Inc., North Chicago, IL, USA. e-mail: stacey.fossey@abbvie.com

that would require qualification in the text of a pathology report. The diagnostic criteria used for terms in this publication are generally those that can be seen with standard hematoxylin and eosin-stained (H&E) paraffin sections. Histochemical or immunohistochemical techniques may be mentioned in the "Comments" section of individual terms as diagnostic aids. Morphologic changes that can be reliably diagnosed grossly are also not covered by this monograph.

Skeletal tissues covered in this document are bones, joints, and teeth. Preferred terms for nonproliferative and proliferative lesions are presented for each tissue. Spontaneous and aging lesions, as appropriate, as well as lesions induced by exposure to test materials, are included. Although some diagnoses have synonyms provided, these terms may not always be recommended as appropriate histologic diagnoses in toxicity studies (i.e., hyperostosis and osteoporosis).

I. Bone

Histological Processing of Bone

Bone is included on the core list of tissues suggested by the STP for histologic examination in nonclinical repeat-dose toxicity studies and carcinogenicity studies. For rodents, the distal femur with an articular surface is recommended. Many institutions also include the proximal tibia, with a more linear physis (growth plate), and intervening meniscus to increase the amount of articular surface available for assessment. Sections of femur for general toxicity evaluation should include articular cartilage, epiphysis, physis, metaphysis, diaphysis, and marrow cavity. For routine toxicity studies, bones are cleaned of most attached skeletal muscle, ligaments, and tendons; fixed by immersion in neutral buffered 10% formalin; decalcified; embedded in paraffin; sectioned at 4–8 μm; and stained with hematoxylin and eosin (H&E). Alternative procedures of decalcification are mentioned in the section "Evaluation of Rodent Joints". In addition to normal transmitted light for microscopic analysis, polarized light may be used to evaluate collagen fiber arrangement in bone. Some specialized investigations require examination of undecalcified bone sections with special stains such as von Kossa or Goldner's trichrome when alterations in bone mineralization are suspected (e.g., increased osteoid) or if *in vivo* fluorochrome labeling is incorporated in the study for histomorphometric assessment of bone formation rates.

Anatomy and Physiology of Bone

Neural crest cells and mesoderm form the early skeleton. The craniofacial skeleton originates from neural crest, while the axial skeleton, ribs, appendicular bones, and the base of the skull are derived from mesoderm. Bone is formed through two different ossification processes, intramembranous and endochondral ossification. Intramembranous ossification occurs in flat bones, with bone formation occurring in condensed mesenchyme. In contrast, as typified in long bones, endochondral ossification is the process by which a cartilage anlage is replaced by bone. The expansion of the primary and secondary ossification centers is limited to retain articular and physeal cartilage, which in rodents serve as sites of continued endochondral growth throughout life. Some bones, such as the mandible, are mixed in origin; this mingling can result in unique structural changes when test articles preferentially affect one form of developmental bone growth. The physis is a highly complex structure in which coordination of endochondral ossification and longitudinal bone growth requires multiple key signaling pathways. Because of the high sustained rate of endochondral ossification and longitudinal bone growth in rats of the age typically used in conventional nonclinical toxicity studies, the rat physis is a sensitive bioassay for test articles that can impact pathways involved in endochondral ossification (e.g., kinase and angiogenesis inhibitors) and subphyseal modeling (e.g., inhibitors of bone resorption).

Mature bone is composed of lamellar bone characterized

by regularly arranged collagen fibers oriented for optimal mechanical function. Woven bone is immature or reactive new bone (typified by bone of the primary spongiosa or an early fracture callus, respectively) that is biomechanically inferior to lamellar bone because it displays increased osteocyte cellularity and more randomly distributed collagen fibers that are not oriented in relation to mechanical stress. Bone tissue is organized at the organ level into either compact (cortical) or cancellous (spongy/trabecular) bone. The relative proportions of trabecular and cortical regions within a specific bone are based on the specific function of that bone. For example, to give the femur the rigidity it needs to function as a mechanical lever during locomotion, the shaft is cylindrical and the diaphysis is composed primarily of inflexible cortical bone. In contrast, the vertebrae require the ability to absorb compressive forces without fracturing and therefore are rich in shock-absorbing trabecular bone with a relatively thin shell of cortical bone.

Osteoblasts are responsible for synthesis and mineralization of bone matrix (osteoid). These cells are distinguished by their single nuclei and tendency to form monolayers lining bone surfaces engaged in active osteoid production. After completing this role, their ultimate fate is either to undergo apoptosis, to become osteocytes (if they become entrapped in the mineralized bone matrix), or to persist as bone-lining cells. Osteoblast differentiation from pluripotential mesenchymal cells is orchestrated through many complex signaling pathways. Major molecules controlling osteoblast activity include transforming growth factor-beta (TGFβ1), bone morphogenetic proteins (BMPs), WNT, NOTCH, and Ephrin-Ephrin receptor interactions among others, with runt-related transcription factor 2 (RUNX2) serving as the master transcription factor that regulates osteoblastogenesis.

Osteoclasts are responsible for demineralization of mature bone and resorption of bone matrix. These cells are recognized by their larger size, multiple nuclei, and close relationship to sites of bone erosion. In mice, a substantial proportion of osteoclasts appear as mononuclear cells, and anti-cathepsin K immunostaining may be needed for their accurate identification. Shallow depressions between osteoclasts and the adjacent bony surface (Howship's lacunae) serve as digestion chambers to concentrate bone-eroding chemicals and enzymes released by active osteoclasts. After fulfilling this function, these cells regress via apoptosis. Osteoclasts are derived from hematopoietic stem cell precursors. Interactions between receptor activator of nuclear factor κB (RANK), an osteoclast surface molecule, and its ligand RANKL are central to osteoclast differentiation from committed precursors. The activity of osteoclasts is modulated by osteoprotegerin (OPG), a soluble decoy receptor for RANKL.

Bone is a highly metabolically active tissue. Maintenance of bones requires the coordination of bone resorption and formation, both of which are regulated by local and systemic hormones, cytokines, biomechanical signals, and dietary factors. Cell-cell interactions and secreted factors mediate signaling between osteoclast and osteoblast precursors that is required for coupling of bone formation and bone resorption during the bone remodeling process. The various signaling pathways are responsive to altered skeletal loading, for which the osteocyte and associated canalicular network is now considered to be the major mechanosensor by producing regulator proteins such as sclerostin, an inhibitor of the canonical WNT signaling pathway and a negative regulator of bone formation. The osteocyte is also a source of RANKL and fibroblast growth factor (FGF)-23, a key signaling molecule regulating phosphate balance. Numerous local mediators of bone metabolism include BMPs, TGFβ1, other FGFs, interleukins (IL-1, -4, -6), interferon-gamma (INFγ), tumor necrosis factors (TNFs), hedgehog proteins, insulin-like growth factors (IGFs), retinoids, and the phosphatidylinositol 3-kinase (PI3K) pathway. Systemic mediators that regulate local factors involved in bone development and metabolism include growth hormone, thyroid hormone, parathyroid hormone (PTH), estrogen, androgen, vitamin D, calcitonin and glucocorticoids.

Perturbations in local and systemic hormones, cytokines, biomechanical signals, and/or dietary factors can manifest as changes in bone mass and structure. Major changes in skeletal mass and structure can be detected by qualitative histopathology, especially in experiments lasting for a protracted period. However, subtle changes that might occur in short-term studies resulting from alterations in the kinetics of bone growth or turnover may require specialized techniques for detection. Densitometry, dynamic histomorphometry, and biomarkers of bone resorption and formation are sensitive methods to detect changes in bone mass and determine the underlying mechanism responsible for test article-related structural changes. Bone mechanical testing may be applied as a coordinated experimental technique to correlate structural changes to functional consequences.

Rat (and mouse) bones have distinct physiological differences from bones of other mammals. Longitudinal bone growth remains active for a greater fraction of the rat's life span compared with other toxicologically relevant animal species (e.g., rabbits, dogs, nonhuman primates) and humans. Although longitudinal growth is minimal by six months of age, physeal closure may be incomplete throughout life at the distal femur and proximal tibia. The physes of male rats ossify more completely than those in females. The predominant bone turnover processes/activities in the young rat skeleton are (endochondral) growth and bone modeling, in which bone resorption and formation are not spatially and temporally coupled. However, with increasing age (from weaning), there is a gradual transition in trabecular bone from modeling to remodeling, in which bone resorption and formation are spatially and temporally coupled. This transition in bone turnover processes/activities is dependent on both age and the skeletal site. Intracortical remodeling is normally absent in the rat skeleton, thereby limiting its utility to evaluate effects of bone-active agents on this process. Despite these biological differences, rats are considered to be a robust model of bone changes (especially for the trabecular compartment) in humans in response to disease and bone-active agents.

References

Anderson and Shapiro (2010), Ballock and O'Keefe (2003), Banks (1993), Bargman et al. (2010), Baron and Kneissel (2013), Bonewald and Johnson (2008), Bonewald and Wacker (2013), Bregman et al. (2003), Chai et al. (2000), Chow et al. (1998), Dallas et al. (2013), EMEA Guidance (2006), Erben (1996), Erden and Glödmsn (2012), Frazier et al. (2007), Gunson et al. (2013), Hall et al. (2006), Jee and Yao (2001), Kharode et al. (2008), Kilborn et al. (2002), Komori et al. (1997), Kronenberg (2003), Leininger and Riley (1990), Lelovas et al. (2008), Mullender and Huiskes (1997), Nakashima et al. (2011), Noden and De Lahunta (1985), Patyna et al. (2008), Roach et al. (2003), Schenk et al. (1986), Sims and Gooi (2008), Wronski et al. (1989), Yamaguchi et al. (2000), Zaidi et al. (2003), Zuo et al. (2012)

Nonproliferative Lesions

Fibro-osseous lesion (FOL) (Figure 1)

Other terms used

Osteofibrosis

Species

Mouse only

Affected structures

All bones, but most commonly observed in sternebrae, long bones, vertebrae, and nasal bones

Biological behavior

Focal to multifocal, non-neoplastic accumulation of mesenchymal cells along endosteal surfaces, associated with localized increases in osteoclastic bone resorption and marrow fibroplasia

Histogenesis/Pathogenesis

The change reflects increased local function of osteoclasts, osteoblasts and fibroblasts. It is uncertain if these changes reflect primary activation of one cell population with a secondary reaction by the other, or secondary activation of both cell populations in response to signals from an as yet unidentified regulatory cell.

Diagnostic features

- Focal resorptive lesions begin in the metaphysis and/or endocortical bone.
- Interface between lytic sites and normal trabeculae has numerous osteoclasts.
- Lesions extend into the adjacent bone marrow with a circumferential or endocortical distribution.
- Fibrous stroma and occasionally trabeculae of woven bone proliferate within the lesion and, in later stages, may replace part of the marrow cavity.
- Osteoblast accumulation and bone formation follow in similar pattern (from the periphery towards the center).
- Character and extent of lesions depends on the local balance of bone resorption and formation.

Differential diagnoses

Fibrous osteodystrophy (FOD)

Use of the term FOL would be the preferred diagnosis to capture the constellation of morphologic changes associated with the syndrome rather than multiple individual morphologic features.

Comment

FOL is observed only in mice, particularly in aging females. It is a common spontaneous lesion in the B6C3F1 and CD-1 strains. FOL is often associated with ovarian cysts or cystic endometrial hyperplasia, and increased serum alkaline phosphatase (ALP) activity. Development is hastened and lesions are more severe in females given estrogen.

A considerable histologic variation is observed during the development of FOL. This variability explains that the condition has been diagnosed as hyperostosis, myelofibrosis, osteoporosis, osteofibrosis, and osteosclerosis in the past. It should be differentiated from fibrous osteodystrophy (FOD), a consequence of parathyroid hormone (PTH)-mediated bone resorption with secondary fibroplasia, by excluding advanced renal disease (generally marked chronic progressive nephropathy) or other causes of increased PTH production.

References

Albassam et al. (1991), Highman et al. (1981), Long and Leininger (1999b), Sass and Montali (1980), Wancket et al. (2008)

Fibrous osteodystrophy (FOD) (Figure 2)

Other terms used

Renal osteodystrophy

Species

Rats and Mice

Affected structures

All bones

Biological behavior

A benign nonneoplastic lesion of stromal cells and fibrous tissue in bone associated with increased bone resorption as a consequence of hyperparathyroidism.

Histogenesis/Pathogenesis

Proliferation of immature fibrous connective tissue to strengthen bones weakened by chronic demineralization in response to systemic metabolic disease. The lesion occurs in two phases:

- Early – accelerated bone resorption, initially endosteal

followed by intracortical, with secondary increase in trabecular bone formation
- Late – trabecular bone and bone marrow are replaced by stromal cells and fibrous stroma that contains coalescing islands of woven bone

Diagnostic features
- Evidence of rapid bone turnover, which is manifested histologically by:
  - o Increased numbers of osteoclasts and osteoblasts
  - o Osteolysis, increased surface excavations resulting in irregular scalloped trabecular surfaces; presence of tunneling resorption
  - o Increased resorption cavities in cortical bone
- Fibrosis/stromal cell proliferation and woven bone production
- Secondary lesions in non-skeletal organs indicative of hyperparathyroidism, such as:
  - o Advanced renal (especially tubular) lesions
  - o Parathyroid gland enlargement due to chief cell hyperplasia/hypertrophy
  - o Metastatic mineralization in soft tissues

Differential diagnoses

Fibro-osseous lesion (FOL; only in mice)

Use of the term FOD would be the preferred diagnosis to capture the constellation of morphologic changes associated with the syndrome rather than multiple individual morphologic features.

Comment

In rats, FOD is typically secondary to longstanding renal disease and attendant increases in serum levels of parathyroid hormone (PTH) in response to absolute or relative hypocalcemia. PTH functions to maintain the blood calcium/phosphorus ratio by inhibiting renal tubular phosphate reabsorption, promoting tubular reabsorption of calcium, and stimulating bone resorption to promote calcium release from bone. The production of fibrous tissue/stromal cell hyperplasia is secondary to sustained elevations in PTH. Chronic renal lesions decrease functional nephron mass, thereby reducing phosphorus excretion and promoting phosphorus retention. Increased serum phosphorus causes increased FGF23 secretion to promote phosphaturia, but this increase also decreases 1,25 dihydroxy vitamin D_3, thus leading to diminished calcium and phosphorus absorption from the intestines. A major additional lesion in FOD is parathyroid enlargement (via hypertrophy and hyperplasia of the PTH-producing chief cells). Intrinsic variability in the balance among these processes contributes to the variable histologic appearance of FOD.

As a spontaneous finding, FOD occurs at a low incidence in mice due to the low incidence of chronic renal failure. In contrast, FOD occurs in many rat strains as an age-related change secondary to the high incidence and severity of chronic progressive nephropathy.

References

Greaves (2000), Leininger and Riley (1990), Long and Leininger (1999b), Malluche (2002)

Increased bone, trabeculae and/or cortex (Figures 3–5)

Other terms used

Hyperostosis (proliferative or nonproliferative types), osteopetrosis, osteosclerosis, trabecular hypertrophy

Species

Rats and Mice

Affected structures

All bones – variably expressed in appendicular long bones (often the most severely affected bones), skull, vertebrae and sternebrae.

Biological behavior

Non-neoplastic augmentation of bone mass (cortical or trabecular, focal or diffuse)

Histogenesis/Pathogenesis

Increased bone matrix production by osteoblasts and/or decreased resorption by osteoclasts

Diagnostic features
- Increased bone matrix (may be lamellar or woven)
- Prominent osteoblasts lining trabecular surfaces early in process
- Trabecular thickness is increased (trabecular hypertrophy), and an apparent increase in trabecular number may be observed
- Increased cortical thickness due to bone deposition at endosteum and/or periosteum
- Diminished marrow cavity volume. In severe cases, extramedullary hematopoiesis (EMH) in the liver and spleen may be pronounced.
- Retained primary spongiosa in young animals

Differential diagnoses
- Osteosarcoma
- Fibro-osseous lesion (FOL; occurs only in mice)

Comment

In rodents, this spontaneous lesion is indicative of increased bone mass arising from enhanced bone formation. Increased cancellous bone occurs in aged rats, where it develops in long bones, the sternum, and vertebrae; this change has been referred to previously as proliferative hyperostosis. Pharmacologically-mediated systemic increases in bone due to increased bone formation have been observed with intermittent administration of PTH or anti-sclerostin antibodies. Focal or multifocal increases in bone in rats may be associated with administration of some an-

ticancer drugs or occur as a secondary response to mononuclear cell (large granular lymphocyte [LGL]) leukemia filling the bone marrow, in which case the deposited bone matrix is of the woven type.

In the presence of an open growth plate and active endochondral ossification, decreased bone resorption results in increased bone mass and altered bone geometry due to retention of primary spongiosa and flared metaphyses due to failed modeling of the "cut-back zone" (at the periosteal surface of the metaphysis of long bones), resulting in an osteopetrotic-like bone phenotype. Bisphosphonates and other inhibitors of osteoclast function or osteoclastogenesis induce these changes. The severity of these changes depends on the magnitude of the inhibition of bone resorption and the rate of longitudinal bone growth.

Decreased bone resorption in the adult rodent skeleton results in only a subtle change in bone mass and structure that cannot be easily appreciated qualitatively. Mechanistically, decreases in osteoclast numbers may result in increased bone; however, due to the challenges of reliably documenting a decrease in osteoclasts with routine methods in a toxicity study, it is not recommended to record "decreased osteoclasts" as a morphologic diagnosis. Morphometric/densitometric measurements of bone may be required to confirm subtle increases in bone mass during adulthood.

References

Courtney et al. (1991), Felix et al. (1996), Hartke (1996), Li et al. (2009), Qi et al. (1995), Stromberg and Vogtsberger (1983)

Increased osteoid (Figures 6, 7)

Other terms used

Hyperosteoidosis, Osteomalacia

Species

Rats and Mice

Affected structures

Trabecular and cortical bone

Biological behavior

Non-neoplastic increase in osteoid (i.e., unmineralized bone matrix)

Histogenesis/Pathogenesis

The quantity of osteoid may be increased by several mechanisms:

- Increased production of normal osteoid
- Defective mineralization of normal osteoid
- Production of defective osteoid matrix that fails to mineralize
- Accelerated osteoid synthesis relative to a normal rate of mineralization

Diagnostic features

- Increased amounts of osteoid (evident as either increased osteoid area or osteoid thickness)

Special diagnostic methods

The presence of increased osteoid can be confirmed only in undecalcified sections. Staining options to demonstrate bone mineral include von Kossa/MacNeal's tetrachrome, Goldner's trichrome, and Movat's pentachrome stains. An alternative method to detect osteoid has been described by Yoshiki et al.

Differential diagnoses

Osteosarcoma

Comment

Increased osteoid occurs with certain metabolic diseases such as rickets and chronic kidney disease-metabolic bone disease (CKD-MBD). Increased osteoid has also been associated experimentally with supraphysiologic doses of vitamin D (1,25 dihydroxy vitamin D_3), which results in a defective osteoid matrix, as well as after high doses of some bisphosphonates and also prostaglandins. Other causes of increased osteoid include aluminum, fluoride, or cadmium toxicity or dietary phosphorus deficiency. Increased osteoid has a negative impact on bone biomechanical properties, and fractures may be observed in advanced cases.

In routine toxicity studies (i.e., where undecalcified sections are not available), a provisional diagnosis of increased osteoid may be made from decalcified H&E-stained sections based on the presence of clearly demarcated zones of abundant, pale-staining bone matrix. However, follow-up studies that include undecalcified sections would be needed to confirm the provisional diagnosis. Importantly, minor variations in the tinctorial qualities of bone matrix in routinely processed (decalcified, H&E-stained) sections should not be interpreted as definitive evidence of increased osteoid.

References

Boyce and Weisbrode (1983), Long et al. (1996), Schenk et al. (1973), Yoshiki et al. (1983)

Increased osteoblastic surface (Figure 8)

Other terms used

Proliferative hyperostosis (when associated with increased bone mass)

Species

Rats and Mice

Affected structures

Axial and long bones

Biological behavior

Non-neoplastic form of increased bone formation, either as remodeling (bone formation temporally and spatially coupled to bone resorption) or a modeling-based process (bone formation occurring on a quiescent bone surface independent of bone resorption)

Histogenesis/Pathogenesis

Increased remodeling or modeling-based bone formation resulting in an increased surface extent of plump osteoblasts (interpreted to be active in matrix synthesis). This change can occur in the face of increased, decreased, or no change in bone mass.

Diagnostic features

- Increased bone formation evidenced by a generally diffuse increased surface extent of plump cuboidal osteoblasts, suggesting an increase in bone formation but without a visible increase in bone matrix
- Bone mass may be unaffected, decreased, or increased depending on the balance between bone resorption and formation; however, whenever there are concurrent increases in both bone matrix and osteoblastic surface area, only the diagnostic term "Increased bone, trabeculae and/or cortex" should be used
- Can occur on any bone surface (trabecular, periosteal, or endocortical)

Special diagnostic methods

Evident in H&E sections based on morphology of osteoblasts. Very active osteoblasts may be identified with a perinuclear vacuole (signifying the Golgi apparatus). Confirmation of diagnosis based on correlation with dynamic histomorphometry based on *in vivo* fluorochrome labeling as qualitative assessment will generally significantly underestimate the magnitude of effects on bone formation.

Differential diagnoses

- Hyperplasia, osteoblast
- Fibrous osteodystrophy (FOD)

Comment

Increased surface extent of osteoblasts interpreted to be active in matrix synthesis that can occur as a consequence of increased bone remodeling or activation of modeling-based bone formation. Classical hormonal changes that can result in these changes are hyperthyroidism, hyperparathyroidism, or estrogen deficiency, with bone mass being unaffected or decreased in these conditions. Increased osteoblastic surface in the absence of changes in bone mass occurs early in the response to increased skeletal loading or inhibition of sclerostin as a consequence of activation of modeling-based formation.

References

Ominsky et al. (2014)

Increased osteoclasts (Figure 9)

Other terms used

Resorption, dissecting osteoclasia (increased osteoclast-mediated resorption)

Species

Rats and Mice

Affected structures

Surfaces of trabecular and cortical bone

Biological behavior

An apparent increase in the number of osteoclasts

Histogenesis/Pathogenesis

Enhanced osteoclastogenesis and/or osteoclast survival

Diagnostic features

- Apparent increase in number of osteoclasts (osteoclast hyperplasia)
- An irregular (eroded) bone surface, with each surface depression representing a Howship′s lacuna (resorptive site or eroded surface)

Special diagnostic methods

Procedures to highlight osteoclasts in tissue sections typically detect an osteoclast biomarker like calcitonin receptor, cathepsin K, tartrate-resistant acid phosphatase (TRAP), or vitronectin receptor. An alternative method is to heighten the eosinophilic hue of osteoclast cytoplasm by adding phloxine B and orange G to the eosin step in the H&E stain.

Differential diagnoses

None

Comment

Osteoclasts are essential for bone modeling during development, remodeling of normal bone during skeletal turnover in adults, and for bone healing. An increase in osteoclasts can be associated with various pathologic processes including metastatic neoplasia, paraneoplastic syndromes, various metabolic/hormonal disturbances that activate osteoclastogenesis (typically via modulation of RANKL), or prolonged osteoclast life span. Importantly, the presence of increased osteoclasts does not always indicate increased bone resorption as is exemplified by bisphosphonates, potent inhibitors of osteoclast function that cause an increase in osteoclasts in rodents. A diagnosis of increased osteoclasts should not be used when the increase in osteoclast numbers is part of the diagnostic features in a more inclusive condition, such as early fibro-osseous lesions (FOL) or fibrous osteodystrophy (FOD) (see above).

References
Bolon et al. (2004), Boyle et al. (2003), Fisher et al. (2000), Schell et al. (2006)

Increased eroded surface

Other terms used
Resorption, dissecting osteoclasia (increased osteoclast-mediated resorption)

Species
Rats and Mice

Affected structures
Surfaces of trabecular and cortical bone

Biological behavior
An apparent increase in the extent of bone surface undergoing resorption

Histogenesis/Pathogenesis
Increased osteoclastogenesis and/or osteoclast survival and bone resorption activity, prolonged life span of the resorptive phase of bone remodeling, or defective/delayed coupling of bone formation as described for certain types of bone metastases that stimulate resorption and inhibit bone formation

Diagnostic features
- An irregular (eroded) bone surface, with each surface depression representing a Howship′s lacuna (resorptive site or eroded surface)
- Disruption of lamellae
- Can be focal (within a single bone, or in multiple bones) instead of systemic (multiple sites in many bones)

Differential diagnoses
None

Comment
Increased eroded surface can be observed with or without an apparent increase in the number of osteoclasts in pathologic processes (neoplasia, paraneoplastic syndromes, metabolic/hormonal disturbances), and thus can suggest an increase in the lifespan of the resorptive surface. This diagnosis can be used when extensive scalloping of bone surfaces is present but an increase in osteoclast number cannot be appreciated. The use of "increased eroded surface" as a sole diagnostic term is suggested if there are both an increased eroded surface and increased number of osteoclasts present.

References
Andersen et al. (2014), Boyce et al. (1995)

Decreased bone, trabeculae and/or cortex (Figure 10)

Other terms used
Bone atrophy, osteoporosis, osteopenia

Species
Rats and Mice

Affected structures
Generalized or localized bone involvement

Biological behavior
Non-neoplastic reduction of bone mass (cortical or trabecular, focal or diffuse)

Histogenesis/Pathogenesis
Decreased bone formation and/or increased bone resorption

Diagnostic features
- Reduced quantity of bone matrix
- Trabecular thickness is decreased (trabecular atrophy), and an apparent decrease in trabecular numbers may be observed
- Reduced cortical bone thickness
- Co-occurrence of both decreased trabecular bone and reduced cortical bone is not a requirement for this diagnosis

Comment
Decreased bone results from an imbalance in bone formation and resorption with a relative reduction in bone formation and/or relative increase in bone resorption. This change occurs as a spontaneous age-related finding in rats. Localized reduction is associated with immobilized/disused limbs. Generalized reduction in bone mass is reported to result from diminished feed intake, cortisone toxicity, thyrotoxicosis, pyridoxine deficiency, heparin, beta-aminopropionitrile, and dextran sulfate.

The terms osteoporosis and osteopenia are not recommended as a qualitative histologic diagnosis in toxicity studies; instead, these terms should be reserved for use in settings in which bone mass has been assessed quantitatively. Morphometric/densitometric measurements of bone may be required to detect subtle decreases in bone mass.

References
Angevine and Clemmons (1957), Benke et al. (1972), Ellis and Peart (1971), Kiebzak et al. (1988a), Kiebzak et al. (1988b), Leininger and Riley (1990), Long et al. (1996), Thompson (1973)

Cyst, bone (Figure 11)

Other terms used
Unicameral bone cyst, solitary bone cyst

Species
Rats and Mice

Affected structure
Bone (most often the metaphysis of long bones)

Biological behavior
Non-neoplastic, space-occupying cavities in the bone, or often in the soft marrow tissues immediately adjacent to bony surfaces

Histogenesis/Pathogenesis
Unknown

Diagnostic features
- Discrete cavities of variable size and shape, often in the metaphysis
- At necropsy, cavities may be filled with fluid
- By histopathologic examination, lesions typically are characterized by:
  - o A thin fibrous membranous lining, with indistinct lining cells; a thin shell of cortical bone may be present
  - o An absence of contents in the cavity
- In many cases, no reaction is seen in the adjacent trabecular or cortical bone
- Certain cystic bone lesions have distinct anatomic features
  - o Aneurysmal cyst – a true cyst with multiple blood-filled spaces that are not lined with vascular endothelium
  - o Subchondral cyst – a pseudocyst (so-called because they lack a discrete cellular lining; see definition below under Joint) most frequently located in the epiphyseal subchondral bone in association with degenerative changes in the joint

Differential diagnoses
Tangential sections of normal tendon and ligament insertions

Comment
Simple bone cysts often represent a focal developmental defect. Aneurysmal bone cysts are thought to arise due to a disturbance in blood flow in the bone marrow. Subchondral bone cysts arise secondary to an inflammatory or degenerative process of the adjacent joint.

True bone cysts appear to be relatively rare in rodents based on published reports. A review of the National Toxicology Program (NTP) Pathology Database revealed sporadic reports of cysts in a variety of bone sites in both male and female rats and mice. Rats administered beta-aminopropionitrile developed aneurysmal-like bone cysts in the mandible. In humans, bone cysts can arise in the context of fibrous osteodystrophy (FOD) secondary to hyperparathyroidism (osteitis fibrosa cystic), but this manifestation is not common in rodents.

Irregular cystic spaces may arise adjacent to lytic bone processes secondary to neoplasia or inflammation, but these secondary lesions do not warrant a separate diagnosis.

References
Baden and Bouissou (1987), Long and Leininger (1999b), National Toxicology Program Data Search (April 2011)

Necrosis (Figure 12)

Other terms used
Osteonecrosis, coxa plana (Legg-Calvé-Perthes disease), flathead

Species
Rats and Mice

Affected structure
Any bone (with femoral head as a predilection site)

Biological behavior
Death (usually localized) of one or more cellular elements within bone (osteocytes, osteoblasts, osteoclasts, and adjacent bone marrow elements)

Histogenesis/Pathogenesis
One or several episodes of ischemia

Diagnostic features
Histologic characteristics of necrosis depend on the location of the lesion.
- General features
  - o Empty osteocyte lacunae
    - ▪ Often involves large expanses of bone
    - ▪ Must be distinguished from:
      - Artifactual loss of osteocytes due to tissue processing
      - A low incidence of empty lacunae that occurs in normal bone
  - o Lesions often are easier to recognize from the simultaneous presence of other changes, including:
    - ▪ Necrosis in adjacent bone marrow
    - ▪ Evidence of bone resorption in the affected area – which is especially marked in osteomyelitis
    - ▪ Islands of necrotic bone surrounded by woven bone foci – a common repair process encountered in aseptic necrosis
- Features specific for femoral head necrosis
  - o Occurs in rats
  - o *Initial Lesion:* Necrosis followed by lysis of bone, usually in the central part of the head of the femur.
    - ▪ The articular cartilage and its subjacent growth cartilage as well as the proximal growth plate of the femur are unaffected at this stage.

- Continual proliferation of the subarticular growth cartilage without concomitant endochondral ossification is responsible for widening of the joint space in radiographs.

o *Repair Phase:* Proliferation of mesenchymal cells and capillaries occurs at the margin of live and dead bone.

- Main histologic characteristics:
  - New woven bone is deposited on existing dead lamellar trabeculae.
  - Later, the new bone is rimmed by osteoblasts, and eventually lamellar bone replaces all the woven bone.
  - The resorptive process may extend into the cartilage of the head, and pannus from the periphery of the joint may destroy articular cartilage from above.
  - Degeneration of the proximal growth plate of the femur may occur, possibly because of injury to germinal cells at the time of the initial insult.
- Outcome – a net loss of subchondral bone

Comment

Necrosis occurs in conditions that result in impaired blood supply to bone. The lesion may be septic or aseptic and frequently is associated with trauma (fracture) or osteomyelitis. A consideration in the choice of the primary diagnosis for a finding that includes necrosis, inflammation and/or fracture is which is the predominant or initiating lesion.

The syndrome of aseptic femoral head necrosis occurs in rats. Causes include idiopathic necrosis of the femoral head, dislocation at the femoral-acetabular joint, and fracture of the proximal part/neck of the femoral head. The pathogenesis appears to stem from venous occlusion, which under natural conditions appears to result from transient synovitis leading to venous occlusion. A sequela of femoral head necrosis is degenerative arthropathy of the coxofemoral ("hip") joint. The histopathologic changes noted above contribute to collapse of the head and development of coxa plana (i.e., flattening of the head and neck of the femur) that is characteristic of Legg-Calvé-Perthes disease (avascular femoral head necrosis) in humans.

References

Boss and Misselevich (2003), Fondi and Franchi (2007), Hirano et al. (1989)

Fracture (Figure 13)

Other terms used

None

Species

Rats and Mice

Affected structure

Any bone

Biological behavior

Localized disruption of bone structure resulting in partial or complete discontinuity in cortical and/or trabecular bone

Histogenesis/Pathogenesis

Fractures develop secondary to exogenous trauma. Additional predisposing factors that lead to bone weakening and susceptibility to low-energy fractures include defective mineralization of normal bone, altered bone matrix with reduced material properties, decreased bone mass, or bone neoplasia.

Diagnostic features

Histologic features of a callus (the bridge that develops during fracture repair) vary with the time that has passed since the fracture occurred.

- Early stages are dominated by hemorrhage, fibrin exudation, and necrosis.
- Intermediate stages are characterized by production of the external and internal calluses.
  - o The external callus is formed by proliferation of fibroblastic mesenchymal cells (osteoprogenitors) in the periosteum proximal and distal to the fracture site. These progenitors migrate to the fracture site along with invading vasculature, where they differentiate and begin producing woven bone and/or cartilage. The external callus gradually is remodeled and replaced by lamellar bone (i.e., occurs by endochondral bone formation). In general, more mature tissue elements are found at the periphery of the external callus.
  - o The internal callus consists of woven bone in the medullary canal without passing first through the intermediate stage of cartilage formation (i.e., occurs by intramembranous bone formation).
- Late stages lead to progressive remodeling and restoration of cortical and trabecular bone structure.

Differential diagnoses

Osteosarcoma (as recent fractures may have abundant, pleomorphic osteoprogenitor cells)

Comment

The histologic features of a fracture/callus are influenced by mechanical and metabolic factors, and they vary with the age of the site. The hallmark of a fracture usually is a pronounced focal distortion of the bone contours. Over time, bone remodeling restores normal bone geometry.

Fractures are uncommon spontaneous findings in rodents. In the authors' experience, fractures secondary to significant test article-related decreases in bone mass are not common. Therefore, the occurrence of fractures in a toxicity study may be more indicative of negative effects on bone quality (e.g., altered matrix, defective mineralization).

References
Marsell and Einhorn (2011)

Increased thickness, physis (Figures 14, 15)

Other terms used
Physeal dysplasia, Physeal hypertrophy, endochondral hypertrophy, cartilage dysplasia, physeal expansion

Species
Rats and Mice

Affected structures
Epiphyseal (articular) and/or physeal (growth plate) cartilage of long bones (rats and mice), vertebrae, and sternum (especially in mice)

Biological behavior
A reversible expansion of cartilage

Histogenesis/Pathogenesis
Perturbation of endochondral ossification

Diagnostic features
- Thickened physis – reported most often in femur and tibia (which are examined most often in routine nonclinical toxicity studies), but thickening may be seen in other bones
  - o Increased thickness of one or more zones of the physeal plate
  - o Expansion may be
    - ▪ Uniform or irregular
    - ▪ Occur with or without dysplasia (i.e., disruption of normal chondrocyte columnar organization and/or changes in cartilaginous matrix)
- When severe, increased subchondral bone may be present

Special diagnostic methods
The change is evident on routinely processed (formalin-fixed, decalcified, paraffin-embedded, H&E-stained) sections but can be seen with other stains designed to highlight cartilage (e.g., safranin O, toluidine blue). Undecalcified preparations are required to determine if expansion is due to or associated with impaired cartilage matrix mineralization.

Differential diagnoses
None

Comment
Alterations result in thickening of the physeal plate by hypertrophy and/or hyperplasia, with or without dysplasia. While in most cases a diagnosis of increased thickness is appropriate, in those cases where there is notable disorganization of the physeal chondrocytes a diagnosis of physeal dysplasia is appropriate. Severity is dependent on test article dose and duration of exposure as well as the rate of endochondral ossification. Therefore, the finding is most notable in young animals due to active endochondral ossification. This lesion is rare as a spontaneous change in rodents.

This lesion often is encountered due to test article-induced impairment of mineralization or alterations in signaling pathways that play a key role in regulation of endochondral ossification, including angiogenesis and physeal chondrocyte proliferation/differentiation. This change has been reported with inhibitors of angiogenesis that target such molecules as vascular endothelial growth factor (VEGF), certain bisphosphonates, fibroblast growth factor (FGF) receptor tyrosine kinase, activin receptor-like kinase (ALK)-5, pp60 SRC kinase, and matrix metalloproteinases (MMPs). Angiogenic inhibitors affect the physis because vascular invasion is required for normal endochondral ossification. ALK5 is a type 1 receptor for TGFβ1, a factor that helps regulate hypertrophic differentiation of chondrocytes in the physis. Osteoclastic bone resorption is dependent on pp60 SRC tyrosine kinase, and MMPs are involved in the degradation of non-mineralized cartilage matrix. Exposure to semicarbazide hydrochloride leads to a similar effect in physes by decreasing polymerization, collagen cross-linking, and mineralization of cartilage matrix.

References
Alvarez et al. (2001), Blair et al. (2002), Brown et al. (2005), Frazier et al. (2007), Hall et al. (2006), Horne et al. (1992), Patyna et al. (2008), Takahashi et al. (2010)

Decreased thickness, physis (Figure 16)

Other terms used
Physeal atrophy, physeal dystrophy

Species
Rats and Mice

Affected structures
Physis (growth plate), especially in long bones

Biological behavior
A reversible regressive change

Histogenesis/Pathogenesis
Transient perturbation of endochondral ossification or a lasting consequence of age-dependent reduction in growth

Diagnostic features
- Decreased thickness of the physis – reported most often in femur and tibia (since these are examined in routine nonclinical toxicity studies), but may be seen in other bones
- Decreased thickness can affect one or more zones of the

physeal plate, but generally appear as a uniform change across the physis

Differential diagnoses
None

Comment
This change can be encountered as a consequence of persistent reduced food consumption affecting signaling pathways that regulate cartilage proliferation and endochondral ossification, such as growth hormone, IGF1, and FGF21. The same effect will be seen following exposure to agents that have a direct effect on chondrocyte proliferation. For example, doxorubicin administration leads to decreased physeal thickness in weanling and aged rats. The effects are most prominent in young animals due to their high rate of endochondral ossification.

Decreases in physeal thickness typically are subtle and challenging to detect using qualitative methods (e.g., histopathologic analysis). If suspected, this change should be confirmed by quantitative methods (e.g., morphometry).

References
Bourrin et al. (2000), Kubicky et al. (2012), Noguchi et al. (2011), Wu et al. (2012), Yakar et al. (2002)

Growth plate closed (Figure 17)

Other terms used
Age-dependent or premature physeal closure

Species
Rats and Mice

Affected structures
Physis (growth plate), typically assessed in long bones

Biological behavior
Closure can arise by physiologic or pharmacologic means
- Physiologic – a normal consequence of skeletal maturation in most species (though growth plates remain open for life in rodents)
- Pharmacologic – the premature closure in juvenile animals following exposure to certain hormones or therapeutic agents

Histogenesis/Pathogenesis
Ossification of the growth plate

Diagnostic features
- Growth plate cartilage is replaced with bone
- Gaps in the ossified growth plate may connect the marrow cavities in the epiphysis and metaphysis
- Closure may be complete or segmental

Differential diagnoses
None

Comment
It is not recommended that it be recorded as a background finding in routine toxicity studies in rodents. However, on a case-by-case basis it may be necessary to record premature closure if the incidence appears to rise following exposure to a test article. For instance, anticoagulant treatment in juvenile rats has been associated with early hemorrhage in the physis followed by segmental to complete closure of growth plate. Retinoids (vitamin A derivatives) have been reported to induce physeal plate closure in guinea pigs; similar premature closure has been linked to vitamin A toxicity in humans and calves. Doxorubicin also has been recorded as an agent capable of inducing this change.

References
Hähnel et al. (1978), Price et al. (1982), Rothenberg et al. (2007), Standeven et al. (1996), Weise et al. (2001)

Proliferative Lesions

Hyperplasia, chondrocyte (Figure 18)

Other terms used
Hyperplasia, cartilage

Species
Rats and Mice

Biologic behavior
Growth may appear expansive but is not invasive

Histogenesis
Chondrocyte proliferation (usually in articular or physeal cartilage, especially in long bones)

Diagnostic features
- Recognized by the presence of an increased amount of well-differentiated but irregularly arranged cartilage
- Chondrocytes often occur in clusters (termed 'chondrones') within more closely arranged lacunae
- The cartilage matrix generally stains highly basophilic with H&E but may stain pale basophilic or pink (chondroid) if depleted of proteoglycans
- Often associated with increased numbers of hypertrophic chondrocytes

Differential diagnoses
None

Comments
Chondrocyte hyperplasia commonly occurs in association with trauma, inflammation, or chondromucinous degeneration (see definition below).

Hyperplasia, osteoblast, focal (Figure 19)

Other terms used
None

Species
Only reported in rats

Affected structure
Trabecular bone

Biological behavior
Non-neoplastic proliferation

Histogenesis
Localized increase in the production of osteoblasts/osteoprogenitors

Diagnostic features
- Single or multiple localized proliferations of well-differentiated, round to columnar osteoblasts organized along bone surfaces
- Occurs concurrently in bones with increased bone (trabecular and/or cortical)
- Often occurs with some evidence of local osteoid production
- May fill inter-trabecular spaces but does not significantly disrupt architecture of pre-existing bone
- Focal osteoblast hyperplasia sometimes is admixed with focal proliferations of fibroblast-like cells (focal fibroplasia) and associated collagenous matrix

Differential diagnoses
- Fibrous osteodystrophy (FOD) – an entity in which osteoclastic bone resorption is a primary feature, and in which the spindle-shaped mesenchymal cells (fibroblasts/osteoprogenitors) are found mainly in inter-trabecular spaces
- Marrow fibrosis/stromal cell hyperplasia – a condition consisting primarily of fibrocellular proliferations within the marrow spaces; the cells lack the cytologic features of osteoblasts
- Osteoblastoma – a benign neoplasm that is more expansile than a hyperplastic focus, induces greater disruption of the trabecular architecture, and is associated with increased pleomorphism of osteoblasts
- Increased osteoblastic surface – this diagnosis is appropriate for diffuse increase in the surface extent of osteoblasts.

Comment
This unusual focal lesion has been reported in rats at a very low incidence and has been described following long-term treatment of rodents with daily injections of PTH or related peptides. These molecules cause a spectrum of benign and malignant bone neoplasms; this lesion has not been reported as a spontaneous finding, but has been observed in a low number of control animals in these studies. Osteoblast hyperplasia often occurs concurrently with increased bone and/or osteoid.

References
Jolette et al. (2006), Lotinun et al. (2005), Riminucci et al. (1997), Vahle et al. (2002)

Osteoma (Figure 20)

Other terms used
Cancellous osteoma, compact osteoma, juxtacortical (parosteal) osteoma, medullary osteoma (enostosis), spongious osteoma, trabecular osteoma

Species
Rats and Mice

Affected structures
Axial and appendicular bones, especially the skull and long bones

Biological behavior
A benign space-occupying neoplasm that arises preferentially from the periosteal surface of cortical bone

Histogenesis
Osteoblasts, osteocytes

Diagnostic features
Some features are common to lesions in both mice and rats, while others are species-specific
- Common characteristics
  - o Expansile growth pattern with sharp demarcation from surrounding tissue
  - o Composed of very dense bone (almost solid in appearance)
  - o Osteoid-rich trabeculae (if present) are located peripherally and may be rimmed with osteoblasts
  - o Mature trabeculae, rich in dense bone, may lack osteoblast rimming altogether, and many osteocyte lacunae may be empty
  - o The inter-trabecular stroma is generally sparse but may contain marrow elements
  - o Smooth outline with inactive or active osteoblasts
  - o Fatty or hematopoietic marrow may be present
- Mouse-specific features
  - o Composed of very dense bone with predominantly woven structure
  - o Lacks spindle cell stroma described for osteofibroma
- Rat-specific traits
  - o Composed of dense mature bone with a predominantly lamellar structure and few cells

Differential diagnoses
Mouse and Rat
- Bony exostosis or reactive bone – distinguishable only

by the absence of any neoplastic cellular characteristics
- Osteosarcoma – low degree of tissue differentiation (immature or atypical bone) and presence of cytologic criteria of malignancy

Mouse
- Osteofibroma – spindle cells are present between the bony trabeculae

Rat
- Osteochondroma – the bony portion is capped by a cartilage layer

Comment

Spontaneous osteomas are rare in most strains of mice. They most often occur in the skull and seem to be more common in females than males. The influence of female sexual hormones on the development of these masses has been suspected. They can be induced in mice by several viruses.

References

Carlton et al. (1992), Charles and Turusov (1974), Ernst et al. (2001), Gimbel et al. (1996), Höger et al. (1994), Leininger and Riley (1990), Long et al. (1993), Long and Leininger (1999b), Nilsson and Stanton (1994), Wilson et al. (1985)

Osteoblastoma (Figure 21)

Other terms used

None

Species

Only reported in rats

Affected structures

Axial (sternebrae) and appendicular (tibia and femur) trabecular and cortical bone

Biological behavior

A benign primary bone tumor

Histogenesis

Osteoblast

Diagnostic features
- Occurs concurrently in bones with increased bone (trabecular and/or cortical)
- Intramedullary growth pattern of disorganized trabeculae of immature bone, often accompanied by a fibrovascular stroma
- Moderate numbers of large active osteoblasts are arranged along the trabecular surfaces
- Cytologically, the osteoblasts have minimal atypia
- Scattered typical-appearing mitotic figures are often present
- Multinucleated cells may be present within the lesion
- The neoplasm may replace a focal region of pre-existing bone, but the leading margin of the osteoblastoma appears to be expansive, sharply demarcated, with minimal invasion
- Within the spaces between interlacing trabeculae of osteoid, a fibrovascular stroma is often prominent

Differential diagnoses
- Osteoblastic osteosarcoma – this entity would include the cytologic features of malignancy, production of tumor osteoid, and produce lysis of adjacent trabecular and/or cortical bone
- Osteoblast hyperplasia – this entity lacks the disruption of trabeculae present in osteoblastoma, and the cells are well differentiated osteoblasts
- Osteofibroma - this entity (observed in mice only) has a prominent fibrous component

Comment

Similar to osteoblast hyperplasia, this is a relatively uncommon entity that has been described in studies with PTH and related peptides.

References

Jolette et al. (2006), Long and Leininger (1999b), Vahle et al. (2002)

Osteofibroma (Figure 22)

Other terms used

None

Species

Mouse only

Biological behavior

A benign primary bone tumor

Histogenesis

Pluripotential mesenchymal stem cells, osteoblasts

Diagnostic features
- Expansively growing mass arising preferentially in the vertebral column
- Appears to arise from the medullary cavity (as opposed to periosteal surface)
- Composed of mature bone trabeculae separated by stroma of spindle cells
- Scattered highly cellular areas with osteoid spicules also typical
- Both active osteoblasts and osteoclasts may be present
- Blood-forming marrow may occur
- Stromal cells are not highly pleomorphic and do not invade surrounding tissue

Differential diagnoses

- Bony exostosis or reactive bone – distinguishable by the absence of any tumor characteristics
- Fibro-osseous lesion (FOL) – characterized by proliferation of fibrovascular stroma, osteoblasts, and osteoclasts. Bone turnover is accelerated with spreading resorption encroaching on the center of the medullary cavity followed by bone formation.
- Osteoma – lacks spindle cell stroma
- Osteosarcoma – low degree of tissue differentiation (immature or atypical bone), infiltrative growth, and presence of cytologic criteria of malignancy

Comment

Osteofibromas have only been reported in mice treated with radionuclides. These tumors may appear as osteosarcoma radiographically (i.e., extensive bone destruction [radiolucent expanses] with evidence of new bone formation [radio-opaque foci]), and they may progress to osteosarcomas. Due to their preferential location in the vertebral column, they may lead to paralysis.

References

Carlton et al. (1992), Ernst et al. (2001), Long et al. (1993), Long and Leininger (1999b), Nilsson and Stanton (1994)

Osteosarcoma (Figures 23, 24)

Other terms used

Osteogenic sarcoma

Species

Rats and Mice

Affected structures

Skeleton in the rat and mouse; may originate from extraskeletal sites such as the subcutaneous tissue, spleen and digestive tract

Biological behavior

A malignant primary bone tumor

Histogenesis

Pluripotential mesenchymal stem cells, osteoblasts, osteocytes

Diagnostic features

- The formation of osteoid by anaplastic mesenchymal cells (neoplastic osteogenesis) is an essential feature
- Various histological types may occur
- Bone formed is typically immature woven bone
- May exhibit the zonation phenomenon with osteoid-rich central region and less productive cells at the periphery
- Marrow cavities with hematopoietic tissues and osteoclasts may be present
- Lysis of normal bone may occur simultaneously with neoplastic osteogenesis
- Foci of collagen, cartilage, and mucoid ground substance may occur in different areas of the same tumor
- Proliferating cells may be pleomorphic, spindle-shaped, or multinucleated often with loss of cellular alignment along the bone surface
- Foci of necrosis and hemorrhage may be extensive
- Mitotic figures variable and can be frequent

Special diagnostic techniques

In research studies, plain film radiographs of animals prior to necropsy can aid in detecting bone lesions which may not be evident at necropsy. Osteosarcomas may produce lytic lesions in which irregular, wispy radio-opaque (white) streaks are seen within the affected tissues.

Differential diagnoses

- Osteoma – well-defined compact osseous tumor consisting of dense woven bone and lacking pleomorphic infiltrating tumor cells indicative of malignancy
- Osteofibroma (mouse only) – well-differentiated spindle cells between bony trabeculae and lacking cytologic criteria of malignancy
- Osteochondroma (rat only) – well-organized, cartilage-capped bony core with fatty and hematopoietic marrow
- Chondrosarcoma, Hemangiosarcoma, or Fibrosarcoma – malignant cells of mesenchymal derivation that do not form osteoid

Comment

This highly invasive and destructive tumor arises in the skeleton, although extra-skeletal sites also may serve as the site of origin in rodents (especially in certain strains of genetically engineered mice). Metastases are common, predominantly occurring in the lung, liver and spleen. A variety of osteosarcoma subtypes (e.g., osteoblastic, osteoplastic, osteoclastic, fibroblastic, telangiectatic, compound) have been described in the literature. Subclassification of osteosarcoma in rodents is possible but not required for risk assessment purposes.

Mouse: Osteosarcomas are rare in strains commonly used in toxicological studies. However in the NMRI strain commonly affected with osteosarcoma, the spine is most commonly involved followed by long bones, particularly at the metaphysis. There is no obvious correlation between histologic differentiation or tumor size and the probability of metastasis. Tumors of the caudal vertebrae have the highest frequency of metastasis.

Rat: Osteosarcomas are readily inducible by exposure of bones to ionizing radiation from external and implanted sources; by administration of PTH, related peptides, or various carcinogens; and by inoculation with Moloney sarcoma virus.

References

Carlton et al. (1992), Charles and Turusov (1974), Ernst et al. (2001), Franks et al. (1973), Frith et al. (1982), Highman et al. (1981), Jolette et al. (2006), Kavirayani et al. (2012), Leininger and Riley (1990), Long et al. (1993), Long and Leininger (1999b), Luz et al. (1991a), Machado and Beauchene (1976), Mii et al. (1988), Minato et al. (1988), Nilsson and Stanton (1994), Olson and Capen (1977), Pybus and Miller (1938), Tucker (1986), Vahle et al. (2002), Wadsworth (1989)

Osteogenic fibrosarcoma (Figure 25)

Other terms used

None

Species

Rats and Mice

Affected structures

Trabecular and cortical bone

Biological behavior

A malignant primary bone tumor

Histogenesis

Fibroblast

Diagnostic features

- Pleomorphic cells intermixed with variable amounts of collagenous matrix
- There is no production of tumor osteoid as would be observed in a fibroblastic osteosarcoma
- Similar to fibrosarcoma in other locations, the mitotic index may be increased and accompanied by cytologic features of malignancy
- Cells may be arranged in interlacing patterns
- Expansion with lysis of adjacent trabecular or cortical bone
- Important to determine that the bone is the site of origin of the tumor, rather than an extension of a subcuticular fibrosarcoma

Differential diagnoses

- Fibroblastic osteosarcoma – this entity would include the production of tumor osteoid
- Marrow fibrosis – primarily spindle cell and collagen matrix without cytologic evidence of malignancy or lysis of adjacent bone

Comment

This relatively uncommon malignant tumor has a metastatic potential that is not well understood. Although not included in most rodent classification schemes previously, fibrosarcoma of bone has been recorded in both control and treated animals in studies conducted by the U.S. National Toxicology Program and has been reported as an induced lesion in rats.

References

Jolette et al. (2006)

Chondroma (Figure 26)

Other terms used

None

Species

Rats and Mice

Affected structures

Cartilage throughout the body, including

- Skeletal system (most common origin), especially at articular surfaces, synchondroses, sites of endochondral ossification, and extensions of bony structures such as ribs, and nasal turbinates
- Extraskeletal sites, such as the ear, nasal cavity, trachea, and lung

Biological behavior

A benign primary cartilage tumor

Histogenesis

Chondroblasts, chondrocytes

Diagnostic features

- Well-circumscribed, expansive tumor consisting of irregular lobules of mature, hyaline cartilage
- Chondrocytes lack orderly arrangement but are well differentiated and generally arranged individually within lacunae
- Individual chondrocytes exhibit minimal cellular and nuclear pleomorphism
- Mitotic figures are rare
- The surrounding matrix is amorphous and lightly basophilic
- As in normal cartilage, occasional bicellular lacunae may be seen, but multinucleated chondrocytes are absent
- Matrix may have areas of osseous metaplasia

Differential diagnoses

Mouse and Rat

- Chondrosarcoma – pleomorphic, binucleated, or multinucleated chondrocytes may be seen in addition to infiltrative growth or metastases

Rat

- Osteochondroma – well-organized cartilage cap on top of a cancellous bony core (resembling growth plate)
- Chordoma – lobules of vacuolated tumor cells with distinct cell borders and central nuclei (‘physaliphorous’ cells), associated with vertebral bodies (i.e., the descendants of the notochord)

Comment

Chondromas do not metastasize or invade surrounding tissues. Areas of osseous metaplasia and/or chondroid formation may occur within chondromas and should not be confused with bone matrix production by neoplastic osteoblasts.

Chondromas are extremely rare in mice. Chondromas are occasionally seen in the nasal turbinates of rats.

References

Carlton et al. (1992), Ernst et al. (2001), Leininger and Riley (1990), Long et al. (1993), Long and Leininger (1999b), Nilsson and Stanton (1994), Wadsworth (1989)

Chondrosarcoma (Figures 27, 28)

Other terms used

None

Species

Rats and Mice

Affected structures

Cartilage in various axial and appendicular skeletal sites, and in mice also in extra-skeletal sites (including third eyelid, external ear, and larynx)

Biological behavior

A malignant primary cartilage tumor

Histogenesis

Pluripotential mesenchymal stem cells, chondroblasts, chondrocytes

Microscopic diagnostic features

Some features are common to lesions in both mice and rats, while others are species-specific

- Common characteristics
  - o Lobulated, highly cellular tumor with minimal tendency to invade surrounding tissues
  - o Usually well-differentiated, large basophilic cells with large nuclei and prominent nucleoli individually in lacunae and surrounded by a hyaline ground substance
  - o Occasional pleomorphic, binucleated, or multinucleated giant cartilage cells
  - o Mitotic figures are rare
  - o Poorly differentiated chondrosarcomas have spindle-shaped cells reminiscent of fetal chondroblasts
  - o No formation of bone or tumor osteoid
- Mouse-specific traits
  - o Sometimes abundant foci of mineralization, extensive necrosis, and cyst formation may occur
- Rat-specific features
  - o Pulmonary metastases are common

Differential diagnoses

Mouse and Rat

- Chondroma – no cellular or nuclear pleomorphism are observed. No cytologic or histologic features of malignancy
- Osteosarcoma – although chondrosarcomatous areas may occur, the production of tumor osteoid or bone is an essential feature of osteosarcoma

Rat

- Osteochondroma – well-organized cartilage cap on a bony core resembling a growth plate
- Chordoma – lobules of vacuolated tumor cells with distinct cell borders and central nuclei ('physaliphorous' cells)

Comment

Local tissue infiltration may occur, and pulmonary metastases are common.

Chondrosarcomas are extremely rare in mice. They may also arise from extra-skeletal cartilage in the third eyelid, external ear, and larynx. In rats, chondrosarcomas have been reported to occur spontaneously and secondary to chemical induction.

Chondrosarcomas have been induced in rats by administration of carcinogens such as 1-(2-hydroxyethyl)-1- nitrosourea (HENU) and 2-acetylaminofluorene. Because chondrosarcomas in rats are often well-differentiated, their distinction from chondromas may be difficult and involve critical assessment of cellular pleomorphism and histologic evidence of invasion or metastases.

References

Carlton et al. (1992), Ernst et al. (2001), Gregson and Offer (1981), Leininger and Riley (1990), Long et al. (1993), Long and Leininger (1999b), Nilsson and Stanton (1994), Pelfrene et al. (1976), Stanton (1979), Wadsworth (1989)

Osteochondroma (Figure 29)

Other terms used

None

Species

Rat only

Affected structures

- Epiphysis, metaphysis, diaphysis
- Trabecular and cortical bone of the appendicular and axial skeleton

Biological behavior

A benign mixed mesenchymal tumor with prominent cartilaginous and osseous components

Histogenesis

Presumed to be chondroblasts (chondrocytes) of the growth plate or pluripotent mesenchymal cells arising from the external surfaces of the bone surface (periosteum)

Diagnostic features

- Cartilage-capped osseous protuberance of the external surface of a bone that is not associated with degenerative joint disease or displacement of the perichondrial ring
- Consists of an outer rim of proliferating growth plate-like cartilage that undergoes endochondral ossification, resulting in an inner zone of lamellar trabecular bone separated by abundant marrow fat and hematopoietic tissue
- Cartilage cap consists of groups or rows of irregular, hypertrophic chondrocytes
- Finger-like projections of the periosteum-covered cartilage cap may be observed extending into the subchondral bone
- Tumor core consists of mature lamellar bone
- Bony core results from endochondral ossification of the expansively growing cartilage layer
- Trabecular bone lined with a uniform population of flat osteoblasts
- Abundant fatty and hematopoietic marrow between the bony trabeculae
- Marrow cavity communicates with that of the parent bone

Differential diagnoses

- Osteophyte – non-neoplastic osseous protuberance with or without a cartilage cap located along the lateral epiphyseal margins that forms as a consequence of degenerative joint disease or displacement of the perichondrial ring
- Chondroma – irregularly oriented lobules of cartilage without significant amounts of bony tissue
- Osteoma – tumor bone is dense, and not capped by a cartilage layer
- Chondrosarcoma – there is no formation of osteoid or bone, and the component cells have the expected cytologic features of malignancy
- Osteosarcoma – if cartilaginous areas are observed within the osteosarcomatous tissue, these are disorderly and usually consist of pleomorphic, atypical chondrocytes. Tumor osteoid is present.

Comment

Osteochondromas and osteochondroma-like lesions have been induced in rats by exposure to vinyl chloride vapors, surgical reflection of the perichondrial ring in radii, and radiation.

Osteochondromas are not associated with degenerative joint disease or displacement of the perichondrial ring.

References

Carlton et al. (1992), Delgado et al. (1985), Delgado et al. (1987), Ernst et al. (2001), Long et al. (1993), Viola et al. (1971)

Chordoma (Figures 30–32)

Other terms used

None

Species

Rats only

Affected structures

Axial skeleton (primarily lumbosacral region, but rarely at the base of the skull)

Biological behavior

A malignant neoplasm

Histogenesis

Rests/remnants of notochord mesenchymal cells (which resemble cartilage in structure and function) along the vertebral axis

Diagnostic features

- Lobulated tumor which may be partially enclosed by a small fibrous capsule
- Lobules consist of syncytial tumor cells with masses divided and surrounded by fibrous trabeculae
- Small to large irregular tumor cells with distinct cell borders; single or multiple cytoplasmic vacuoles; and round to oval, centrally located, basophilic nuclei (bubble-bearing or "physaliphorous" cells)
- ″Signet-ring cells″ with peripherally located nuclei and tumor cells with homogeneous or granulated cytoplasm also present
- Mucin production may be observed using special stains
- Mitotic figures are few
- Necrosis and spicules of reactive bone may be seen within the tumor
- Invasion and destruction of adjacent bones and soft tissue
- Distant metastases occur frequently, especially to the lung

Special diagnostic techniques

Chordomas can be distinguished by histochemistry and immunohistochemistry from other tumors. They are lipid-negative (oil-red-O, Sudan IV), glycogen-positive (periodic acid-Schiff [PAS]-labeled cytoplasmic granules), keratin-positive, vimentin-positive, neuron-specific enolase (NSE)-positive, and S100 protein-positive. Toluidine blue stain demonstrates mucin well.

Differential diagnoses

- Hibernoma – tumor cells (of brown adipose tissue origin) stain positively for lipid
- Chondrosarcoma – large basophilic cells in lacunae and surrounded by a hyaline ground substance
- Liposarcoma – variably sized, sometimes vacuolated cells (of white adipose tissue origin) that often are lipid-positive and PAS-negative
- Chondromas and chondrosarcomas – negative for keratin

Comment

Chordomas are rare and have been observed mostly in Fischer 344 and Donruy rats; however, a chordoma has been reported in a Sprague-Dawley rat. Diagnosed chordomas in rats are generally malignant because the primary site is only rarely subjected to routine evaluation unless grossly abnormal. The diagnosis is often based on sole detection of metastases in the lung. The incidence is greater in males than females, which is also true of this neoplasm in humans.

References

Carlton et al. (1992), Ernst et al. (2001), Leininger and Riley (1990), Long et al. (1993), Maekawa et al. (1984), Reuber and Reznik-Schüller (1984), Reznik and Russfield (1981), Stefanski et al. (1988), Wimberly (1988), Zwicker and Eyster (1991)

II. Joint

Normal Rodent Joints

The front and rear paws (carpus/metacarpus or tarsus/metatarsus, respectively, with associated phalanges), "knees" (femorotibial joint), and "ankles" (tibiotarsal joint) are the synovial joint-containing sites that are most commonly evaluated microscopically in rodents during the course of efficacy (e.g., animal models of osteoarthritis [OA] and rheumatoid arthritis [RA]) and toxicity studies. A typical synovial joint is shown in Figure 33. Covering the inner (i.e., adluminal) surfaces of joint capsules as well as intraarticular ligaments and tendons, synovial membranes are formed by a thin (1 to 3 cells thick), discontinuous layer comprised of type A (i.e., macrophage-like), type B (i.e., fibroblast-like), and intermediate-type synoviocytes supported by loose fibroadipose tissue within which are blood and lymphatic vessels and unmyelinated nerves. Normal regional anatomic variations include infrapatellar "fat pads", villous projections of synovial membranes at sites of insertion on the periosteum/perichondrium (i.e., transition zones) of apposed articulating bones, and fibrocartilaginous metaplasia of the femorotibial menisci with ossicle formation. Transition zones are also believed to be the sites from which pannus and osteophytes develop (Figures 33–36).

Evaluation of Rodent Joints

Morphologic assessments of rodent joints are generally dependent on the objectives of the necropsy and the information that needs to be obtained. To minimize the possibility of dissection-induced iatrogenic damage and because rat and mouse joints are small enough to be displayed in their entirety (often as groups of multiple adjacent joints) on a single microscopic slide, macroscopic evaluation of rat and mouse joints is not routinely conducted. Instead, evaluation of joint architecture in terms of both overall form and cellular detail typically is undertaken on slide-mounted tissue sections.

Routine processing of rodent joints is comparable to the steps taken for other bony structures. Rat and mouse joints usually are fixed by immersion in neutral buffered 10% formalin for 3 days and 24 hours, respectively. Next, fixed specimens typically are demineralized by immersion in a solution like 20% ethylenediaminetetraacetic acid (EDTA, a calcium-chelating agent) and 5% or 10% formic acid; commercially available demineralization products (e.g., Decal®, Immunocal®) have been used successfully to process rodent joints. In general, specimens are transferred to fresh demineralizing solution every 24 to 48 hours until the bone can be cut without resistance using a sharp blade. The choice of an agent for demineralization is influenced by several factors, chiefly the desired speed of processing and the need to preserve delicate antigenic epitopes. Chelating agents (e.g., EDTA) generally provide slower and gentler demineralization compared with acids. Combinations of acids and chelators (e.g., Formical®) represent a reasonable compromise between increased processing speed and molecu-

lar preservation.

Demineralized joints must be trimmed to an appropriate plane to ensure that all joint elements (i.e., articular cartilage, joint cavity, subchondral bone, synovium, and periarticular soft tissues) are present in an optimal orientation for analysis. The choice of trimming plane varies depending on the joint and typically is dictated by anatomic considerations such as (1) the conformation in which most joint tissues are routinely observed and (2) the available landmarks needed to ensure such reproducible sampling. The most frequently used trimming plane to prepare rat and mouse femorotibial joints for microscopic evaluation, the objective of which is to examine the largest expanses of articular cartilage, is the frontal orientation (Figure 33). In contrast, for general toxicity studies designed to survey joint health as one of many potential target organs, the rodent femorotibial joint typically is evaluated in parasagittal orientation (taken off-center through one femoral condyle, a portion of meniscus, and the corresponding tibial plateau, Figure 34). Hind paw (usually tibiotarsal and intertarsal) joints generally are assessed using a longitudinal ("mid-axial") orientation (Figure 35), while forepaw (typically intercarpal with radiocarpal ["wrist"] and/or carpometacarpal) joints often are inspected by placing the volar ("palm") surface down in the cassette and then facing the paraffin block to reach the carpal bones. After trimming, fixed and demineralized joint specimens usually are processed by routine methods into paraffin blocks.

The choice of stains used for histopathological evaluation also depends on the desired endpoints. Hematoxylin and eosin (H&E)-stained tissue sections are generally used to survey the basic morphologic features of all joint tissues, and often may serve as a standalone screen for joint lesions in general toxicity studies or if the primary experimental endpoints are scoring of non-cartilaginous effects (Figure 36). The most frequently used stains to assess matrix integrity in the articular cartilage are toluidine blue and safranin O/fast green. For some studies, special procedures (e.g., anti-cathepsin K immunohistochemistry to count osteoclasts or anti-von Willebrand factor to examine vessel numbers) may be undertaken as well.

Joint pathology may be evaluated in multiple fashions. Depending on the model, the most common options are qualitative assessments of structural abnormalities and semi-quantitative scoring systems for endpoints such as articular cartilage integrity, bone erosion, inflammation, and pannus. Histomorphometry and noninvasive imaging by contrast-enhanced magnetic resonance imaging (MRI) and microcomputed tomography (μCT) or even routine bench-top radiography are additional tools to facilitate the evaluation of the structural integrity of the joint.

References

Bendele et al. (1999), Bolon et al. (2004), Bolon et al. (2011), Coxon et al. (2002), Gerwin et al. (2010), Glasson et al. (2010), Greaves (2012), Long and Leininger (1999b), Palmer et al. (2006), Pastoureau et al. (2010), Wong et al. (2006), Woodard et al. (2002)

Nonproliferative Lesions

Inflammation (Figures 37–40)

Other terms used

Arthritis, synovitis

Species

Rats and Mice

Affected structures

Synovial membrane, articular cavity, articular cartilage, intra-articular ligaments, subchondral bone, fibrous joint capsule, tendons, and/or intra-articular and periarticular adipose tissue

Biological behavior

Locally infiltrative and often destructive accumulation of dedicated and facultative immunoreactive and phagocytic cells.

Histogenesis/Pathogenesis

The chief components of inflammatory joint infiltrates typically include one or more leukocyte types and locally recruited phagocytes (including osteoclasts for attacking bone and/or type A synoviocytes). The infiltrating cells generally will include a preponderance of neutrophils for acute (especially bacteria-induced) conditions but will have more mononuclear elements (usually lymphocytes, with fewer plasma cells and macrophages) as the disease becomes chronic, especially if it represents an autoimmune response to some intra-articular antigen. "Pannus" is an aggressive layer of fibrovascular ("granulation") tissue that in some diseases originates from the inflamed synovium at the transitional zone to grow across the adluminal surface of the articular cartilage, where it may act to destroy the articular surface as well as periarticular and subchondral bone.

The location of the infiltrating cells depends on the target tissue. Leukocytic infiltrates in OA models initially are beneath the synovial lining cells and later become more diffuse. In contrast, leukocytic infiltrates in RA models are initially perivascular; later they diffusely infiltrate the synovial membrane and periarticular tissues. In collagen-induced arthritis (CIA) models of RA in rats and mice, neutrophils are commonly seen in the articular cavity, on the surface of the articular cartilage, and in periarticular soft tissues adjacent to synovium-lined surfaces.

Diagnostic features

Inflammation is diagnosed by the presence of the following primary changes

- Edema of intra-articular and periarticular soft tissues
- Congested blood vessels within intra-articular and periarticular soft tissues

- Infiltration of inflammatory cells (e.g., neutrophils, lymphocytes, plasma cells, and/or macrophages) in the synovial membrane and/or intra-articular and periarticular soft tissues
- Influx of neutrophils, often accompanied by deposits of fibrin, into the joint cavity

Secondary changes induced over time by persistence of the primary inflammatory response may include

- Synoviocyte hypertrophy and hyperplasia (see definition below)
- Fibrosis (proliferation of fibrous connective tissue in and around joints)
- Pannus formation
- Erosion and/or ulceration of articular cartilage
- Resorption of subchondral bone
- Production of chondrophytes or osteophytes
- Bony ankylosis (the typical "end-stage" lesion)

Special diagnostic techniques

In general, a diagnosis of "inflammation" may be made reliably using H&E-stained sections. Special procedures may be utilized to evaluate the nature of the inflammatory process:

- Major cell type-specific markers (immunohistochemical [IHC] methods, which work well on formalin-fixed, acid-demineralized, paraffin-embedded joints):
  - o Neutrophils – myeloperoxidase
  - o B-lymphocytes – B220 (mouse)
  - o T-lymphocytes – CD3
  - o Macrophages – ED1/CD68 (rat) or F4/80 (mouse)
- Markers for sequelae of chronic inflammation
  - o Cartilage matrix destruction – safranin O/fast green, toluidine blue (histochemistry)
  - o Fibrous connective tissue – Masson's trichrome (histochemistry)
  - o Neovascularization – CD31 (IHC)
  - o Osteoclasts – cathepsin K (IHC)
- Microbes and microbial products
  - o Bacterial detection – Gram stain (histochemical)
  - o Organism identification – demonstration of organism-specific gene transcripts (*in situ* hybridization [ISH] techniques) or proteins (IHC methods)

Differential diagnoses

None

Comment

Spontaneous inflammation in the joints of rodents is uncommon. Inflammation associated with spontaneous and surgically-induced models of OA is usually mild and consists of mononuclear inflammatory cells (typically lymphocytes) infiltrating into the synovial membrane. In contrast, inflammation in rodent models of RA (e.g., models induced by type II collagen [CIA] or adjuvant [i.e., adjuvant-induced arthritis, or AIA]) often is characterized acutely by infiltration of neutrophils and at later stages by infiltration of lymphocytes, plasma cells, and macrophages widely throughout the synovial membrane and periarticular soft tissues.

Rodent CIA models of RA result in aggressive inflammatory changes in the synovial membrane, articular cartilage, and subchondral bone of knees, ankles, and paws of both mice and rats. Rodent AIA models of RA develop exclusively in rats; lesions typically are most severe in the tibiotarsal region, although the femorotibial joints also are involved reproducibly when certain adjuvants are employed. Compared with CIA in rats, damage to articular cartilage is less severe and bone resorption is much more rapid and severe in rats with AIA. Infiltrates in both these rodent models are mainly neutrophilic with fewer macrophages and lymphocytes; an explanation for their different time course and severity, despite having similar intra-articular complements of leukocytes, is not known. The recent development of a novel modification of the K/BxN mouse has added significant logistical and platform advantages compared with the K/BxN serum transfer and CIA models in mice, and provided investigators with additional opportunities to study pathways and mechanisms involved in the pathogenesis of human RA.

Infectious forms of arthritis in mice and rats are chiefly bacterial, and are much less common compared with non-infectious forms. Microbial agents can gain access to a joint by inoculation, extension from a previously established infection in the periarticular soft tissue, or by hematogenous dissemination.

Xenobiotic exposure may result in the induction of joint inflammation. Administration of ciprofloxacin, levofloxacin, and other fluorinated derivatives of the quinolone class of antibiotics has been associated rarely with tendonitis and tendon rupture in people. Although the administration of nalidixic acid, a first-generation quinolone, to guinea pigs induced a distinctive, blister-like focus of degeneration and necrosis affecting articular cartilage, the absence of an adequate and reproducible rodent model has been a barrier to identifying the pathogenesis of those debilitating tendon/joint disorders in people.

The long-term administration of non-selective matrix metalloproteinase (MMP) inhibitors (e.g., marimastat) to humans elicits musculoskeletal syndrome (MSS), a condition characterized by joint damage including pain, stiffness, and inflammation. In a rat model of MSS, the administration of marimastat results in clinical signs (e.g., reluctance or inability to move, hind paw swelling, high-stepping gait) and microscopic findings in the periarticular soft tissue (e.g., synoviocyte hypertrophy and hyperplasia, fibrosis of perisynovial adipose tissue, and lymphocytic infiltrates) that is thought to mimic changes in human MSS.

References
Bendele (2001a), Bendele (2001b), Bolon et al. (2011), Brand (2005), Ghoreschi et al. (2011), Greaves (2012), LaBranche et al. (2010), LaBranche et al. (2012), Liu (2010), Long and Leininger (1999b), Mazurek et al. (2011), Melhus (2005), Renkiewicz et al. (2003), Rosenberg (2010)

Osteophyte (Figures 41, 42, 44)

Other terms used
Osteochondrophyte, chondrophyte

Species
Rats and Mice

Affected structures
Periosteum, joint capsule

Biological behavior
These periarticular bony nodules are a unique example of neochondrogenesis in adult animals

Histogenesis/Pathogenesis
Precursor cells in the periosteum spatially associated with the transition zone (i.e., the area between the periosteum-covered metaphysis and the epiphyseal site of attachment of the synovium)

Diagnostic features
Early lesions presaging the eventual development of osteophytes include:
- Synovial cell hyperplasia (see definition below)
- Chondrocytogenesis near the capsular attachments to bone, with subsequent cell differentiation, hypertrophy and hyperplasia

Secondary changes that result in osteophyte generation include:
- Endochondral ossification (leading to ossification at the base of the nodule) that culminates in the following:
  - o Full integration of the bony nodule with the original subchondral bone
  - o Formation of marrow cavities inside the bone (populated by bone marrow and/or white adipose tissue), which are not connected to the pre-existing marrow cavities
  - o Retention of a cartilage cap that extends the original joint surface

Special diagnostic techniques
None

Differential diagnoses
None

Comment
An osteophyte is a fibrocartilage-capped bony growth that forms in response to chronic periosteal irritation, commonly that associated with degenerative joint disease (DJD). Developing osteophytes are composed of fibroblasts, mesenchymal prechondrocytes, maturing chondrocytes, hypertrophic chondrocytes, and osteoblasts, and their growth is regulated by growth factors in the transforming growth factor beta (TGFβ1) superfamily. Gene expression patterns associated with developing osteophytes indicate that chondrogenesis and bone deposition resemble a healing fracture callus. It is unclear whether osteophytes develop as a functional adaptation to joint instability or alternatively from remodeling processes as a result of joint changes.

Osteophytes commonly form during the development of OA and RA. In experimental arthritis models, osteophyte formation is a rapid process (i.e., within 2–3 days). Although a cause and effect relationship to cartilage damage has not been definitively established, osteophytes arise from the periosteum covering the bone at the cartilage-bone junction. In advanced lesions, osteophytes on adjacent bones may become so extensive that they fuse, leading to joint ankylosis.

References
Bolon et al. (2015), Matyas et al. (1997), van der Kraan and van den Berg (2007)

Chondromucinous degeneration (Figure 43)

Other terms used
Cartilage degeneration, sternal cartilage degeneration

Species
Rats and Mice

Affected structures
Cartilage of the articular surface and physes (i.e., growth plates) of long bones and intervertebral joints, intervertebral discs, and synarthroses of the sternum

Biological behavior
Incidental background finding in many rodent strains, the prevalence of which appears to be higher in aged animals

Histogenesis/Pathogenesis
The initial biochemical change is believed to occur in the extracellular matrix; chondrocytes are affected secondarily

Diagnostic features
Typical features include the following:
- Focal to locally extensive areas of cartilage necrosis in cartilage characterized by:
  - o Absence of chondrocytes
  - o Disordered and/or fragmented ground substance
  - o Cavitation (in some but not all instances)
- Chondrocytes at the periphery appear in nests or "clones" (i.e., a proliferative response)

Special diagnostic techniques
Histochemical stains demonstrating cartilage matrix degeneration—safranin O/fast green, toluidine blue—may be employed to detect subtle (i.e., early) degenerative lesions that occur in the matrix prior to chondrocyte loss

Differential diagnoses
Degenerative joint disease (DJD)

Comment
The etiopathogenesis is unknown. When occurring in articular joints, the localized degeneration does not appear to progress to degenerative joint disease.

References
Long and Leininger (1999b)

Degenerative joint disease (DJD) (Figures 41, 42, 44)

Other terms used
Osteoarthritis (OA)

Species
Rats and Mice

Affected tissues
Articular cartilage, meniscus, marginal zones, subchondral bone, synovium

Biological behavior
Primary degeneration and gradual loss of articular cartilage leading to secondary bony changes

Histogenesis/Pathogenesis
Primary chondrocyte dysfunction leads to aberrant maintenance of the matrix in articular cartilage. The resulting alterations in the shape and continuity of cartilage surfaces permits the release of pro-inflammatory factors and promotes joint instability, thereby leading to secondary reactions in other joint components.

Diagnostic Features
Macroscopic findings may be absent. Microscopic findings, from least to most severe, include the following primary changes in the articular cartilage:
- Irregular contours of articular surfaces
- Thickening of articular cartilage
- Tinctorial changes in articular cartilage matrix (e.g., focal loss of basophilia in H&E-stained sections, or metachromasia in toluidine blue-stained sections)
- Fibrillation of cartilage matrix; erosion/ulceration of cartilage
- Chondrocytes arranged in closely packed clusters/nests or "clones" (i.e., proliferative response)
- Chondrocyte degeneration and necrosis
- Microfissures in articular cartilage

The gradual progression of the primary cartilage lesion through the entire articular surface leads to involvement of other joint structures and the following secondary morphologic changes:
- Subchondral bone resorption
- Cyst / pseudocyst formation
- Hyperplasia of synovial lining cells
- Thickening and ossification of the joint capsule

Special diagnostic techniques
The biochemical integrity of articular cartilage matrix is assessed by tinctorial changes in its glycosaminoglycan (GAG) content. The most frequently used histochemical stains for this purpose are toluidine blue, safranin O/fast green, and H&E.

Differential diagnoses
Chondromucinous degeneration (an incidental, typically focal change affecting articular cartilage that does not progress to degenerative joint disease)

Comment
The characteristic lesion of DJD is primary degeneration and gradual loss of articular cartilage with secondary thickening of underlying bone, formation of subchondral cysts/pseudocysts, and osteophyte formation. It typically develops as the end-stage lesion for OA, a chronic, disabling condition affecting synovial joints. Although separated from "inflammatory" (e.g., immune-mediated) arthritis to differentiate the condition from rheumatic disease, inflammation and angiogenesis both play a role in the pathogenesis of OA. Species and strain differences, as well as sampling and tissue orientation, influence reporting of this finding in rodents. Optimal fixation, processing, and scoring systems have been established for investigating DJD; the femorotibial joint is most commonly assessed due to its heavy biomechanical load and large expanses of cartilage for evaluation. Morphometry is also an important tool in animal models of OA.

Erosion of the degenerated cartilage as well as secondary bony and soft tissue reactions increase in severity and extent with age. Naturally-occurring DJD occurs in guinea pigs, hamsters, non-human primates and mice. For example, many strains of mice have age-related spontaneous cartilage degeneration that involves the medial side of the knee joint with lesions generally originating in an area not protected by the meniscus. In a few strains, the lateral compartment of the knee is affected. Those lesions progress with age and can be quite severe with areas of full-thickness (i.e., to the tidemark) cartilage degeneration or eburnation (i.e., loss of calcified cartilage and exposure of subchondral bone). In contrast, rats have rare, minor spontaneous cartilage degeneration, generally on the medial side and in an area not protected by the meniscus. Lesions in rats have been reported to begin at approximately 13 months of age.

Unfortunately, the slow onset of natural disease in animals that experience DJD makes them suboptimal models for translational medicine studies. Accordingly, more rapid-onset OA models have been devised in skeletally mature individuals in which a large joint (e.g., generally the femorotibial ["knee"]) space is injected with chondrocyte toxicants to initiate primary cartilage-centered damage or manipulated surgically to promote joint instability capable of accelerating cartilage wear. Conditionally engineered genes that are expressed in chondrocytes and that can be activated in adult animals have been argued to more closely model human disease. Genetically engineered mouse models including knock-in, knock-out, and transgenic animals develop early cartilage degeneration. For example, the Del1 transgenic mouse with deletion mutations in type II collagen develops OA-like lesions by 4 months of age. Regardless of the many available options, no animal models of DJD completely reproduce the human disease.

References

Aigner et al. (2010), Bendele (2001a), Bonnet and Walsh (2005), Gerwin et al. (2010), Glasson (2007), Glasson et al. (2010), Long and Leininger (1999b), Pastoureau et al. (2010), Pritzker (1994), Säämänen et al. (2007), Wancket et al. (2008), Wieland et al. (2005)

Proliferative Lesions

Hyperplasia, synovial cell

Other terms used

Hyperplasia/hypertrophy, synovial cell

Species

Rats and Mice

Affected tissue

Synovium

Biological behavior

Adaptive, non-neoplastic increase in the number of synovial cells

Histogenesis/Pathogenesis

Synovial cells are activated to proliferate in response to injury/irritation in which the responsible stimulus may be present within the joint cavity or alternatively within the synovium

Macroscopic diagnostic features

Macroscopic findings may be absent, but if present the synovial lining will exhibit thickening by multiple, often coalescing, tan/white, firm nodules of variable size

Microscopic diagnostic features

Findings generally include both:

- Hypertrophy (i.e., enlarged cell size)
- Hyperplasia (evident as an increased number of synovial cell layers and/or undulation of the synovium)

Special diagnostic techniques

None

Differential diagnoses

None

Comment

Regardless of its pathogenesis, hyperplasia of synoviocytes, which often is accompanied by hypertrophy of the synovium, is a commonly observed feature of inflammatory and degenerative diseases of the joints in rats and mice. The mechanism(s) by which synoviocytes proliferate remains elusive, even in a disease like RA in which synovial cell hyperplasia is striking. The chemokine- or cytokine-driven activation of signaling pathways that stimulate cell proliferation or result in the expression of anti-apoptotic molecules might be responsible.

References

Leininger and Riley (1990), Long and Leininger (1999b), Wachsmann and Sibilia (2011)

Synovial sarcoma (Figures 45, 46)

Other terms used

None

Species

Rats and Mice

Affected tissue

Synovium

Biological behavior

Malignant tumor that is locally invasive/destructive but generally has a low propensity for metastasis

Histogenesis/Pathogenesis

Although synovial sarcomas are spatially associated with tendon sheaths, bursae, and joint capsules, the exact cell of origin is unclear

Diagnostic features

Synovial sarcomas are morphologically biphasic or monophasic

- Biphasic tumors exhibit dual lines of differentiation (i.e., epithelial cell-like and mesenchymal cell-like elements) within a single neoplasm.
  - o Epithelial cell-like regions are comprised of cuboidal to columnar cells arranged in pseudoglandular formations, clefts, fronds, or solid cords
  - o Mesenchymal cell-like foci contain densely cellular fascicles of spindle cells

- Monophasic tumors have a single (usually epithelial-like) line of differentiation

Special diagnostic techniques

Due to their rarity in rodents, diagnostic markers of synovial sarcoma have not been identified for use in mice and rats

Diagnosis of human synovial sarcomas has been facilitated by immunohistochemical and genetic studies:

- Cell type-specific markers (IHC methods)
  - o Epithelial lineage (partial list)
    - HMW-CK (high-molecular-weight cytokeratin)
    - EMA/MUC1 (epithelial membrane antigen)
  - o Mesenchymal lineages (partial list)
    - MART-1/MLANA (melanoma antigen recognized by T cells 1, a melanocytic differentiation antigen)
    - SMA (smooth muscle actin)
    - DES (desmin)
    - MYOG (myogenin)
    - KIT (CD117, receptor tyrosine kinase)
- Genetic abnormalities
  - o Approximately 90% of human synovial sarcomas exhibit a characteristic chromosomal translocation (i.e., t[x;18][p11.2;q11.2]); a single gene SS18 (*SYT*) has been implicated on 18q11.2
  - o Fluorescence *in situ* hybridization (FISH) analysis for *SYT* gene rearrangement was positive in ≥ 96% of cases of monophasic synovial sarcoma that were evaluated

Differential diagnoses

Fibrosarcoma, Sarcoma NOS (i.e., not otherwise specified)

Comment

Synovial sarcomas have been reported in 0.1% of 2320 male F344/N rats used as untreated controls in approximately 300, 2-year carcinogenesis bioassays conducted by the U.S. National Cancer Institute (NCI) and U.S. National Toxicology Program (NTP). No synovial sarcomas were reported in 2370 female F344/N untreated control rats in that same historical control database. The frequency of spontaneous synovial sarcomas is reported to be very low (i.e., between 0% and 10%) in mice, including the BALB/c strain. Recently, investigators, using a tamoxifen-inducible CreER system in mice, demonstrated that the sporadic expression of the human translocation-derived SYT-SSX2 fusion protein across multiple tissue types led to the exclusive formation of synovial sarcoma-like tumors.

References

Bahrami and Folpe (2010), Haldar et al. (2009), Long and Leininger (1999b), Mouse Tumor Biology Database (MTB) (accessed May 2011), Rosenberg (2010), Stinson (1990), Tanas et al. (2010)

III. Tooth

Normal Rodent Teeth

Teeth are formed by a series of reciprocal inductive phenomena that occur between odontogenic epithelium and mesenchymal cells of the dental papilla and dental follicle. In rodents, crown formation is a continuous process. Crown formation is initiated by the inner dental epithelium of the dental organ. Cells of the inner dental epithelium induce the underlying mesenchymal cells of the dental papilla to differentiate into odontoblasts. Odontoblasts then deposit dentin which has a reciprocal inductive effect on the inner dental epithelial cells, stimulating them to differentiate into ameloblasts and deposit enamel. Rodent incisors have no roots (Figure 47).

Formation of molar roots is initiated by an extension of the dental organ called Hertwig's root sheath, a fusion of the inner and outer dental epithelium. Cells of the root sheath induce the underlying mesenchymal cells to differentiate into odontoblasts and deposit dentin. In response to dentin formation, epithelial cells of the root sheath deposit enamel matrix protein within a thin non-collagenous layer (known as intermediate cementum and afibrillar cementum) along the outer root surface. As the epithelial root sheath involutes or fenestrates, the enamel matrix protein induces adjacent mesenchymal cells to differentiate into cementoblasts and deposit cementum on the root surface.

Rats and mice have only one set of teeth and therefore lack deciduous or temporary teeth. The normal dentition consists of an incisor and three molars in each quadrant, giving a dental formula of 2 (I1/1, M3/3) = 16. Incisors consist of crown only, with extra-alveolar and intra-alveolar parts. In contrast, each molar consists of a crown and roots. The junction between the crown and root is the cervical margin or neck. The clinical term crown refers to the part of the tooth that is visible in the oral cavity. The peridontium is defined as the attachment apparatus of the tooth and consists of cementum, periodontal ligament, the bone lining the alveolus, and the junctional epithelium of the gingiva.

The labial or convex side of the incisors is covered by a layer of enamel. A film of iron is deposited between the dentin and enamel, giving rodent incisors a yellow appearance. The lingual or concave side of the incisors is enamel-free, but does have a very thin layer of cementum into which fibers of the periodontal ligament are embedded. Enamel is not formed over the top of the incisors. Before eruption, the tip is filled with dentin produced by odontoblasts of the pulp. As the tip wears away with use, the odontoblasts form more dentin (secondary dentin) so that the pulp is never exposed. Incisors have a widely open apical foramen. Rodent molars have an enamel-free area on the cusps.

Ameloblasts are columnar epithelial cells responsible for producing enamel. Enamel is usually completely removed during decalcification leaving a clear vacant area in its place; matrix of immature enamel may be visible in some decalcified specimens. Beneath the single row of ameloblasts is a stratified

epithelial layer representing the remainder of the dental organ. Odontoblasts are columnar mesenchymal cells that line the perimeter of the pulp cavity and are responsible for dentin production. Dentin is deposited in an unmineralized form known as predentin, which subsequently mineralizes to form primary dentin. The odontoblasts retreat from the predentin they deposit, gradually encroaching on the pulp cavity. Each odontoblast has a cytoplasmic process extending into the dentin, encased in a dentin tubule that arborizes at the dentin-enamel/intermediate cementum junction. Dentin lacks blood vessels and nerves.

The dental pulp is contained within the pulp cavity and is composed of delicate connective tissue interspersed with small blood vessels, lymphatics, sensory nerves, and primitive connective tissue cells. The apical foramen, at the end of each tooth, allows for passage of blood vessels, and nerves. Progressive narrowing of the molar pulp cavity with age is normal and should not be confused with abnormal development or a test article-induced change.

Cementum is an avascular bone-like material produced by cells of the periodontal ligament, often referred to as cementoblasts. Cementum covers the molar root surfaces and the lingual aspect of the incisors and serves as an anchor for collagen fibers, also known as Sharpey's fibers. Sharpey's fibers are embedded in both cementum and alveolar bone that lines the alveolus (tooth socket). Cementum is thickest at the apex of the tooth and gradually thins as it extends coronally. Microscopically, two forms of cementum exist. One form is cellular and the other is acellular. Cellular cementum predominates along the apex of the root and acellular cementum predominates along the coronal aspect of the root with the two blending imperceptibly. Progressive thickening of the cementum layer with age is normal and should not be confused with abnormal development or a test article-induced change.

References

Ahmad and Ruch (1987), Hay (1961), Kuijpers et al. (1996)

Nonproliferative Lesions

Degeneration (Figure 48)

Other terms used

None

Species

Rats and Mice

Biological behavior

Attenuation of cells from tooth structure

Histogenesis/Pathogenesis

Altered cytoarchitecture and function of cells, potentially reversible, typically due to unknown metabolic or toxic insults

Diagnostic features

- Focal or diffuse loss of cells
- Loss of ameloblasts may be associated with irregularities in the contour of the enamel or enamel may be abnormal in appearance or diminished in amount (difficult to determine in decalcified sections)
- Focal or diffuse loss or attenuation of odontoblasts may be associated with irregularities in the contour of the dentin or the dentin may be abnormal in appearance or diminished in amount

Differential diagnoses

- Necrosis – usually accompanied by nuclear pyknosis, karyorrhexis, cellular debris, and inflammation

Comment

Ameloblasts are columnar epithelial cells responsible for the production of enamel. Enamel is not usually seen in decalcified sections because it is 95% mineral, and most is removed during the decalcification process. A clear vacant area, the enamel space, is usually present in place of existing enamel. Beneath the single row of ameloblasts is a stratified epithelial layer representing the remainder of the dental organ. Loss or degeneration of ameloblasts may be diffuse or focal, resulting in irregularities in the ameloblast layer. Enamel formation (or lack of formation) mirrors the changes in the ameloblast layer and therefore may also appear irregular in contour. In chronic fluorosis, loss of ameloblasts may be accompanied by flattening of the underlying stratum intermedium, herniation of ameloblasts into the enamel, and inclusions of enamel within the ameloblastic layer.

Basophilic granules/bodies noted in teeth (or bones) from fluoride-treated rats are reported to represent decalcification-related precipitation artifact (calcium fluoride crystal formation), not pathology. Similar structures can form as a precipitate in normal bone following decalcification if fluoride is added to the fixative and also as a precipitation artifact during decalcification of bone from animals dosed with fluoride/fluoride-containing chemicals, in which case the precipitation artifact may appear dose-related. Regardless of the presence/absence of fluoride, to confirm this as artifact one could prepare undecalcified sections (could be ground or thin sections) and examine them unstained and stained. If the pigment/structures are not present in undecalcified sections, then this is solid proof that they occurred as an artifact during decalcification.

Degenerative changes in ameloblasts have also been described in rats following administration of puromycin and tetracycline hydrochloride. In addition, colchicine (which disrupts microtubule formation) is reported to disrupt enamel formation and pigmentation.

Odontoblasts are columnar mesenchymal cells that line the perimeter of the pulp cavity and are responsible for dentin

formation. A sharp line of demarcation separates the uncalcified predentin from the calcified dentin. Degeneration of odontoblasts may be subtle with minimal irregularity in dentin formation, or it may be more pronounced with displacement of odontoblasts leading to displaced dentin production within the pulp. Complete infarction (i.e., coagulative necrosis) of odontoblasts with failure to form dentin is possible in the absence of damage to other adjacent cell types.

References
Bucher et al. (1991), Hashimoto (1984), Lindemann and Nylen (1979), Long and Leininger (1999a), Maurer et al. (1990), Maurer et al. (1993), Weinstock (1970), Westergaard (1980)

Necrosis (Figure 48)

Other terms used
None

Species
Rats and Mice

Biological behavior
Regional, non-neoplastic loss of multiple cells/tissues within the tooth structure

Histogenesis/Pathogenesis
A local insult of aseptic or septic nature that disrupts the function and precludes the survival of injured cells within the region

Diagnostic features
- Pyknosis, karyorrhexis, and karyolysis of nuclei (or presence of ghost cells if the lesion is of the coagulative type)
- May be accompanied by an acute inflammatory response
- May be accompanied by cell debris and/or small cavities

Differential diagnoses
- Postmortem autolysis – uniform dissolution of the entire tissue section with no change in organization or depth of cell layers

Comment
Necrosis is most often seen within the pulp chamber. Common causes include fracture and infection. Coagulative necrosis can occur secondary to thrombosis of pulp vessels.

References
Bucher et al. (1991), Long and Leininger (1999a), Maurer et al. (1993)

Periodontal pocket (Figure 49)

Other terms used
None

Species
Rats and Mice

Affected structures
Spaces between the teeth and the periodontium (especially near upper molar teeth)

Biological behavior
Presence of foreign bodies within spaces, sometimes with regional secondary inflammation

Histogenesis/Pathogenesis
The lesion arises from impaction of hair, feed, and/or bedding material around teeth/within periodontium

Diagnostic features
- Dilation/expansion of periodontium (especially near upper molars in rodents)
- Impacted hair, feed, and/or bedding material (sometimes including bacterial colonies) within the widened spaces or adjacent connective tissue
- Secondary inflammation may be evident (generally viable or degenerating neutrophils within the periodontal spaces and/or adjacent connective tissue)
- Severe lesions may be associated with erosion of the bony sockets

Differential diagnoses
- Cyst – discrete membrane-lined, fluid-filled cavity that does not contain hair, feed, or bedding material

Comment
Communication of the periodontal pocket with the oral cavity may not be apparent due to the plane of section.

References
Losco (1995), Sakura (1997)

Dentin niches (Figures 50, 51)

Other terms used
None

Species
Rats and Mice

Biological behavior
Non-neoplastic developmental defect

Histogenesis/Pathogenesis
Focal or multifocal failure of odontoblasts to form dentin

Diagnostic features
- Focal or multifocal recesses within the dentin
- May be bilaterally symmetrical

Differential diagnoses
- Decreased dentin – affects the entire tooth

Comment
Odontoblast degeneration and subsequent failure to form dentin is an occasional focal or multifocal process that may result in the formation of recesses within the dentin.

References
Long et al. (2004)

Dentin, decreased

Other terms used
None

Species
Rats and Mice

Biological behavior
Non-neoplastic developmental defect

Histogenesis/Pathogenesis
Generalized failure of odontoblasts to form dentin

Diagnostic features
- Entire tooth wall is abnormally thin
- May be bilateral

Differential diagnoses
- Dentin niche – focal or multifocal recess within the dentin

Comment
A decrease in odontoblast activity may result in decreased dentin formation resulting in a tooth (usually an incisor) in which the entire wall is abnormally thin. These teeth are susceptible to fracture.

Dentin matrix alteration (Figure 52)

Other terms used
None

Species
Rats and Mice

Biological behavior
Non-neoplastic developmental defect

Histogenesis/Pathogenesis
Odontoblasts form abnormal dentin

Diagnostic features
- Dentin appears abnormal (i.e., tubules may be arranged in disorderly fashion)
- Dentin may contain trapped cells or inclusions

Differential diagnoses
- Dysplasia – aberrant development of odontogenic tissues, characterized by irregular mass of dentin-like material surrounded by fragments of the original tooth and small islands of bone. Displaced odontogenic tissues may form tooth-like structures (denticles) in the adjacent connective tissue, in which tissue resembling the dental papilla may also form, but these tend to remain relatively small and solitary. The change usually is associated with injury/fracture.

Comment
Odontoblast degeneration and subsequent attempts at repair may result in alterations in the appearance of dentin. Such alterations, although secondary, may be noteworthy.

References
Hashimoto (1984), Lindemann and Nylen (1979), Maurer et al. (1990), Weinstock (1970), Westergaard (1980)

Dental dysplasia (Figure 53)

Other terms used
None

Species
Rats and Mice

Affected structures
Primarily incisor teeth

Biological behavior
Non-neoplastic developmental defect

Histogenesis/Pathogenesis
Abnormal development of odontogenic tissues

Diagnostic features
- Tooth socket may become partly filled with an irregular mass of dentin-like material surrounded by fragments of the original tooth and small islands of bone
- Displaced odontogenic tissues may form tooth-like structures (denticles) in the adjacent connective tissue, in which tissue resembling the dental papilla may also form, but these tend to remain relatively small and solitary
- Often associated with injury/fracture
- May exhibit cytologic overlap with odontoma (see definition below)

Differential diagnoses
- Odontogenic neoplasia – space-occupying masses associated with unregulated proliferation (± matrix production) by one or more odontogenic cell lineages

Comment

Incisors grow throughout life in rodents. This characteristic coupled with infection, chronic inflammation, nutritional/metabolic/vascular alterations, and injury/fracture can result in abnormal development of odontogenic tissues at any time during the animal's life span. The appearance of such lesions can vary considerably depending on the nature and extent of injury, the tissues affected, and the plane of section. Alveolar bone, cementum, dentin, enamel, and/or connective tissue resembling that of the dental papilla may develop in various combinations and abnormal patterns.

References

Long and Leininger (1999a), Losco (1995)

Fracture

Other terms used

None

Species

Rats and Mice

Affected structures

Primarily incisor teeth

Biological behavior

Disruption of tooth structural integrity

Histogenesis/Pathogenesis

Discontinuity ("break") in the tooth, chiefly due to mechanical trauma

Diagnostic features

- Histology is influenced by mechanical stability and the amount of time since the fracture occurred
- May see inflammation and/or reactive osteodentin formation within the pulp
- May be accompanied by dysplasia if dental organ of incisor is injured or displaced

Differential diagnoses

- Dental dysplasia – aberrant development of odontogenic tissues without an accompanying fracture.
- Odontogenic neoplasia – space-occupying masses associated with unregulated proliferation (± matrix production) by one or more odontogenic cell lineages

Comment

Fractures are usually accompanied by some form of dental dysplasia (abnormal development). Given that most teeth are cross-sectioned, actual breaks may not be easily identified. In some cases, fracture and dysplasia may be evident, in which case diagnoses of both fracture and dysplasia would be appropriate.

References

Long and Leininger (1999a), Kuijpers et al. (1996)

Resorption

Other terms used

None

Species

Rats and Mice

Affected structures

Any tooth

Biological behavior

Non-neoplastic loss of tooth mass

Histogenesis/Pathogenesis

Osteoclastic resorption of dental hard tissues

Diagnostic features

- Abnormal resorption/removal of dental hard tissues (cementum/dentin)
- May be accompanied by inflammation, fracture, and/or ankylosis (fusion of alveolar bone to cementum or dentin of the affected tooth)

Differential diagnoses

- Dentin niche – focal or multifocal defect in dentin formation
- Decreased dentin – widespread defect in dentin formation

Comment

Resorption of dental hard tissues (cementum and/or dentin, and possibly including the bone of the tooth socket) commonly is initiated by primary factors including malocclusion, infection/inflammation, and trauma/injury. Resorption may progress to complete loss of the tooth and replacement with fibrous connective tissue. In other cases, resorption may be accompanied by abnormal development of remaining viable odontogenic tissue (see dental dysplasia).

References

Long and Leininger (1999a)

Denticle(s) (Figure 54)

Other terms used

None

Species

Rats and Mice

Affected structures

Primarily incisor teeth

Biological behavior

Abnormal formation of small tooth-like entities

Histogenesis/Pathogenesis
These lesions arise from folds/outcroppings in the epithelial root sheath that are shed into the pulp cavity

Diagnostic features
- Round to slightly oval structures within the pulp
- Comprised of dentin with dentin tubules
- Center appears hollow but may contain ameloblasts or fragments of ameloblasts
- Outer margin may or may not be lined with odontoblasts
- May collide with inner wall of tooth where they may be associated with irregularities in the contour of the dentin along the inner margin of the pulp cavity
- May become incorporated into the wall of the tooth

Differential diagnoses
- Pulp concretions – concentric layers of mineralized tissue around dead/injured cells or collagen fibers.

References
Long and Herbert (2002)

Pulp concretion

Other terms used
Pulp stone

Species
Rats and Mice

Affected structures
Primarily incisor teeth

Biological behavior
Repair process

Histogenesis/Pathogenesis
Mineral deposition around dead/injured cells or collagen fibers

Diagnostic features
- Mineralized tissue forms around dead/injured cells or degenerating collagen fibers
- Mineral is deposited in irregular linear or concentric layers

Differential diagnoses
- Denticle(s) – round to slightly oval structures within the pulp comprised of dentin with dentin tubules, in which the hollow center may contain ameloblasts but the outer margin may or may not be lined with odontoblasts

Comment
Pulp concretions (single or multiple) represent areas of dystrophic mineralization.

References
Long and Herbert (2002)

Cyst(s) (Figure 55)

Other terms used
None

Species
Rats and Mice

Affected structures
Any tooth

Biological behavior
Non-neoplastic, space-occupying cavity

Histogenesis/Pathogenesis
Unknown

Diagnostic features
- Discrete membrane-lined, fluid-filled cavity
- Typically located near the apex of the affected tooth

Differential diagnoses
None

References
Long and Leininger (1999a)

Thrombus

Other terms used
None

Species
Rats and Mice

Affected structures
Vessels of tooth pulp and alveolus

Biological behavior
Transient occlusion (partial or complete) of regional vessels

Histogenesis/Pathogenesis
Activation of the clotting cascade (typically due to systemic rather than local factors)

Diagnostic features
- Granular or laminated and partly organized mass of fibrin and thrombocytes (platelets) within a vessel lumen
- Contains variable numbers of erythrocytes and leukocytes
- May or may not be associated with hemorrhage in nearby tissues

Differential diagnoses
- Postmortem clot – intravascular mass of fibrin and platelets containing few or no leukocytes and with lamination either absent or present as very fine filaments

Comment
Thrombosis of pulp blood vessels has been reported in incisors from rats treated with 2-butoxyethanol. Thrombosis may result in coagulative necrosis of odontoblasts and/or pulp mesenchymal cells.

References
Long et al. (2000)

Proliferative Lesions

Odontoma (Figure 56)

Other terms used
None

Species
Rats and Mice

Biological behavior
Hamartoma (developmental malformation comprised of a disorganized mass of normal tissue elements)

Histogenesis/Pathogenesis
Epithelial cells (ameloblasts) and ectomesenchymal cells (odontoblasts, cementoblasts) of the tooth germ

Diagnostic features
The diagnosis depends on the degree of morphologic differentiation:
- Common features
  - All dental hard tissues (enamel, dentin and cementum as well as odontoblasts, cementoblasts and dental pulp mesenchymal cells) are present
  - Absence of distinct areas of ameloblastic (ameloblastoma-like) epithelium unassociated with dental hard tissues
  - Not uncommonly associated with an unerupted tooth
- Variants
  - Complex odontoma
    - dental tissues show a characteristic poor morphologic differentiation
    - little resemblance to normal teeth
  - Compound odontoma
    - dental tissues exhibit a high degree of morphologic differentiation and histodifferentiation resembling that of normal teeth
    - usually presents as a small and well-circumscribed lesion

Differential diagnoses
- Ameloblastoma – a neoplasm that does not produce dental hard tissues. Radiographs (if available) reveal a radiolucent lesion.
- Ameloblastic Odontoma – a neoplasm that has proliferating ameloblastoma-like epithelium in the tumor periphery that is unassociated with dental hard tissues and often shows aggressive behavior
- Fibroma, odontogenic – a neoplasm composed of dental follicle-like mesenchyme (i.e., enamel and dentin do not form)
- Dental dysplasia – abnormal development, usually involving inflamed or traumatized incisor teeth, that consists mainly of dentin-like material but which may contain other odontogenic tissues

Comment
Complex as well as compound odontomas are considered to be malformations (hamartomas) rather than true neoplasms, although they have also been described to be chemically inducible by application of different *N*-nitrosourea derivatives. The odontogenic tumors described by Nozue and Kayano (1978) and by Goessner and Luz (1994) are considered to represent odontomas rather than dentinomas. Odontomas of the jaws may be diagnosed as "cementomas", when cementum-like bony substance is present. If the cementum-like structures are surrounded by fibrous tissue with cementoblasts, such tumors may be diagnosed as "cementoblastomas."

References
Berman and Rice (1980), Dayan et al. (1994), Eisenberg et al. (1983), Ernst and Mohr (1991), Finkel et al. (1979), Gibson et al. (1992), Goessner and Luz (1994), Humphreys et al. (1985), Kimura et al. (2012), Long et al. (1993), Long and Leininger (1999a), Nozue and Kayano (1978), Rivenson et al. (1984), Robins and Rowlatt (1971), Smulow et al. (1983), Sokoloff and Zipkin (1967), Stoica and Koestner (1984)

Ameloblastic odontoma (Figure 57)

Other terms used
Odontoameloblastoma

Species
Rats and Mice

Biological behavior
Benign but locally aggressive neoplasm

Histogenesis/Pathogenesis
Epithelial cells (ameloblasts) and ectomesenchymal cells (odontoblasts, cementoblasts) of the tooth germ

Diagnostic features

- Usually well-circumscribed, concentrically growing tumor
- Different degrees of morphologic differentiation ranging from primitive tooth buds to mature tooth structures
- All dental tissues are found including ameloblastic epithelium, stellate reticulum-like cells, enamel matrix, enamel, dentin, odontoblasts, cementum, cementoblasts and pulpal tissue
- The proliferating ameloblastic (ameloblastoma-like) epithelium is located in the tumor periphery and contains no or minimal amounts of dental hard tissues
- Formation of the dental hard tissues occurs within the central areas of the tumor
- Degenerating keratinized ("ghost cells") and calcified odontogenic epithelium may also be observed
- Formation of reactive multinucleated giant cells within the tumor tissue in response to accumulation of keratin debris may occur
- Ameloblastic odontomas usually are locally aggressive (invasive and destructive) but do not metastasize
- One variant (ameloblastic fibro-odontoma) exhibits substantial proliferation of fibroblasts in association with the tissues derived from teeth

Differential diagnoses

- Ameloblastoma – a neoplasm that does not produce dental hard tissues. Radiographs (if available) reveal a radiolucent lesion.
- Odontoma (complex or compound) – a developmental malformation (hamartoma) consisting of differentiated mineralized dental hard tissues, which do not contain significant amounts of ameloblastic (ameloblastoma-like) epithelium that is not associated with dental hard tissues
- Fibroma, odontogenic – a neoplasm composed of dental follicle-like mesenchyme (i.e., enamel and dentin do not form)
- Dental dysplasia – abnormal development, usually involving inflamed or traumatized incisor teeth, that consists mainly of dentin-like material but which may contain other odontogenic tissues

Comment

Spontaneous ameloblastic odontomas are rare in rats and mice. They are, however, chemically inducible by application of different *N*-nitrosourea derivatives. Similar "odontogenic tumors" have been observed in genetically altered mice carrying albumin-Myc (*Alb-Myc*) and albumin-Ras (*Alb-Ras*) transgenes.

References

Barbolt and Bhandari (1983), Berman and Rice (1980), Boorman and Hollander (1973), Eisenberg et al. (1983), Ernst and Mohr (1991), Fitzgerald (1987), Long et al. (1993), Rivenson et al. (1984), Smulow et al. (1983), Stoica and Koestner (1984), Wang et al. (1975)

Ameloblastoma (Figure 58)

Other terms used

None

Species

Rats and Mice

Biological behavior

Benign but locally aggressive neoplasm

Histogenesis/Pathogenesis

Epithelium of dentigerous cysts; remnants of the dental lamina and of the enamel organ; basal cell layer of the oral mucosa

Diagnostic features

- Usually large and concentrically growing tumor which is locally invasive and destructive but which does not metastasize
- Composed of islands (follicular type), nests or anastomosing strands (plexiform type) of epithelial cells embedded in a collagenous stroma
- Epithelium consists of a peripheral layer of tall columnar cells resembling the inner enamel epithelium and loosely arranged central cells similar to stellate reticulum
- The epithelial islands may be solid (solid type) or may show degenerative changes in the stellate cells resulting in cyst formation (cystic type)
- The stroma may be focally hyalinized, but dental hard tissues (enamel, dentin, or cementum) are not produced
- In one variant (acanthomatous ameloblastoma), epithelial cells of the stellate reticulum may undergo squamous metaplasia

Differential diagnoses

- Ameloblastic Odontoma – the proliferating ameloblastic (ameloblastoma-like) epithelium is located in the tumor periphery and contains no or minimal amounts of dental hard tissues. Formation of the dental hard tissues occurs within the central areas of the tumor. Often shows aggressive behavior
- Fibro-odontoma, ameloblastic – a mouse-specific non-aggressive neoplasm of odontogenic epithelium in which formation of hard dental tissues does occur
- Odontoma (complex or compound) – a developmental malformation (hamartoma) consisting of differentiated mineralized dental hard tissues, which do not contain significant amounts of ameloblastic (ameloblastoma-like) epithelium
- Fibroma, odontogenic – a neoplasm composed of dental follicle-like mesenchyme (i.e., enamel and dentin do not form)

Comment

Spontaneous ameloblastomas are extremely rare in rats and mice. In rats, they are chemically inducible by appli-

cation of different *N*-nitrosourea derivatives. Ameloblastoma-like tumors (ameloblastic carcinoma, adamantoblastoma) have been induced in mice by polyoma virus and by local application of 3-methylcholanthrene.

References

Berman and Rice (1980), Dawe et al. (1959), Ernst and Mirea (1995), Goessner and Luz (1994), Gollard et al. (1992), Greene et al. (1960), Lewis et al. (1980), Long and Leininger (1999a), Long et al. (1993), Pearl and Takei (1981), Smulow et al. (1983), Stanley et al. (1965), Stanley et al. (1964), Van Rijssel and Mühlbock (1955), Zegarelli (1944)

Odontogenic fibroma (Figure 59)

Other terms used

None

Species

Rats and Mice

Biological behavior

Benign but locally expansile neoplasm

Histogenesis/Pathogenesis

Mesenchymal cells of the periodontal ligament or of the developing dental apparatus, the dental papilla or dental sac

Diagnostic features

- Well-circumscribed expansile tumor usually associated with the pulp of a continuously erupting incisor tooth
- Mainly composed of cellular whorls of primitive-appearing dental follicle-like mesenchyme separated by distinct areas of collagen formation
- Strands and islands of non-neoplastic, small and mostly undifferentiated epithelial cells, representing rests of the dental epithelium, are scattered throughout the tumor
- Epithelial nests consisting of squamous cells and ghost cells are occasionally seen
- Formation of round or irregular foci of cementum-like material can also be observed within the mesenchymal tissue

Differential diagnoses

- Ameloblastoma – a neoplasm in which cuboidal to columnar ameloblastoma-like epithelium encloses a stellate reticulum
- Ameloblastic Odontoma – a neoplasm that has proliferating ameloblastoma-like epithelium in the tumor periphery that is associated with dental hard tissues and often shows aggressive behavior
- Fibro-odontoma, ameloblastic – a mouse-specific non-aggressive neoplasm of odontogenic epithelium in which formation of hard dental tissues does occur
- Odontoma (complex or compound) – a developmental malformation (hamartoma) consisting of differentiated mineralized dental hard tissues
- Fibroma, odontogenic – a neoplasm composed of dental follicle-like mesenchyme (i.e., enamel and dentin do not form)

Comment

Spontaneous odontogenic fibromas have been reported in rats and mice. Odontogenic tumors with similar morphological features have been induced in Fischer rats by feeding of aflatoxins and an agar-based diet, but they were not classified as odontogenic fibromas.

References

Cullen et al. (1987), Ernst et al. (1998), Goessner and Luz (1994), Long and Leininger (1999a)

Cementifying/ossifying fibroma (Figures 60, 61)

Other terms used

None

Species

Mice

Affected structures

Mandible or maxilla, commonly near incisor teeth

Biological behavior

Benign but locally expansile neoplasm

Histogenesis/Pathogenesis

Pluripotential mesenchymal stem cells, osteoblasts (cementoblasts)

Diagnostic features

- Well-demarcated tumor
- Appearance is suggestive of a fibroma in which bone/cementum forms by osseous metaplasia of the fibrous connective tissue component
- The proliferating component consists of spindle cells resembling fibroblasts that undergo transformation to cuboidal osteoblasts/cementoblasts and form multiple rounded cementicle-like bodies or cementum-like trabeculae with blue-staining borders.
- Cell processes run perpendicular to the hard-tissue surface
- Bone spicules are composed almost entirely of woven bone
- Bone spicules often appear as letter-like “C” and “Y” profiles
- Usually separated from surrounding tissue by a thin shell of newly-formed cortical bone
- Low number of mitotic figures

Differential diagnoses

- Fibro-osseous lesion (FOL) – a mouse-specific lesion that is distinguishable by the heterogeneous cell population and absence of any morphologic criteria consistent with tumor
- Osteoma – a benign bone tumor that lacks any spindle cell stroma
- Osteofibroma – a benign tumor with fewer spindle cells, less fibrous tissue, and lacking bony trabeculae
- Osteosarcoma – a malignant neoplasm exhibiting a low degree of tissue differentiation (immature or atypical bone) and highly infiltrative growth

Comment

Spontaneous ossifying fibromas are rare in mice and occur in the mandible or maxilla. They often contain cementicles (oval to round, mineralized tooth-like structures comprised chiefly of cementum) and are considered to originate from the periodontal membrane.

References

Faccini et al. (1990), Long and Leininger (1999a), Luz et al. (1991b), Nilsson and Stanton (1994)

Tumor, odontogenic, benign

Other terms used

None

Species

Rats and Mice

Biological behavior

Benign neoplasm

Histogenesis/Pathogenesis

Epithelial and/or ectomesenchymal cells of the tooth germ

Diagnostic features

- Odontogenic structures are present.

Comment

This general diagnosis may be applied for benign odontogenic tumors, which are not otherwise specifiable as one of the particular odontogenic tumor categories listed above.

Tumor, odontogenic, malignant

Other terms used

None

Species

Rats and Mice

Biological behavior

Malignant neoplasm

Histogenesis/Pathogenesis

Epithelial and/or ectomesenchymal cells of the tooth germ

Diagnostic features

- Odontogenic structures are present

Comment

This general diagnosis may be applied for malignant odontogenic tumors, which are not otherwise specifiable as one of the particular odontogenic tumor categories listed above.

Acknowledgements

The authors wish to express their sincere appreciation to Drs. Jerrold Ward, Bing Ong, Andrew Suttie, Armando Irizarry, Thomas J. Wronski, Diane Gunson, Ken Frazier, and John Sundberg for contributing images, and to Dr. Robert Maronpot for his critical review of the bone portion of this document.

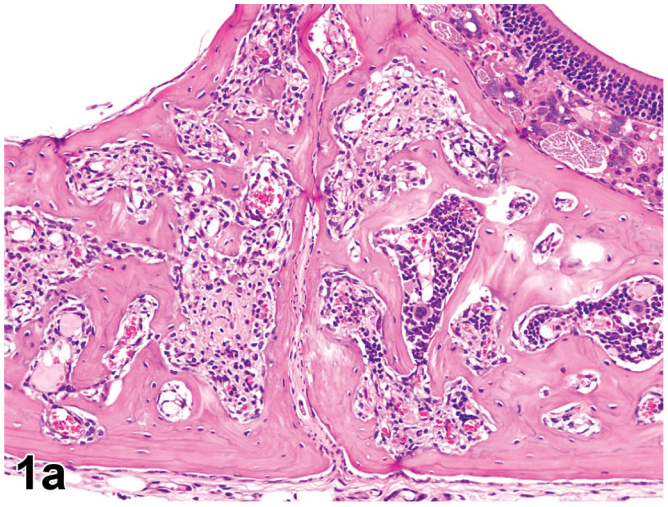

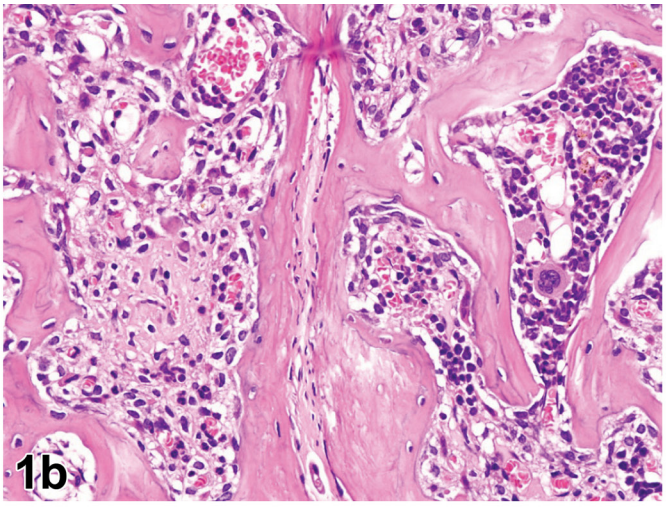

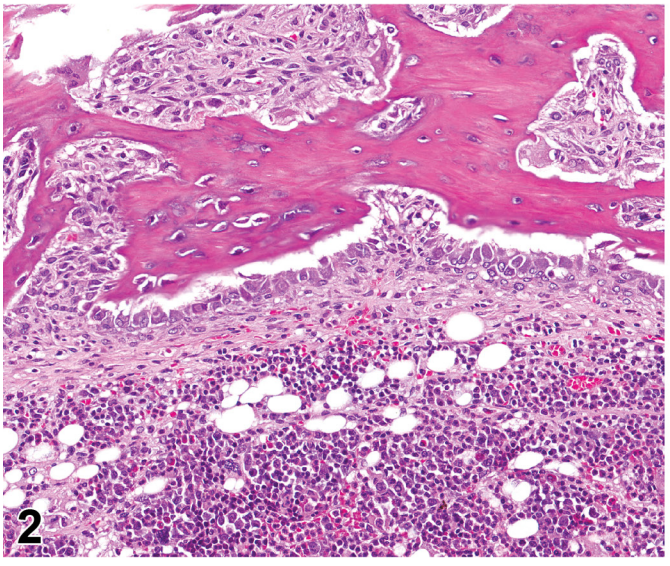

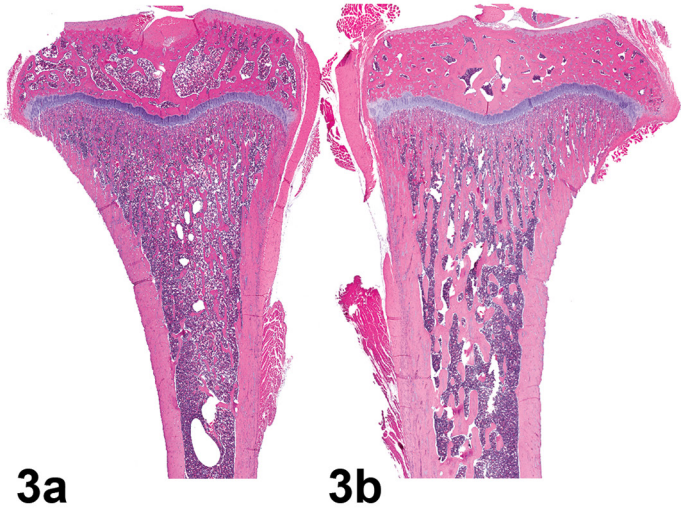

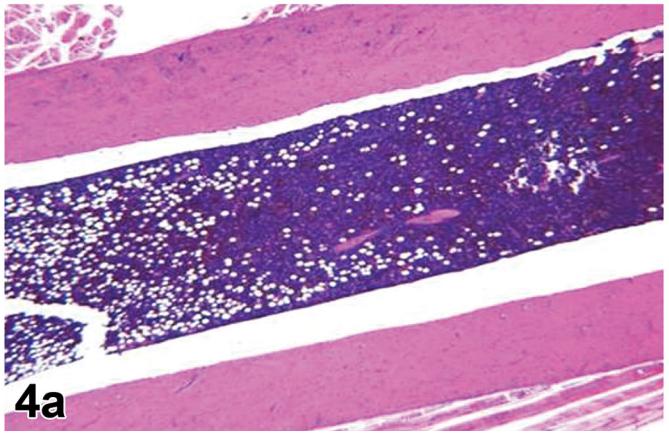

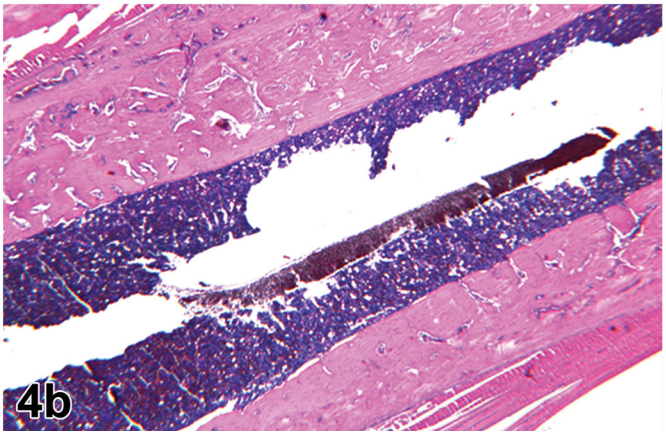

Figure 1. — Fibro-osseous lesion (FOL), skull, mouse. Localized increases of bone trabeculae and osteoclasts with fibrous stroma proliferation within the marrow cavity. (A) Low magnification, (B) Higher magnification. Decalcified bone, H&E. Images courtesy of Dr. Jerrold Ward.

Figure 2. — Fibrous osteodystrophy (FOD), rat. Dense peri-trabecular fibrosis with prominent osteoblast rims along some bone surfaces (lower middle) and increased scalloping (erosion in shallow depressions [Howship's lacunae]) associated with osteoclasts along other surfaces (upper middle). Decalcified bone, H&E. Image courtesy of Dr. Andrew Suttie.

Figure 3. — Increased bone, trabeculae, tibia, rat that had been given an anti-sclerostin antibody. Increased bone is characterized by trabecular hypertrophy (expanded thickness) in the metaphysis (B) compared to an untreated rat (A). Decalcified bone, H&E.

Figure 4. — Increased bone, cortex, diaphysis of a long bone, rat (B). The cortex is thicker relative to that of normal cortex in a rat long bone (A). Decalcified bone, H&E.

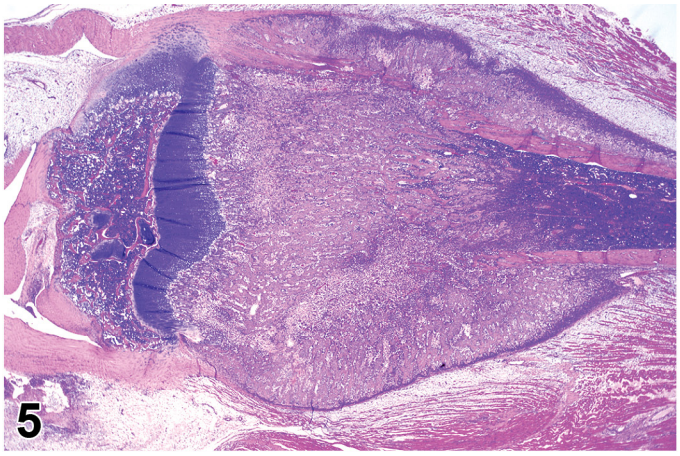

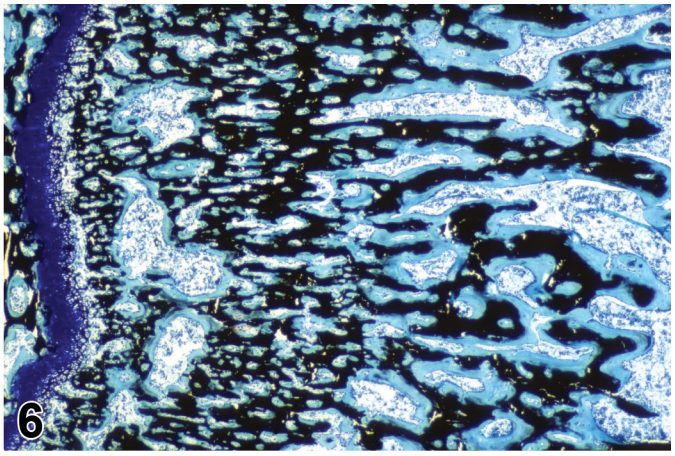

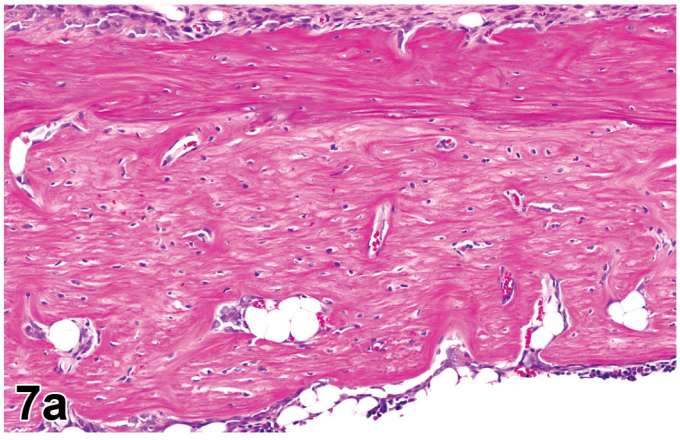

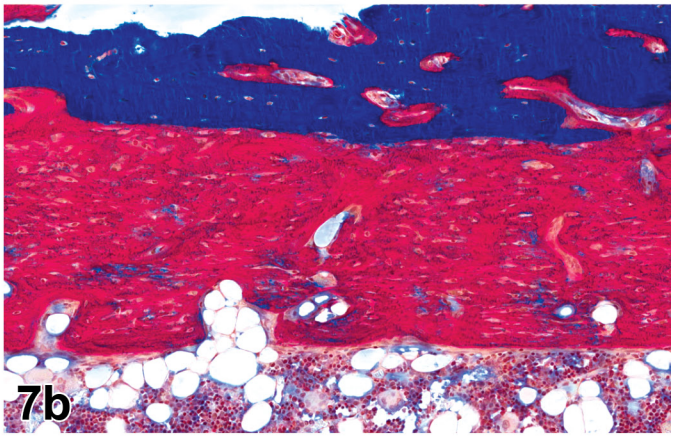

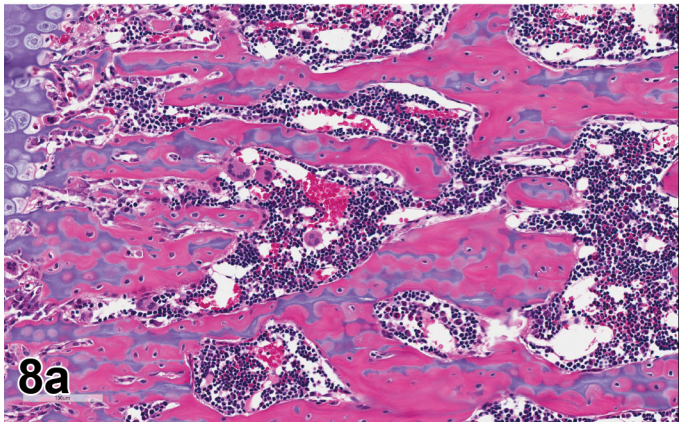

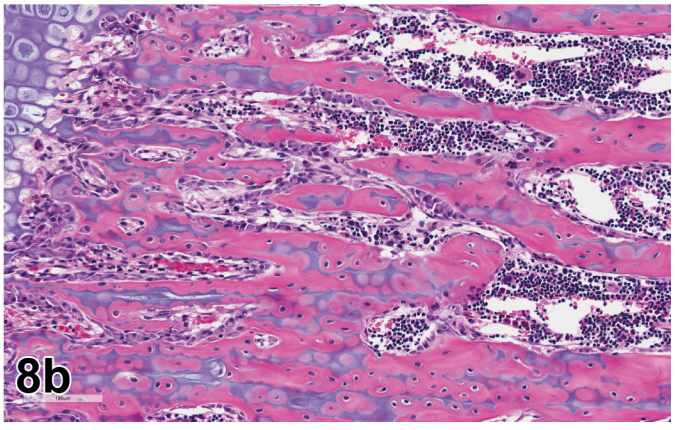

FIGURE 5. — Increased bone, periosteum and endosteum, metaphysis, tibia, rat. Decalcified bone, H&E. Image courtesy of Dr. Bing Ong.

FIGURE 6. — Increased osteoid, tibia, rat, following administration of high doses of 1,25 dihydroxy vitamin D_3. Abundant accumulation of osteoid (pale blue) lining the mineralized (black) matrix in trabeculae of the primary spongiosa in the metaphysis. Undecalcified section, von Kossa/MacNeal's tetrachrome.

FIGURE 7. — Increased osteoid, cortex, tibia, rat. The increase is evident as a thick plaque of pale eosinophilic woven bone (A, decalcified bone, H&E) or bright red woven bone (B, undecalcified bone, modified trichrome) adjacent to the bone marrow.

FIGURE 8. — Increased osteoblastic surface, tibia, rat. Increased surface extent of osteoblasts, interpreted to be active in matrix synthesis, along the trabeculae of the primary spongiosa in a rat given recombinant human parathyroid hormone (PTH) (B), compared to control (A). Decalcified bone, H&E.

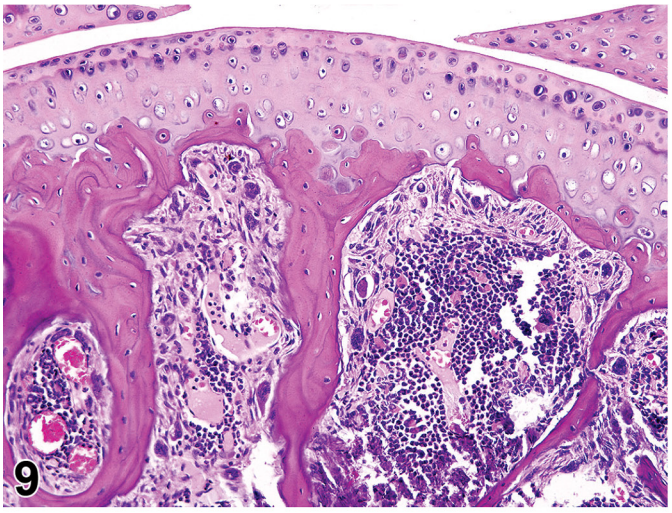

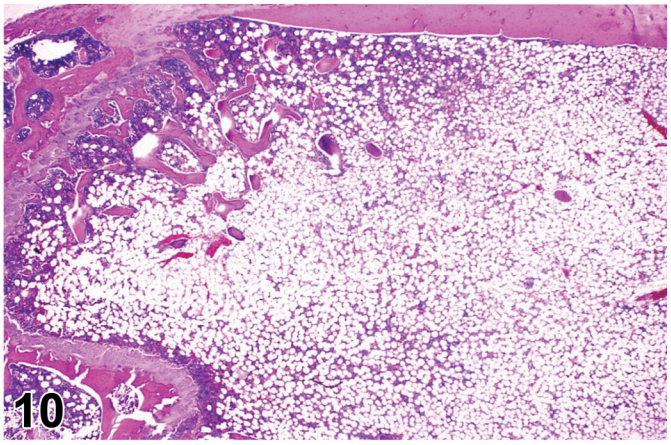

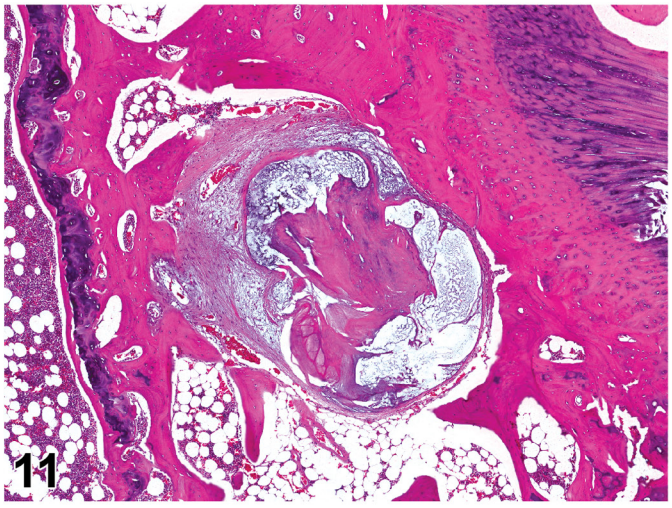

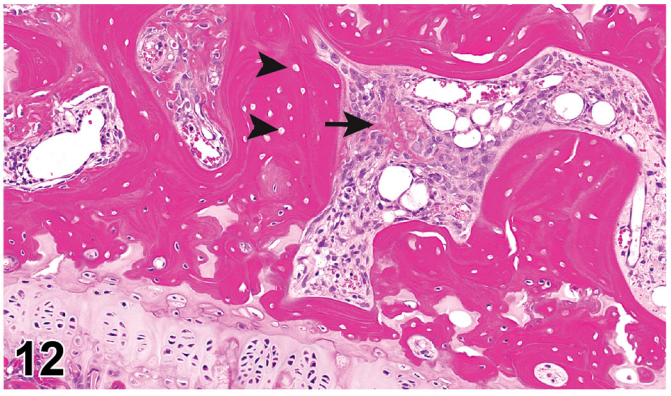

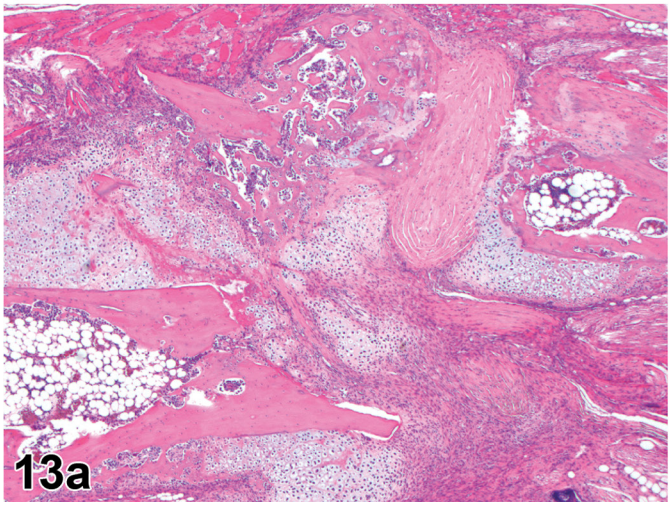

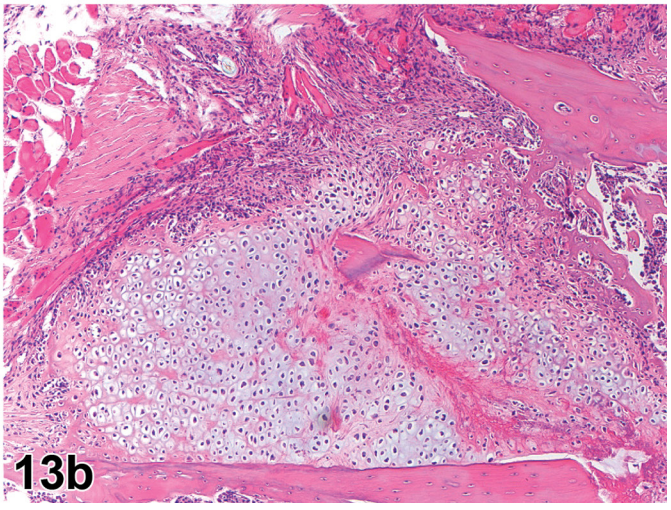

FIGURE 9. — Increased osteoclasts with fibrosis, genetically engineered mouse. Both changes follow the trabecular surfaces; the osteoclasts are very large, multinucleated elements with basophilic cytoplasm. Decalcified bone, H&E. Image courtesy of Dr. Jerrold Ward.

FIGURE 10. — Decreased bone, metaphysis, distal femur, rat. Both the number and size of trabeculae in the primary spongiosa are reduced markedly. Decalcified bone, H&E.

FIGURE 11. — Cyst, bone, rat. The cavity is lined by a continuous membrane (visible as a thin eosinophilic layer) while the wall is expanded by fibrous connective tissue. Decalcified bone, H&E. Image courtesy of Dr. Andrew Suttie.

FIGURE 12. — Necrosis, femoral head, rat. Empty osteocyte lacunae (arrowheads) are numerous in epiphyseal trabecular bone, while reactive woven bone (arrow) in the adjacent viable marrow is indicative of a tissue response. Decalcified bone, H&E.

FIGURE 13. — Fracture with callus, vertebrae of tail, mouse. (A) Lower magnification, (B) Higher magnification. The proliferating cartilage forms multiple, coalescing, pale blue nodules (center) spanning the gap between the ends of the displaced bone fragments. The sharp bony margins visible along the fracture line indicate that bony remodeling has yet to begin in earnest. Decalcified bone, H&E.

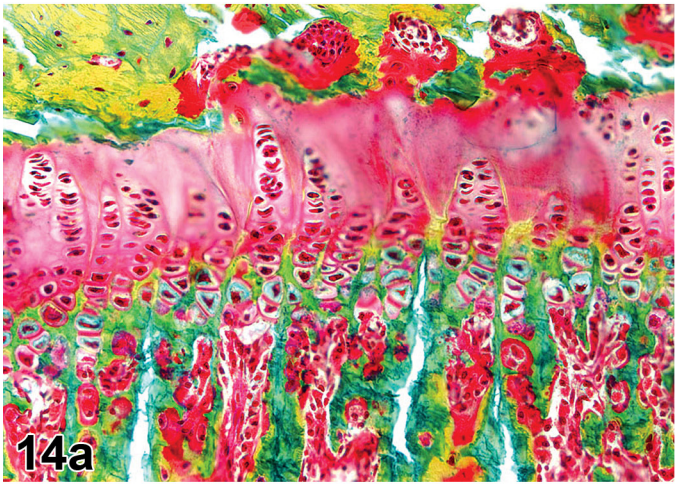

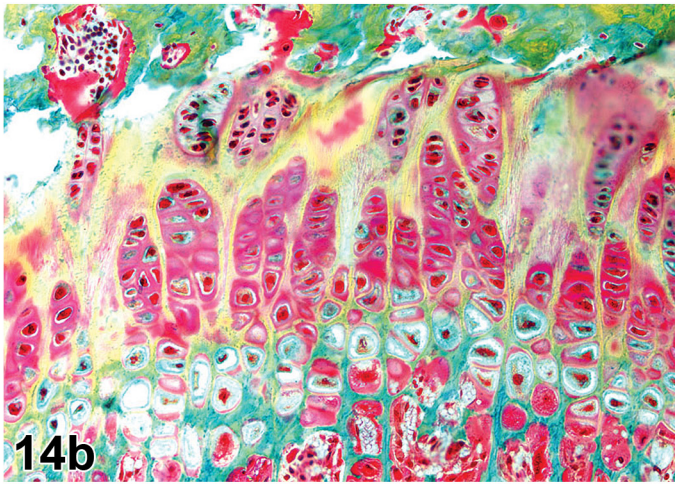

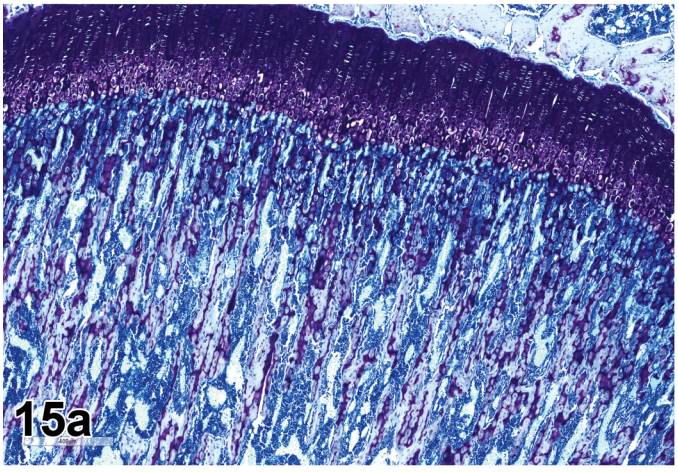

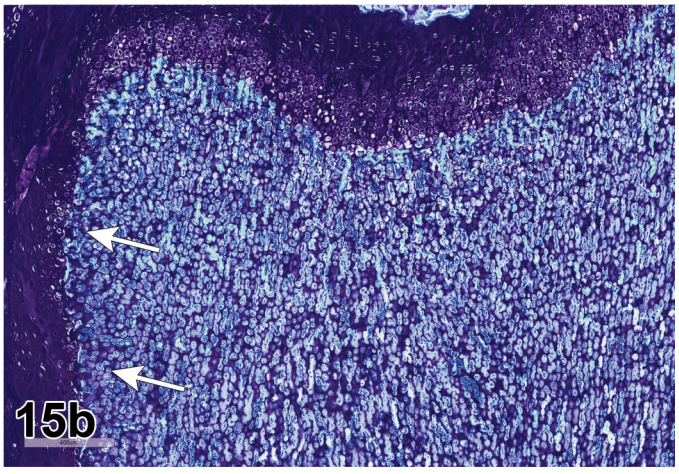

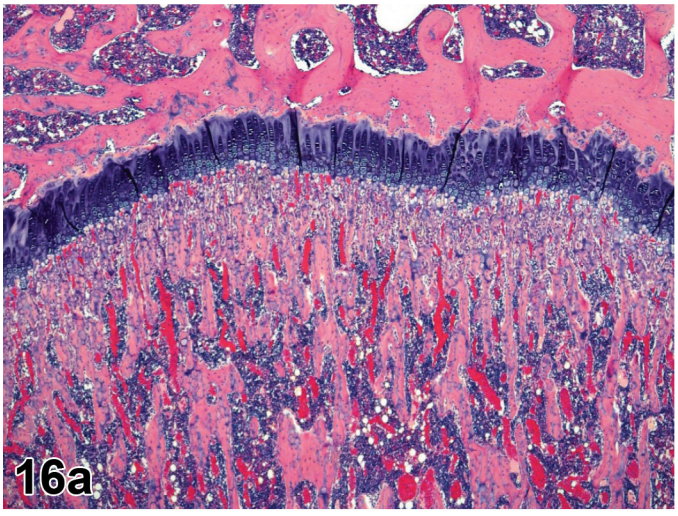

FIGURE 14. — Increased thickness, physis, tibia, rat that received a TGFβ1 inhibitor (B). Relative to an age-matched control rat (A), the treated animal exhibited increased thickness of the physeal hypertrophic zone along with altered staining of cartilagenous matrix (the latter indicating changes in matrix components indicative of dysplasia). Decalcified bone, Movat's pentachrome stain. Images republished from Frazier et al (2007) by permission of SAGE.

FIGURE 15. — Increased thickness, physis, long bone, neonatal male rat that received the engineered fusion protein OPG-Fc (combining osteoprotegerin [OPG] and the constant region [Fc] of human immunoglobin), an inhibitor of RANKL (B). Relative to an age-matched control animal (A), the treated rat exhibits a hypertrophic lesion characterized by thickening and disorganization of the physeal hypertrophic zone with marked focal thickening (arrows) and increased trabecular bone. The two images are taken at the same magnification to highlight the thickened physis and overproduction of bone. Decalcified bone, Toluidine blue.

FIGURE 16. — Decreased thickness, physis, femur, rat. In images taken at the same magnification, the treated rat (B) has a slightly narrowed growth plate—confirmed subsequently by quantitative endpoints—compared to a control animal (A). Decalcified bone, H&E.

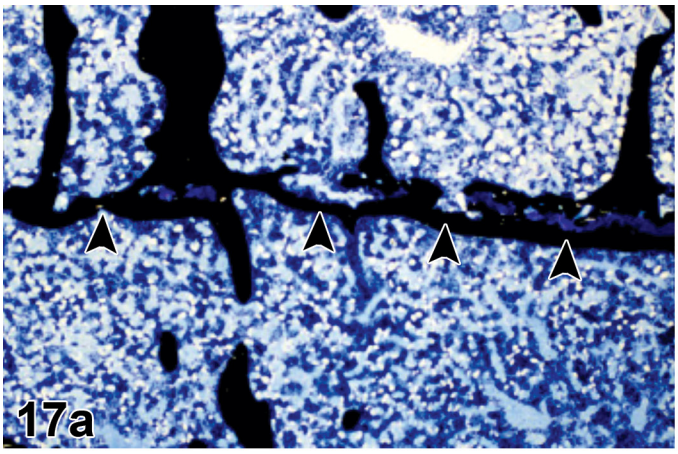

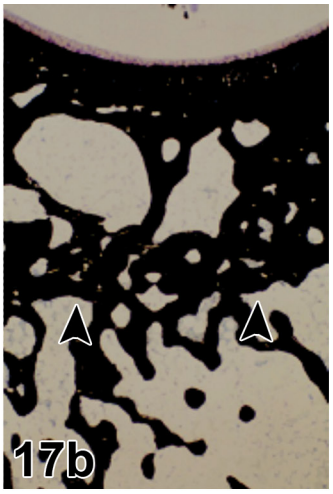

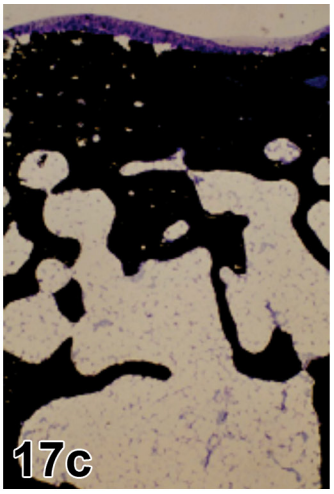

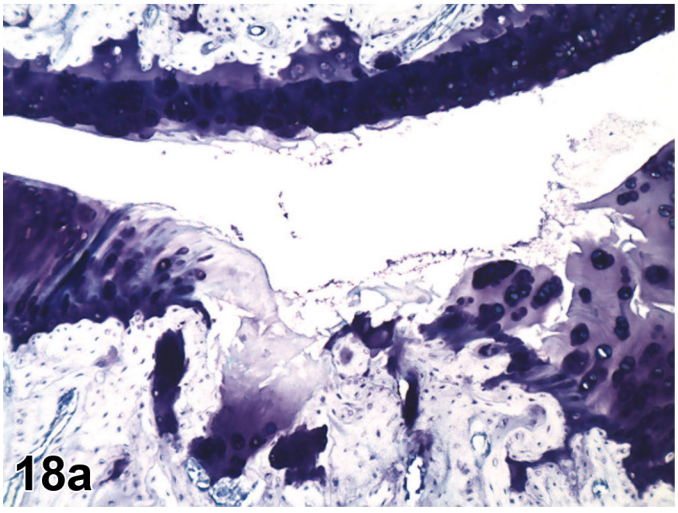

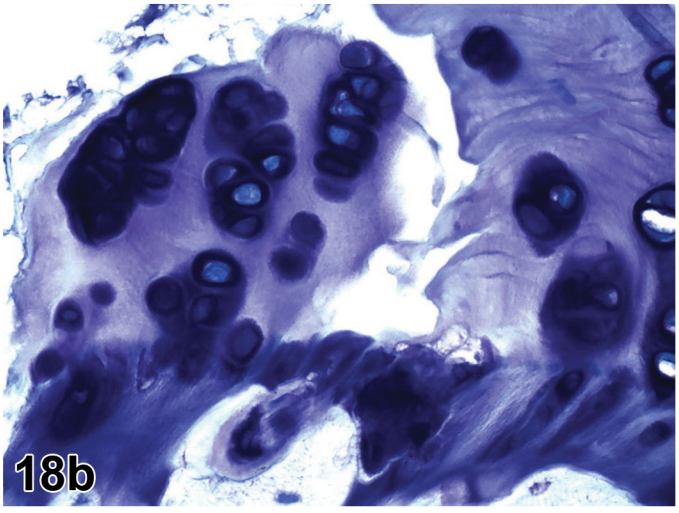

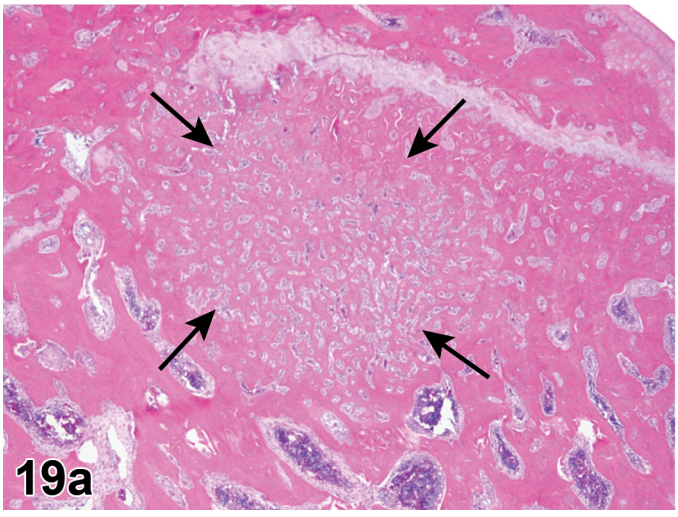

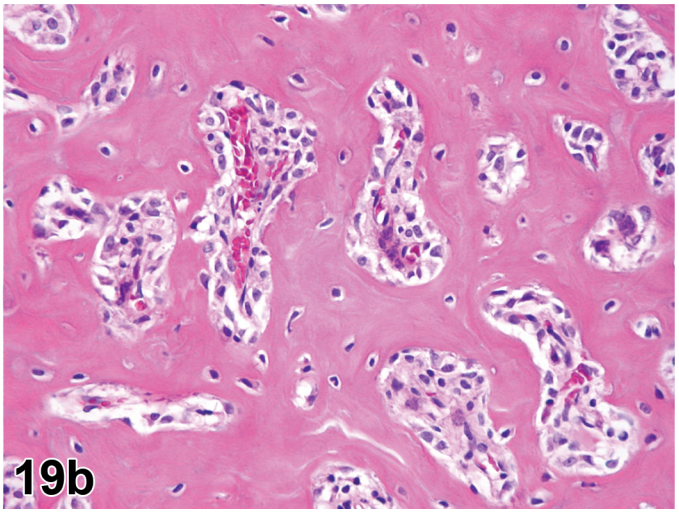

FIGURE 17. — Growth plate closed, female rats, 15-21 months of age. (A) With hyaline cartilage remnants, proximal tibia with red marrow (growth plate labelled with arrowheads). (B) and (C) Distal tibia with fatty marrow. (C) There is complete disappearance of the growth plate and fusion of the epiphysis and metaphysis. (B) Arrowheads mark the position of the ossified growth plate. Undecalcified bone, Von Kossa/MacNeal's tetrachrome. Images courtesy of Dr. Thomas J. Wronski.

FIGURE 18. — Hyperplasia, chondrocyte with subchondral bone, calcified cartilage fractures, and collapse of the articular cartilage, femorotibial joint of a rat model of medial meniscal tear-induced osteoarthritis (OA). (A) Low magnification, (B) Higher magnification to demonstrate clonal clusters of hypertrophied chondrocytes. (As an approximate comparison, the normal appearance of chondrocytes in articular cartilage of the mouse femur is shown in Figure 9.) Decalcified bone, Toluidine blue.

FIGURE 19. — Hyperplasia, osteoblast, focal, femur with increased bone trabeculae, male rat given recombinant human parathyroid hormone (PTH). (A) Low magnification, (B) higher magnification. Note poorly demarcated areas of irregular trabecular bone with bone surfaces lined by plump cuboidal osteoblasts. Decalcified bone, H&E. Images republished from Jolette J et al. (2006), by permission of SAGE.

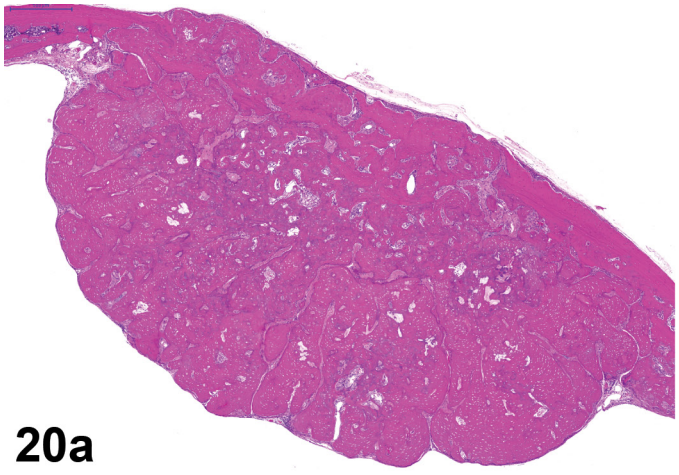

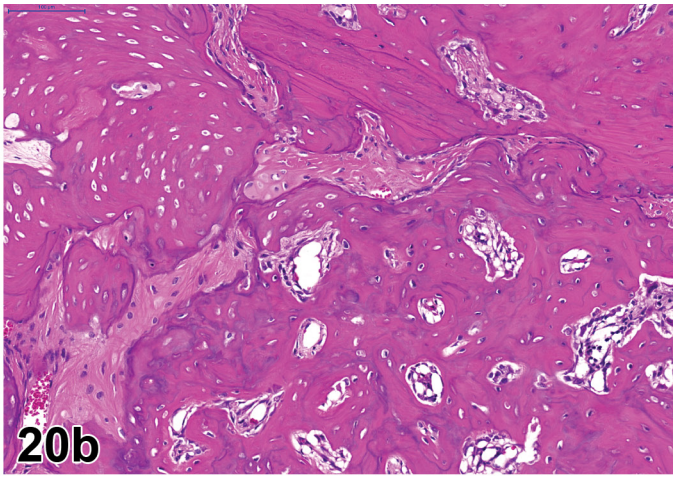

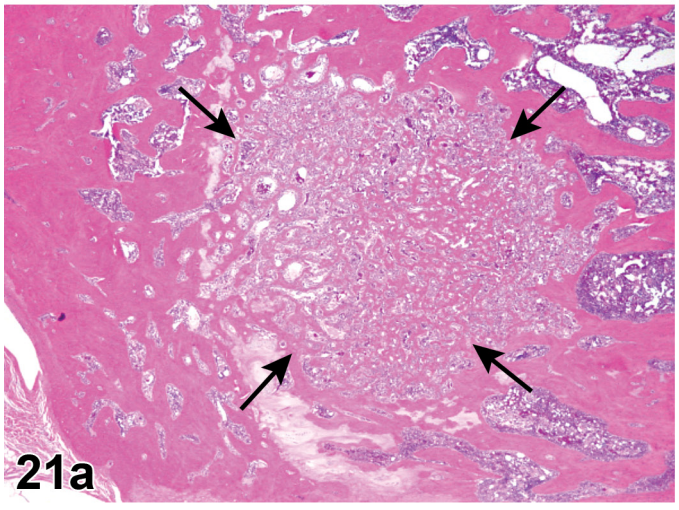

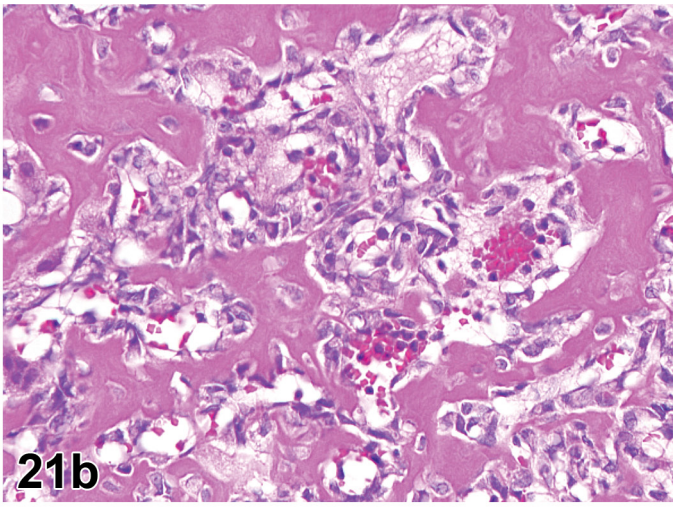

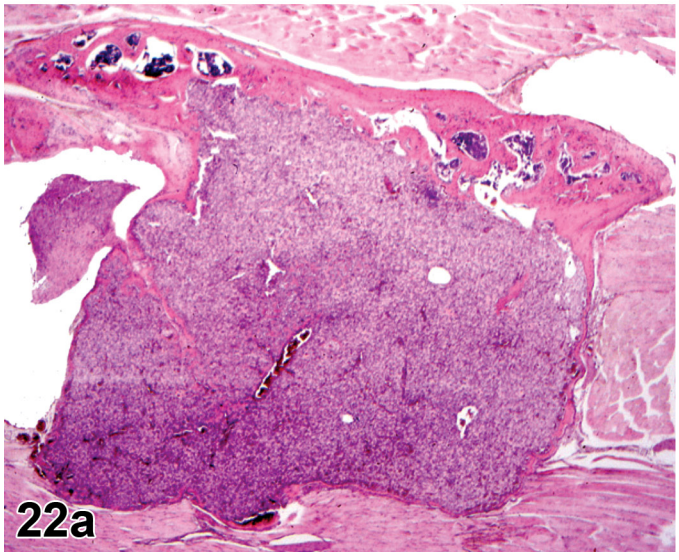

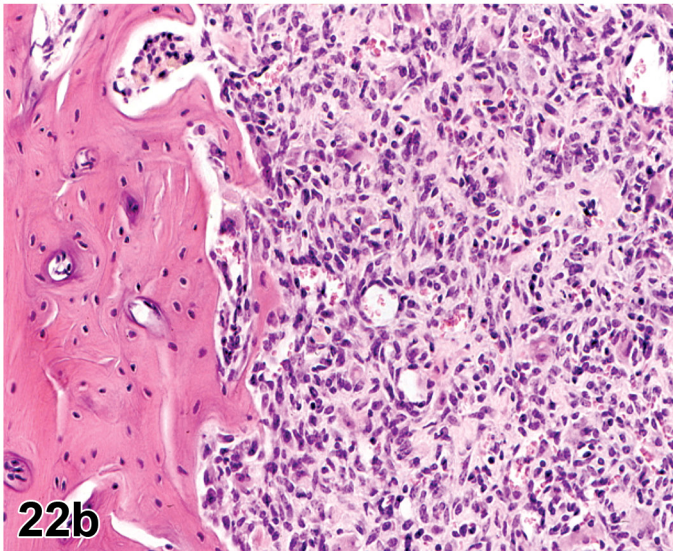

FIGURE 20. — Osteoma, mouse. (A) Low magnification, (B) higher magnification. (A) An expansile, well-demarcated, benign neoplasm of osteocytic or osteoblastic origin consisting of irregular lobules of well-differentiated bone separated by narrow bands of fibrous connective tissue. (B) The disorganized arrangement of lacunae in the woven bone of the well-differentiated benign neoplasm contrasts with the regular laminated architecture of the cortical bone (upper right quadrant). Decalcified bone, H&E.

FIGURE 21. — Osteoblastoma, proximal tibia, rat given recombinant human parathyroid hormone (PTH). (A) Low magnification, (B) higher magnification. A focal benign neoplasm of osteoblast origin with irregular borders replacing metaphyseal bone. The neoplastic cells in this lesion are more pleomorphic (i.e., less differentiated) than those in an osteoma. Decalcified bone, H&E. Images republished from Jolette J et al. (2006), by permission of SAGE.

FIGURE 22. — Osteofibroma, mouse. (A) Low magnification, (B) higher magnification. An expansile, highly cellular, mildly pleomorphic benign bone neoplasm that lacks tumor osteoid or other features of osteosarcoma but has a dense fibrous stroma. Decalcified bone, H&E.

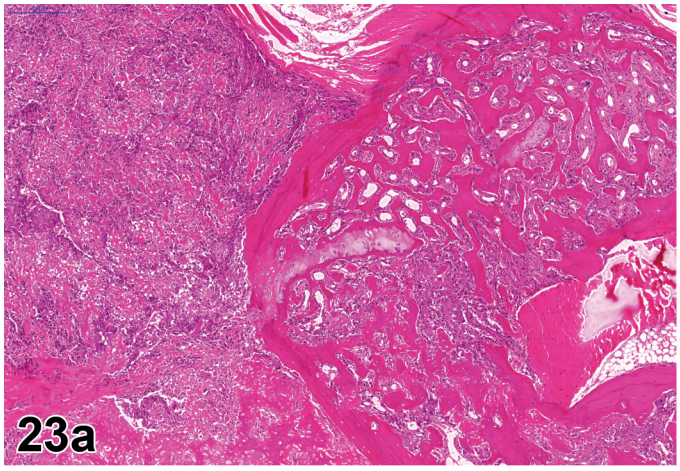

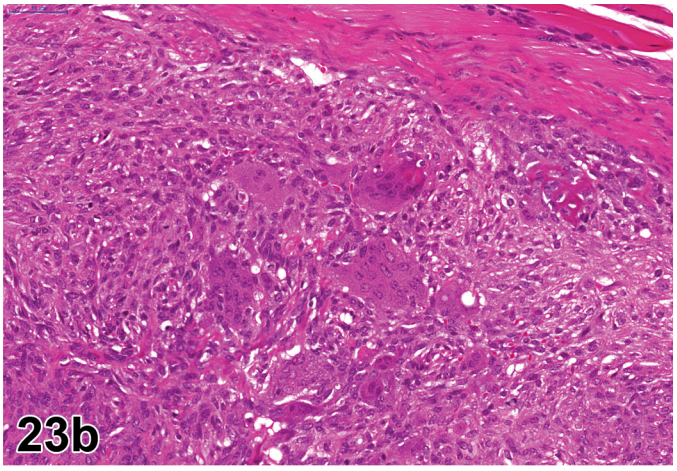

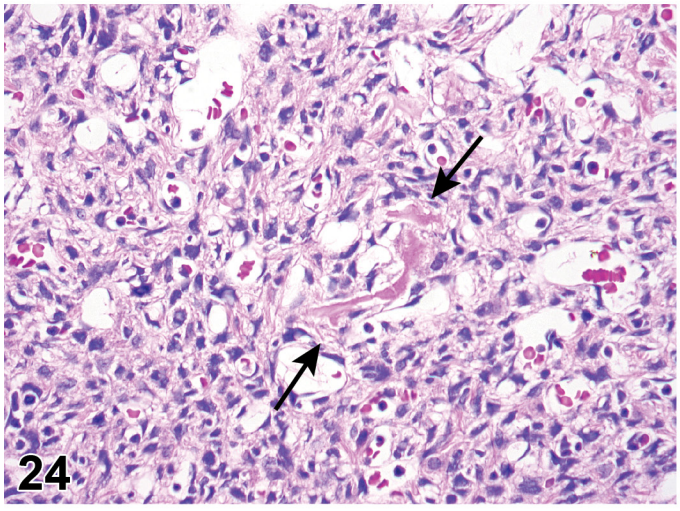

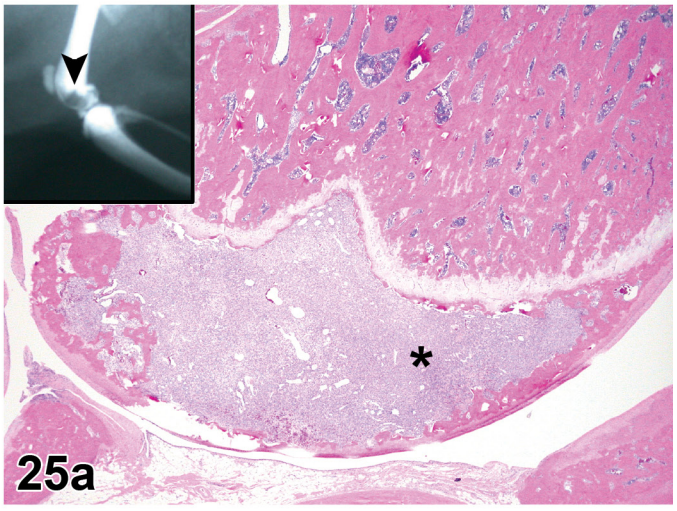

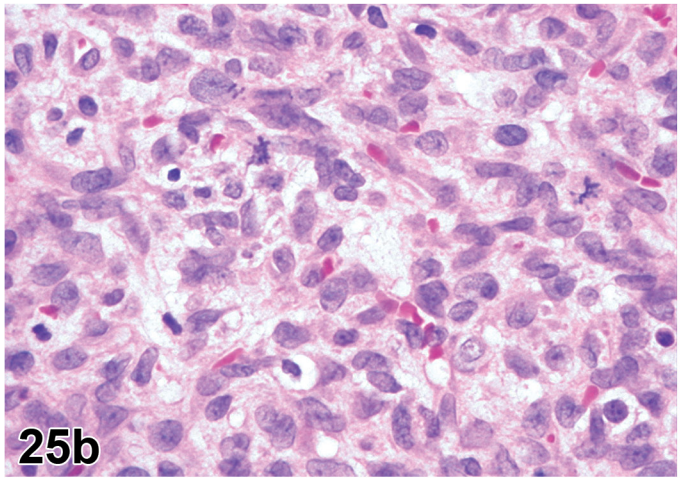

FIGURE 23. — Osteosarcoma, mouse. (A) Low magnification, (B) higher magnification. An aggressively invasive, highly cellular, variably anaplastic malignant spindle cell neoplasm of bone characterized by formation of osteoid by tumor cells. Decalcified bone, H&E.

FIGURE 24. — Osteosarcoma, fibroblastic, tibia, rat given recombinant human parathyroid hormone (PTH). The tumor was lytic and produced scant tumor osteoid (arrows) but a fairly abundant fibrous stroma. Decalcified bone, H&E. Image republished from Jolette J et al. (2006), by permission of SAGE.

FIGURE 25. — Osteogenic fibrosarcoma, intramedullary, with increased bone in metaphysis, distal femur (*), rat administered recombinant human parathyroid hormone (PTH). (A) Low magnification, (B) higher magnification. This malignant tumor forms from fibroblasts within a bone, and thus does not produce osteoid. Decalcified bone, H&E. Radiographic evidence of focal osteolysis of the femoral epiphysis (arrowhead) with bone sclerosis of the metaphysis and diaphysis (left insert) is a common clinical presentation in osteosarcomas. Image republished from Jolette J et al. (2006), by permission of SAGE.

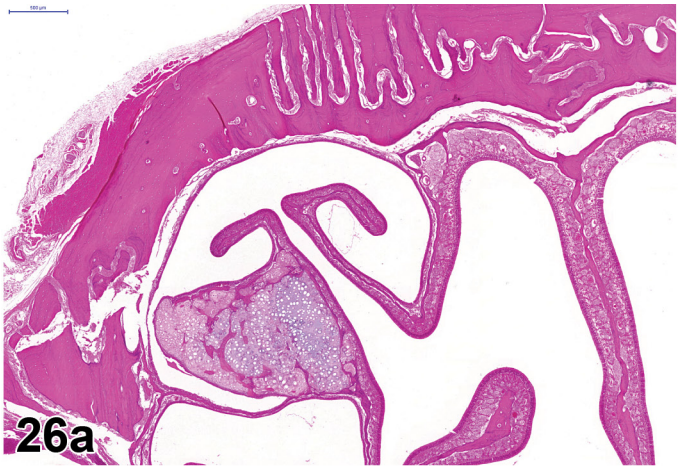

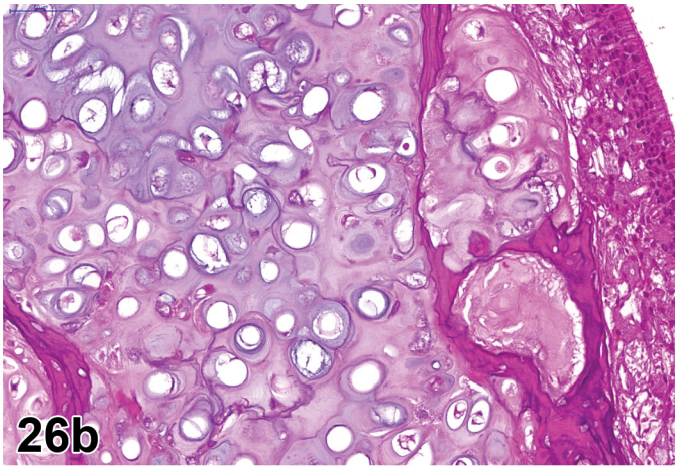

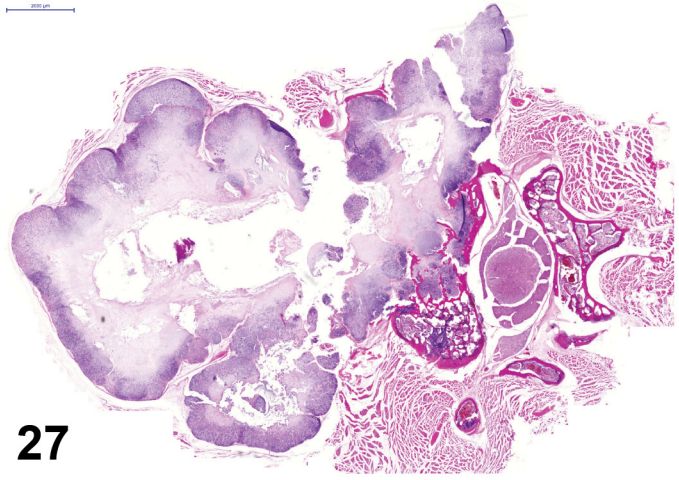

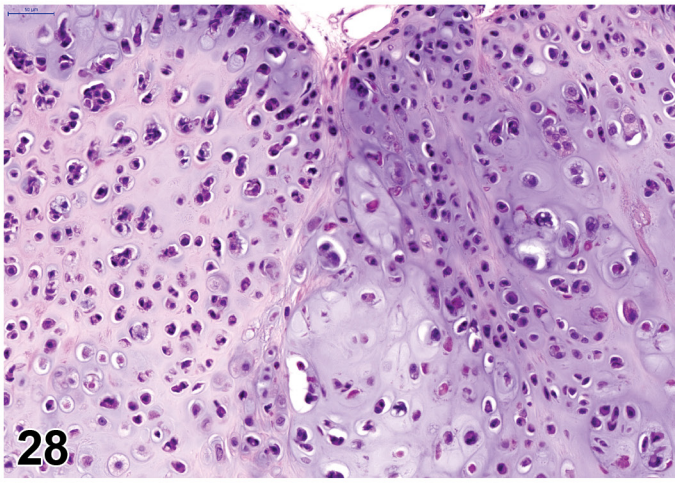

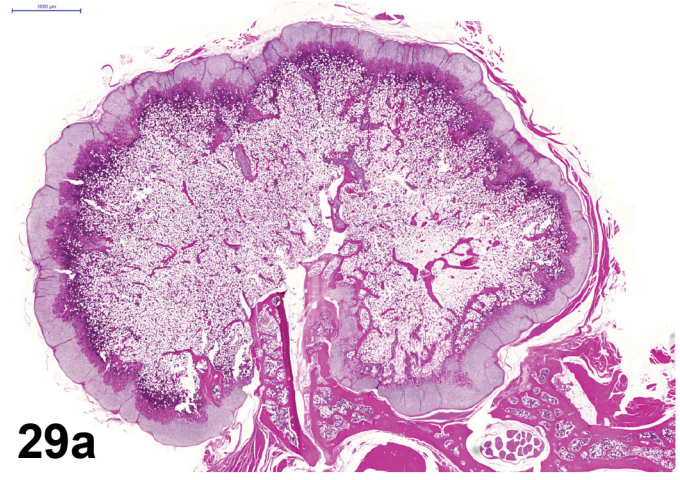

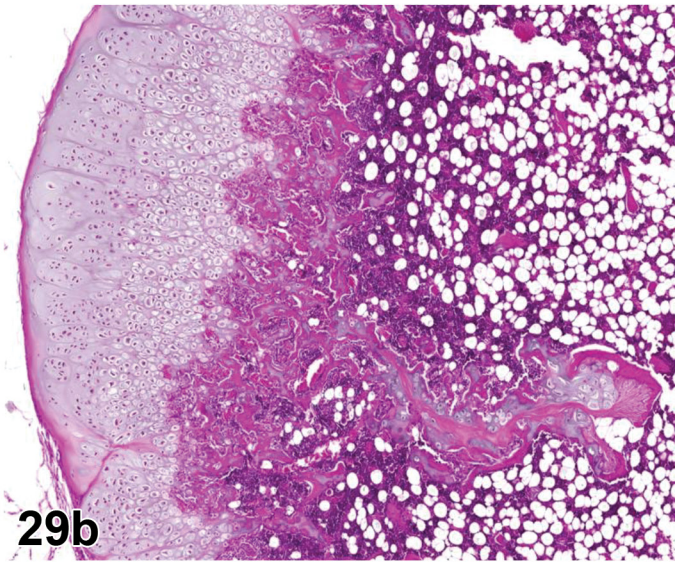

FIGURE 26. — Chondroma, nasal turbinate, rat. (A) Low magnification, (B) higher magnification. An expansile, benign tumor of chondrocyte or chondroblast origin formed of irregular lobules of disorganized hyaline cartilage. Decalcified bone, H&E.

FIGURE 27. — Chondrosarcoma, vertebra, rat. A large, highly expansile and destructive, malignant neoplasm of chondrocytic or chondroblastic origin. Decalcified bone, H&E.

FIGURE 28. — Chondrosarcoma, rat. Extensive pleomorphism is characteristic of malignant cells in this tumor. Decalcified bone, H&E.

FIGURE 29. — Osteochondroma, rat. (A) Low magnification, (B) higher magnification. A benign mixed mesenchymal neoplasm characterized by both cartilaginous and osseous components. The orderly cap of hyaline cartilage is a distinctive feature of this tumor. Decalcified bone, H&E.

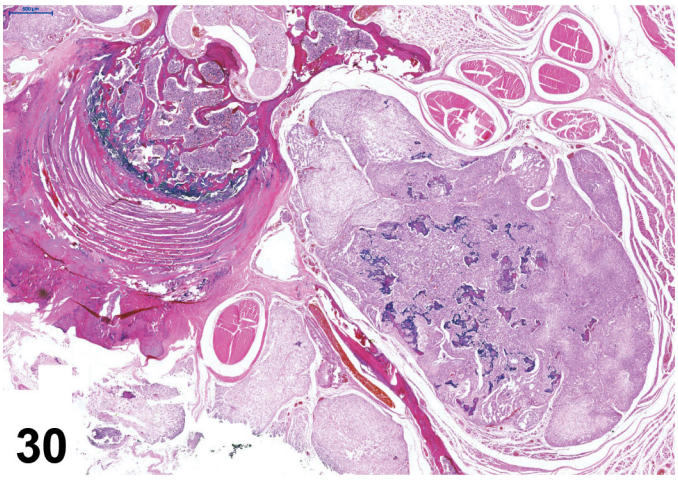

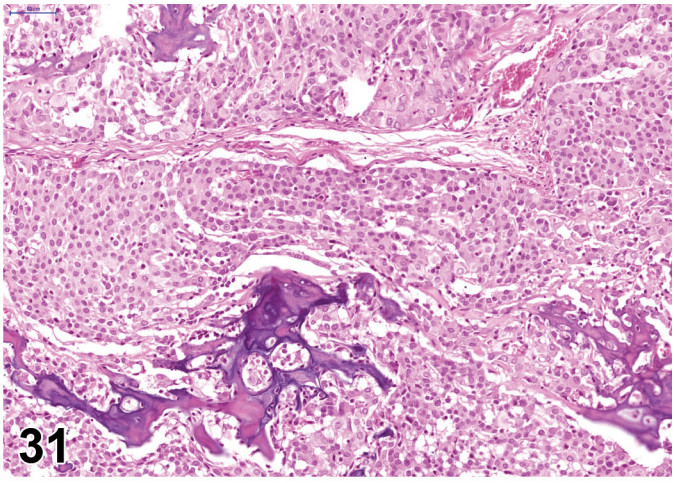

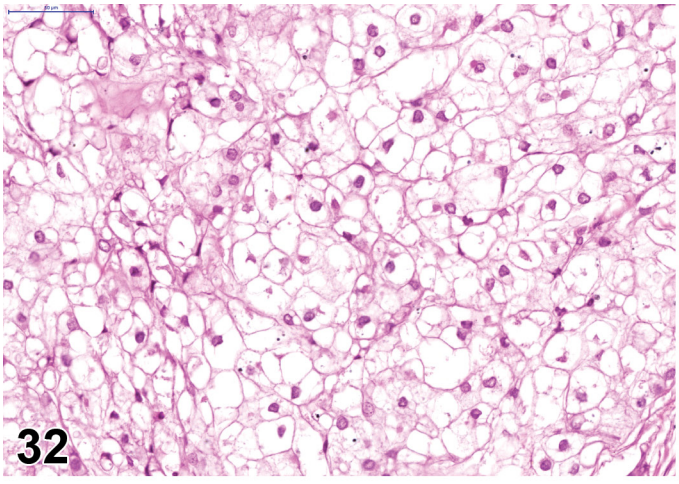

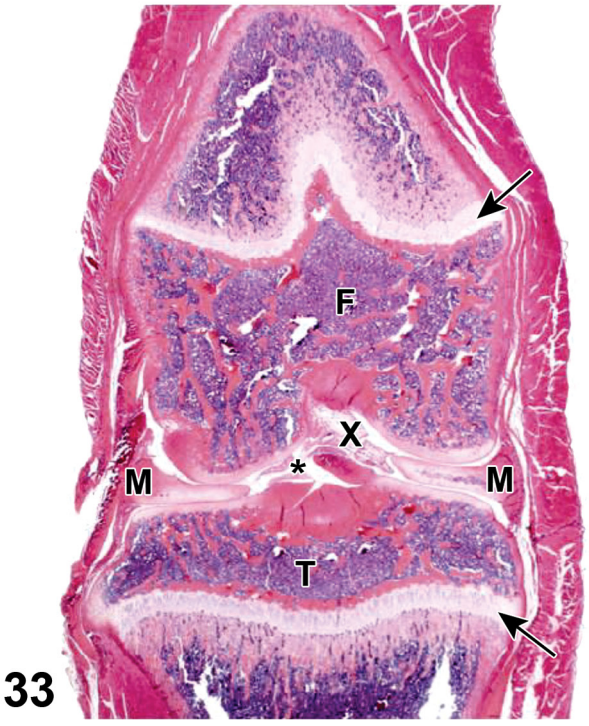

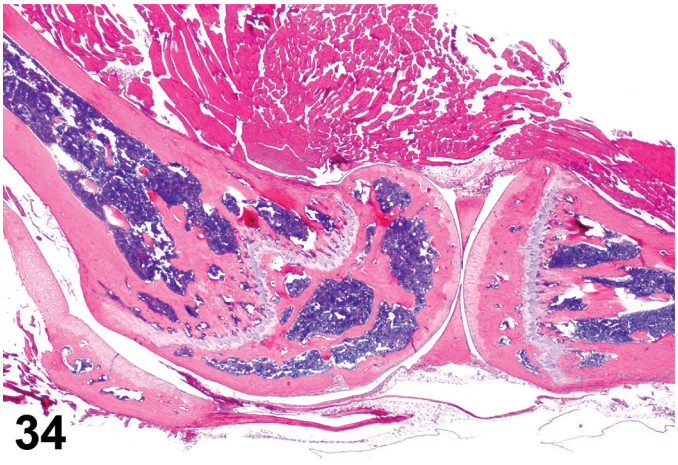

FIGURE 30. — Chordoma, malignant, vertebral column, rat. This aggressive, lobulated neoplasm arises from notochord mesenchyme within the axial skeleton (commonly a vertebral body). Decalcified bone, H&E.

FIGURE 31. — Chordoma, malignant, rat. Lobules consist of densly packed aggregates of tumor cells separated by fibrous trabeculae. Spicules of bone encompassed by the tumor represent eroded remnants of bone rather than a product of the tumor cells. Decalcified bone, H&E.

FIGURE 32. — Chordoma, malignant, rat. Highly vacuolated cytoplasm ("physaliphorous cells") is a characteristic feature of neoplastic cells within chordomas. Decalcified bone, H&E.

FIGURE 33. — Normal femorotibial joint (i.e., stifle, or "knee"), adult Lewis rat. This synovial joint features a narrow joint cavity (asterisk) that is partially filled by dense, fibrous cruciate ligaments (X) and triangular fibrocartilaginous menisci (M). Both the distal femur (F) and proximal tibia (T) have well-formed physes (arrows). Marrow cavities of these long bones generally are filled with hematopoietic precursors in healthy animals. Decalcified bone, H&E. Image republished from Bolon B et al. (2011) by permission of the publisher.

FIGURE 34. — Normal femorotibial joint (parasagittal section), 3-month-old mouse. This section shows articular surfaces, menisci, and synovium. Decalcified bone, H&E.

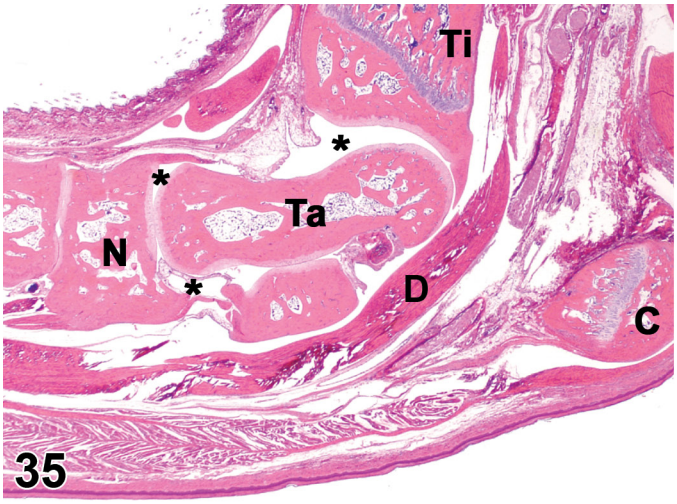

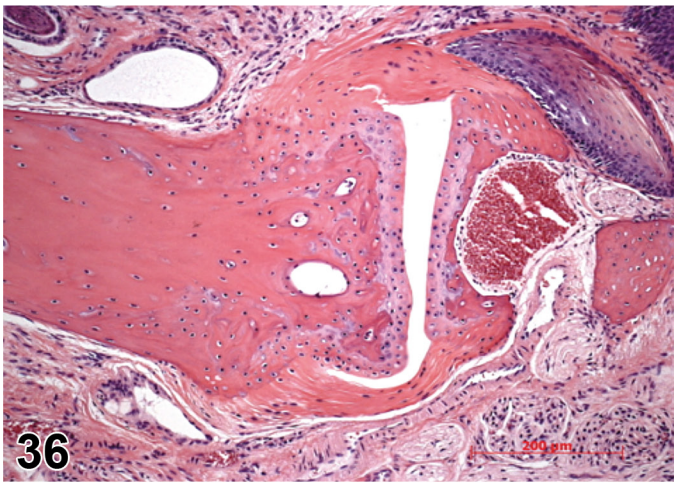

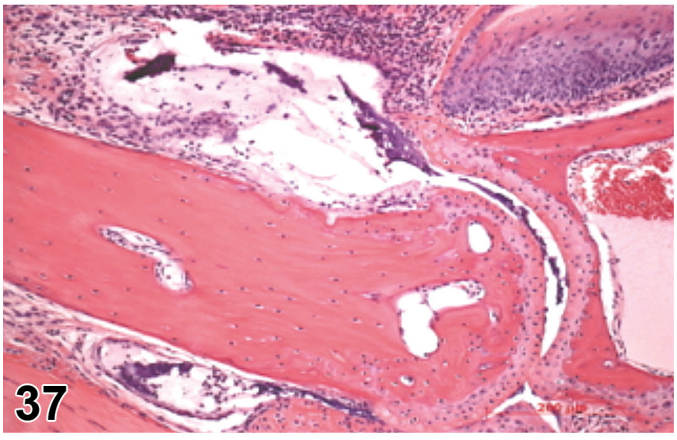

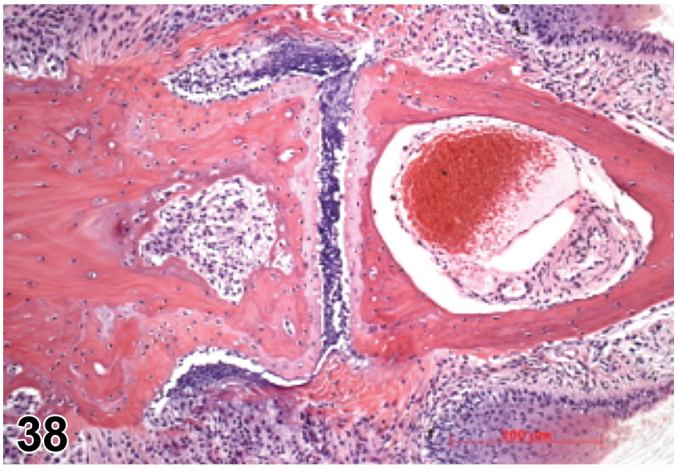

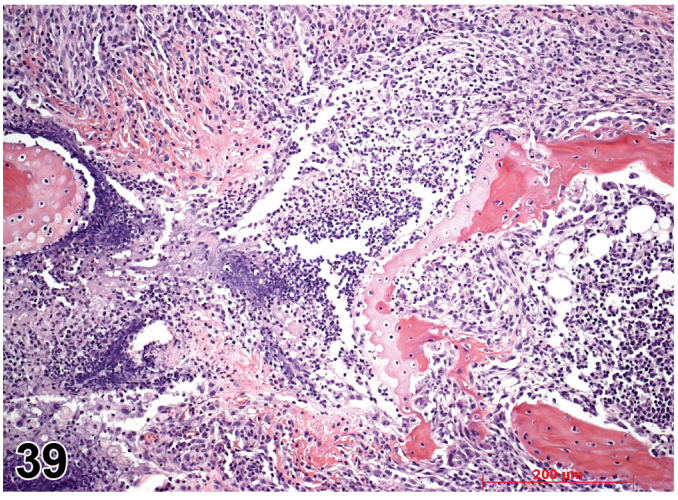

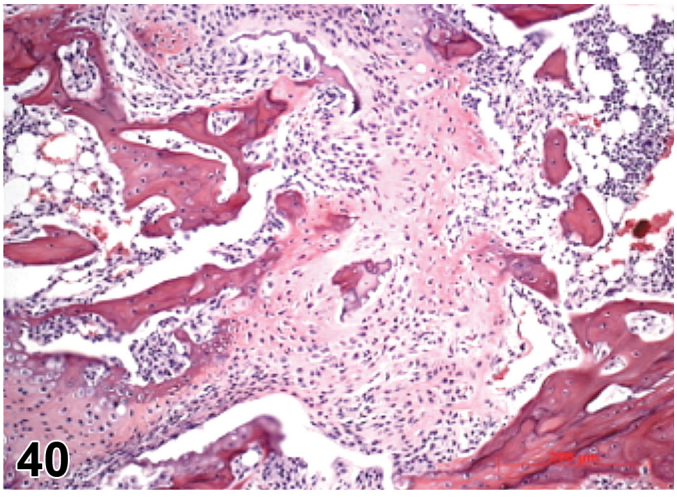

FIGURE 35. — Normal tibiotarsal joints (i.e. hock, or "ankle"), adult Lewis rat. These synovial joints demonstrate the characteristic thin synovial lining subtended by a thin fibrous joint capsule and abundant peri-articular soft tissue (in this case, white adipose tissue). The multiple joint cavities (asterisks) separate the articular surfaces of the navicular bone (N), talus (Ta), and distal tibia (Ti). In normal rodents, bone marrow cavities in this region typically contain white adipose tissue rather than hematopoietic cells. The deep digital flexor tendon (D) and calcaneus (C) are also shown. Decalcified bone, H&E. Image republished from Bolon B et al. (2011) by permission of the publisher.

FIGURE 36. — Normal distal interphalangeal joint, 10-week-old DBA/1JBomTac mouse. The joint cavity, synovium-lined cul-de-sacs, ligament-reinforced joint capsule, articular cartilage, subchondral bone, and transition zones are shown. Decalcified bone, H&E.

FIGURE 37. — Inflammation, distal interphalangeal joint, 10-week-old DBA/1JBomTac mouse. A minimal to mild, acute, neutrophil-dominated cellular infiltrate accompanied by fibrin distends the synovial cul-de-sacs and extends within the peri-articular connective tissue. The bone marrow contains the expected white adipose tissue but no inflammatory cells. Decalcified bone, H&E.

FIGURE 38. — Inflammation, distal interphalangeal joint, 10-week-old DBA/1JBomTac mouse. A mild to moderate, subacute infiltrate of neutrophils within the articular cavity and peri-articular connective tissue is associated with superficial erosion of the articular cartilage, disruption of the ligament-reinforced joint capsule, and incipient pannus formation. Decalcified bone, H&E.

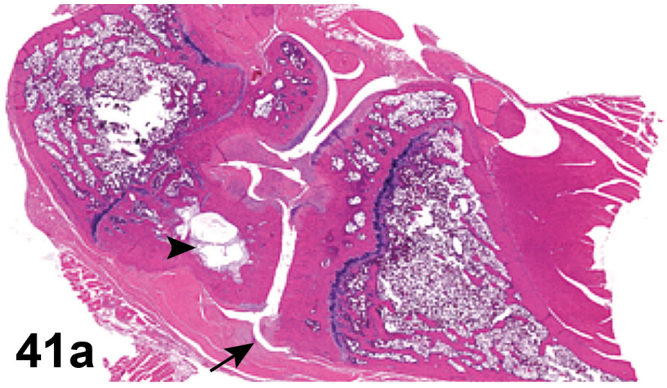

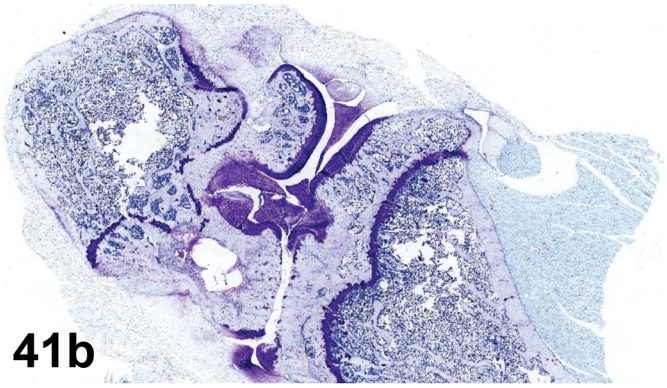

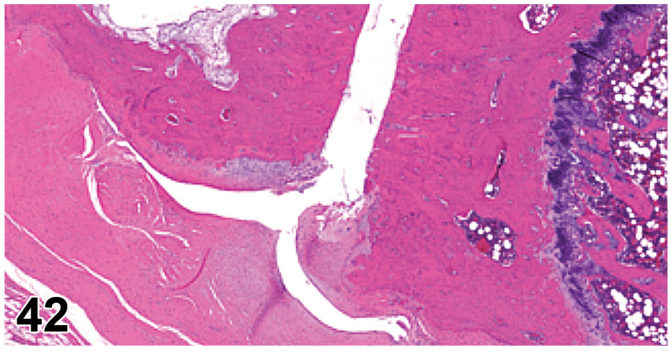

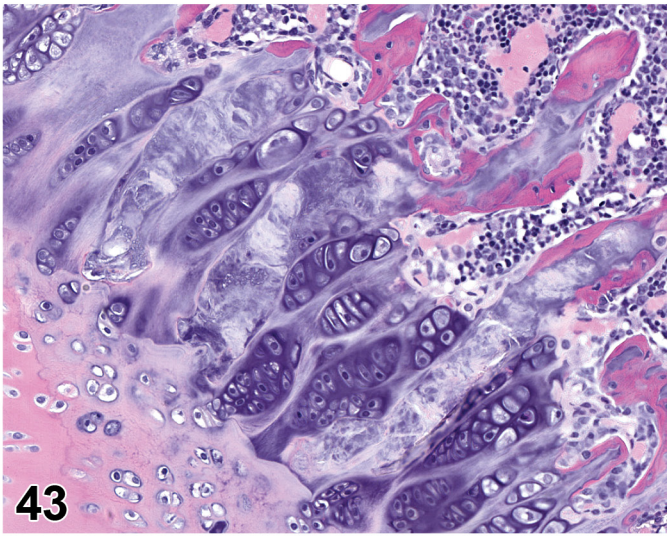

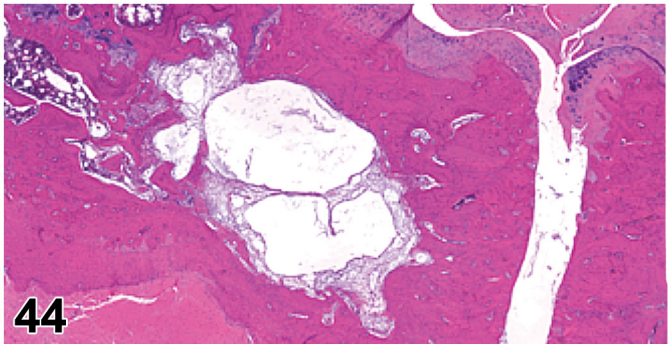

FIGURE 39. — Inflammation, metatarsophalangeal joint, 10-week-old DBA/1JBomTac mouse. A moderate to marked, chronic infiltrate of neutrophils and macrophages accompanied by cellular debris obscures the natural boundaries of the joint; superficial erosion of articular cartilage, pannus formation, undermining of articular cartilage/subchondral bone, resorption of subchondral bone, and myelofibrosis are evident. The bone marrow is filled with inflammatory cells rather than white adipose tissue. Decalcified bone, H&E.

FIGURE 40. — Inflammation, metatarsophalangeal joint, 10-week-old DBA/1JBomTac mouse. This chronic lesion is characterized by complete loss of joint integrity; opposed bone ends are devoid of articular cartilage caps, and their medullary cavities are united by contiguous deposits of woven bone, fibrocartilage, and fibrous connective tissue. Decalcified bone, H&E.

FIGURE 41. — Osteophyte with degenerative joint disease (DJD), femorotibial joint, medial meniscal tear model of osteoarthritis (OA), rat. (A) On the left side of image, the medial tibial plateau (lower bone) and medial femoral condyle (upper bone) are devoid of articular cartilage, the subchondral bone plates at those sites are thickened, an osteophyte (arrow) projects above the eburnated surface of the medial tibial plateau, and a pseudocyst (arrowhead) is evident within the medial femoral condyle. Decalcified bone, H&E. (B) A toluidine blue-stained serial section of the specimen shown in (A), taken at the same magnification, showing that the osteophyte is formed mainly of cartilage.

FIGURE 42. — Osteophyte with degenerative joint disease (DJD), femorotibial joint, medial meniscal tear model of OA, rat. A higher magnification of the H&E-stained section in Figure 41A to highlight the loss of articular cartilage in the femur (left bone) and tibia (right bone) and osteophyte.

FIGURE 43. — Chondromucinous degeneration, sternebra, 10-week-old Sprague-Dawley rat. Multiple, discrete foci of matrix dissolution/fragmentation and chondrocyte loss are evident as pale, acellular areas within the cartilage of the synarthrosis. Decalcified bone, H&E.

FIGURE 44. — Pseudocyst, femorotibial joint, medial meniscal tear model of OA, rat. The cavity within the medial femoral condyle (left bone) is designated a pseudocyst because it lacks the definitive cellular lining of a true cyst (shown in Figure 11). This lesion is found most frequently in the epiphyseal subchondral bone of joints with advanced degenerative joint disease, evident here through the loss of articular cartilage from the medial tibial plateau (right bone) and medial femoral condyle and osteophyte at the joint margin. Decalcified bone, H&E.

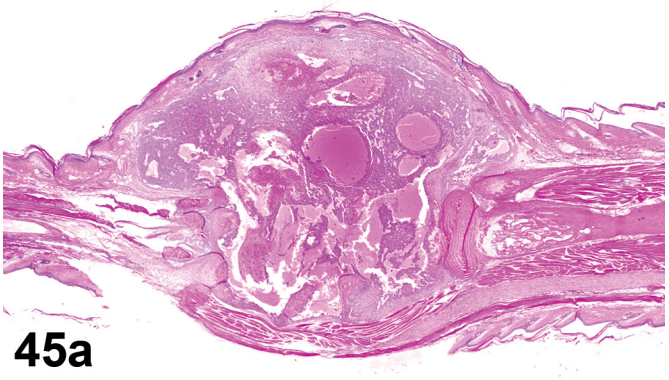

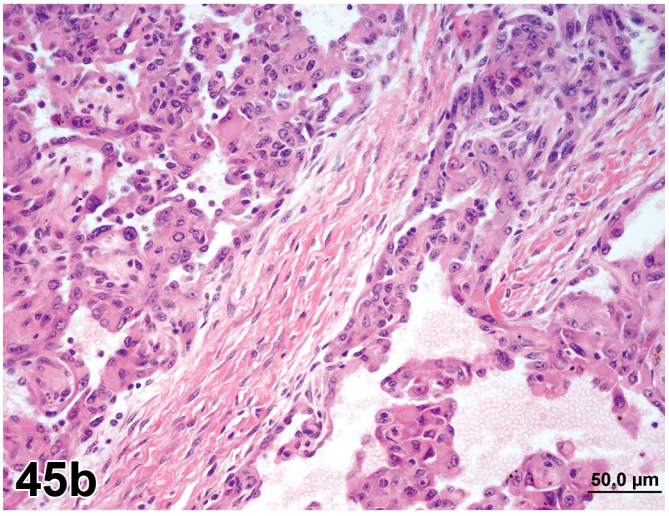

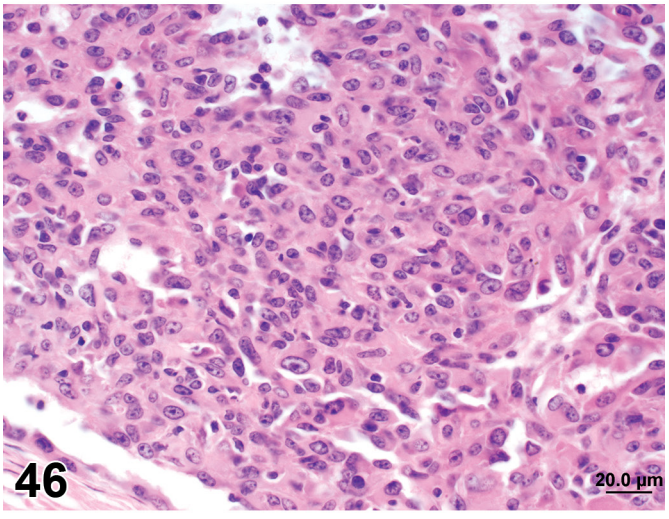

FIGURE 45. — Synovial sarcoma, vertebra, tail, 165-day-old BALB/cJ mouse. (A) Low magnification, (B) higher magnification. (A) The architecture of a coccygeal vertebra is completely effaced by an expansile, cystic, and unencapsulated malignant neoplasm arising from synoviocytes. (B) The neoplasm is composed of a labyrinth of variably sized, interconnected spaces that contain a faintly stained, fine granular, eosinophilic substance and are bordered by papillary displays of monomorphic, histiocyte-like tumor cells (i.e., resembling type A synoviocytes) supported by a sparse collagenous stroma. Decalcified bone, H&E. Image courtesy of Dr. John Sundberg.

FIGURE 46. — Synovial sarcoma, vertebra, tail, 165-day-old BALB/cJ mouse. Higher magnification of the mass shown in Figure 45A. In this portion of the mass, the monomorphic, histiocyte-like cells are more solidly arranged and have indistinct cell borders. Individual cells are characterized by an oval, euchromatic nucleus and generally single nucleolus. Decalcified bone, H&E. Image courtesy of Dr. John Sundberg.

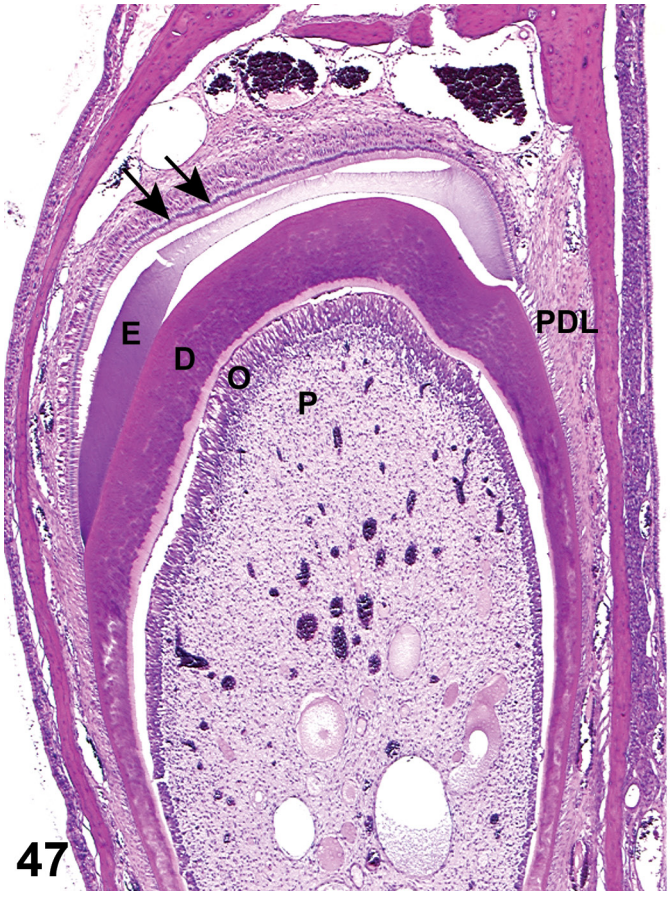

FIGURE 47. — Normal incisor, rat, showing ameloblasts (arrows), enamel (E), dentin (D), odontoblasts (O), pulp (P), and the periodontal ligament (PDL). Decalcified tooth, H&E.

FIGURE 48. — Degeneration and necrosis, ameloblast, with degeneration, odontoblast, mouse. Incisor showing ameloblast degeneration (short arrow) and necrosis (long arrow) as well as odontoblast degeneration (intermediate arrow). Degeneration is characterized by attenuation of the normal cell size, while necrosis is associated with destruction of the affected cells. Decalcified tooth, H&E.

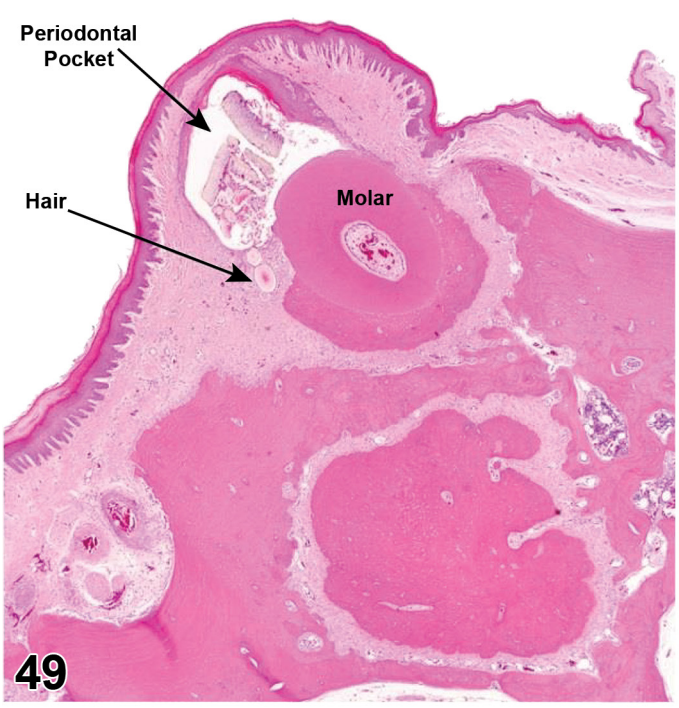

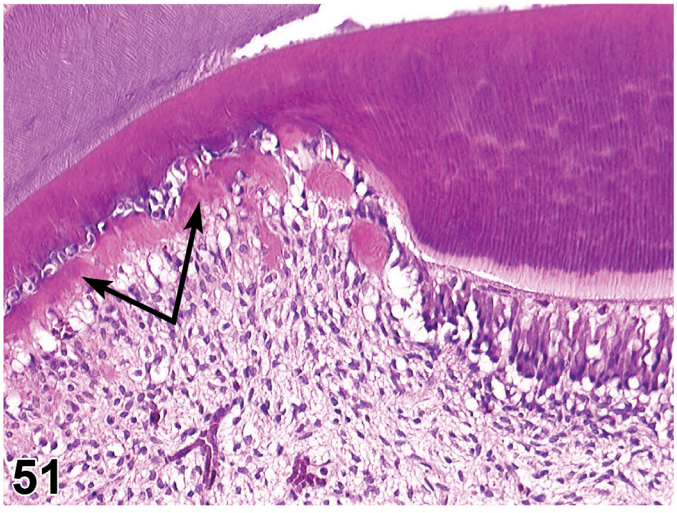

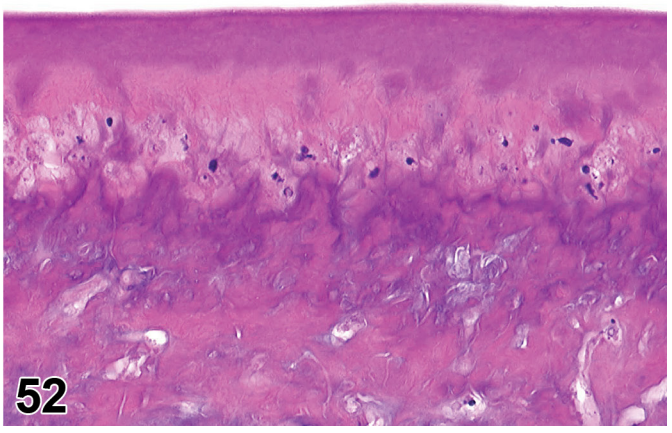

FIGURE 49. — Periodontal pocket, rat. The potential space between the tooth and periodontium, which usually is spanned by the periodontal ligament, is disrupted by distension with impacted feed/bedding material and a hair cross section within the surrounding periodontal connective tissue. Decalcified tooth, H&E.

FIGURE 50. — Dentin niches (arrows), incisor, rat. This represents the localized failure of odontoblasts to form dentin. Decalcified tooth, H&E.

FIGURE 51. — Dentin niche, incisor, rat. Higher magnification of dentin niche region from Figure 50. Note the thin dentin layer, degeneration/loss of odontoblasts, and attempted repair seen as tertiary dentin (osteodentin) formation (arrows). Decalcified tooth, H&E.

FIGURE 52. — Dentin matrix alteration, incisor, rat. Dentin is not normal in morphology or staining, and it contains cellular inclusions. Decalcified tooth, H&E.

FIGURE 53. — Dental dysplasia (abnormal development), incisor, rat. This defect results from abnormal development of one or more odontogenic cell lineages and typically presents as a tooth socket containing a disorganized mass of dentin-like material surrounded by fragments of the original tooth and small islands of bone; because rodent incisors grow throughout life, this developmental anomaly may arise during adulthood, commonly in association with trauma. Decalcified tooth, H&E.

FIGURE 54. — Denticle, incisor, rat. These lesions represent abnormal formation of small tooth-like structures in the pulp cavity. Note odontoblasts along one edge (upper right), tubules within the dentin matrix, and central space containing degenerate ameloblasts and a small amount of enamel (purple) matrix. Decalcified tooth, H&E.

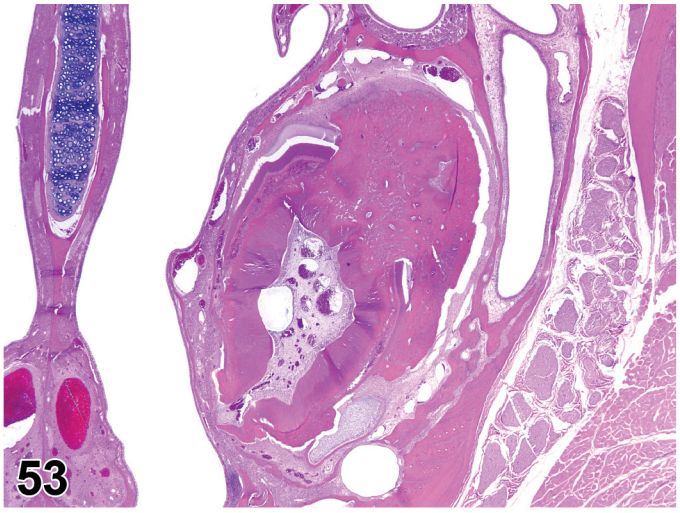

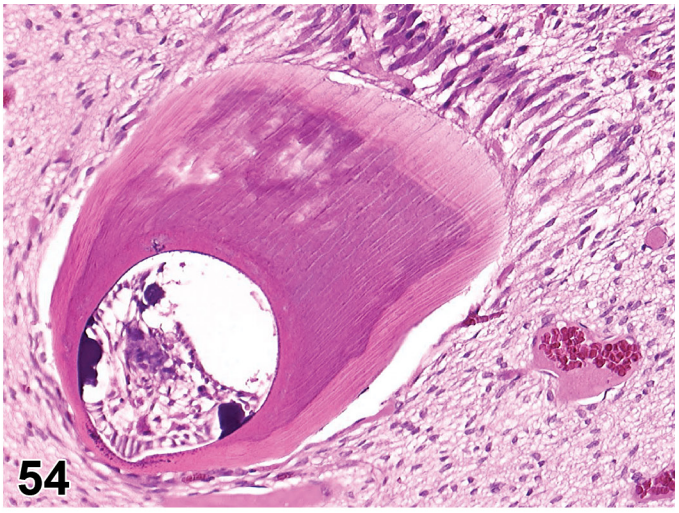

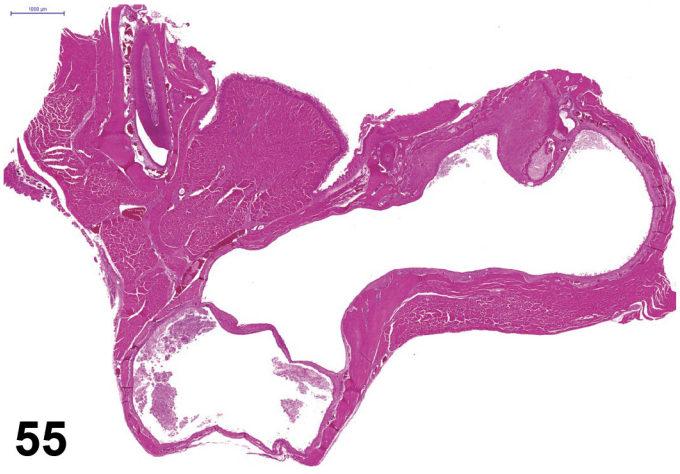

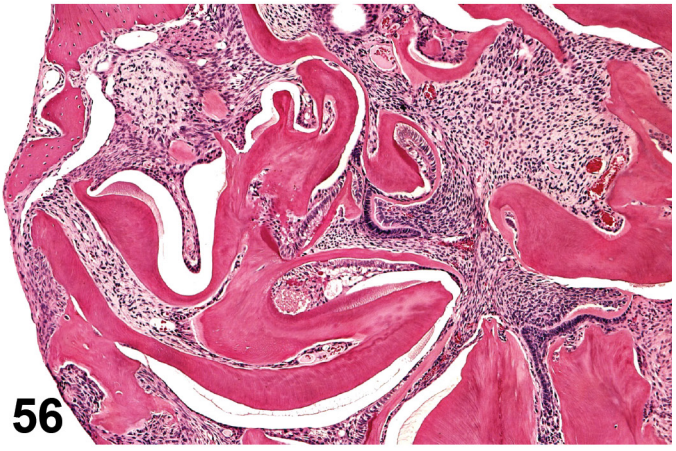

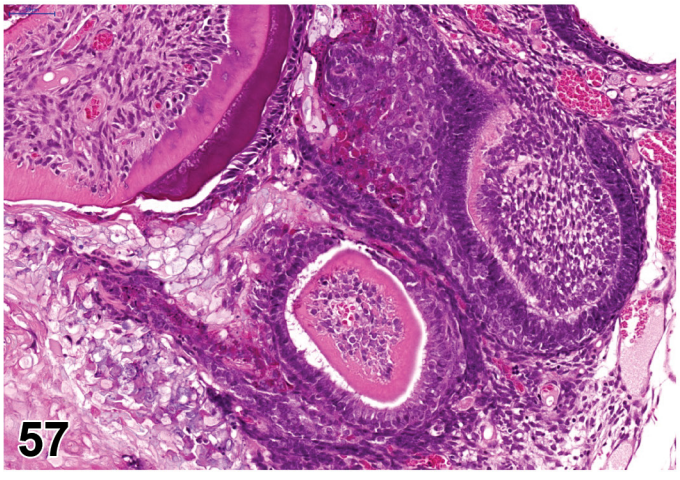

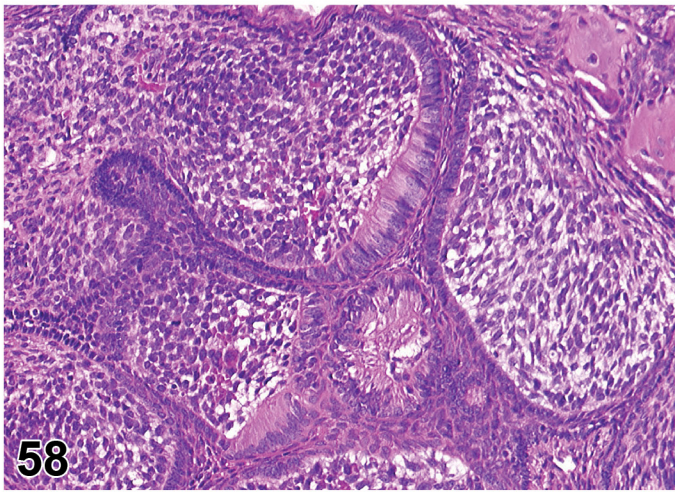

FIGURE 55. — Cyst, incisor, mouse. Odontogenic cysts are membrane-lined, fluid-filled cavities of unknown origin, typically arising at the apex of a tooth (seen here as a cross section at the upper left margin of the section). Decalcified tooth, H&E.

FIGURE 56. — Odontoma, rat. This lesion represents a developmental malformation (not neoplasm) in which all dental hard tissues including enamel (appears as clear spaces due to its loss during decalcification), dentin and cementum as well as odontoblasts, cementoblasts and dental pulp mesenchymal cells are present within a disorganized mass. Decalcified tooth, H&E.

FIGURE 57. — Ameloblastic odontoma, rat. This locally expansile neoplasm is comprised of proliferating, well-differentiated ameloblastoma-like epithelium located at the tumor periphery and minimal amounts of more centrally located dental hard tissues. Decalcified tooth, H&E.

FIGURE 58. — Ameloblastoma, rat. This locally expansile neoplasm consists of intersecting columns of mildly pleomorphic epithelial cells resembling the inner enamel epithelium encompassing aggregates of loosely arranged central cells similar to stellate reticulum. Decalcified tooth, H&E.

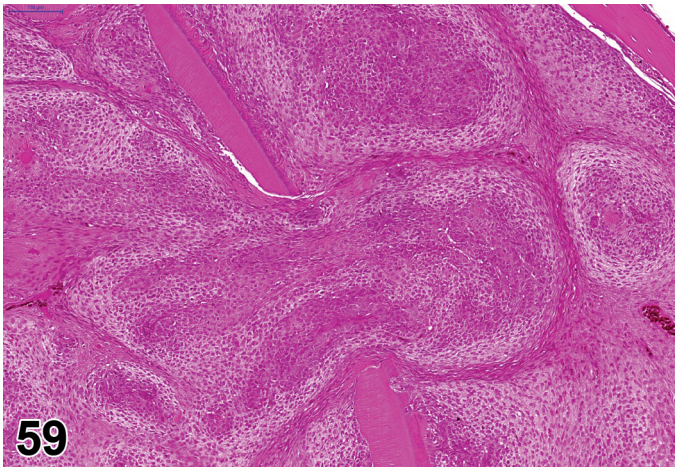

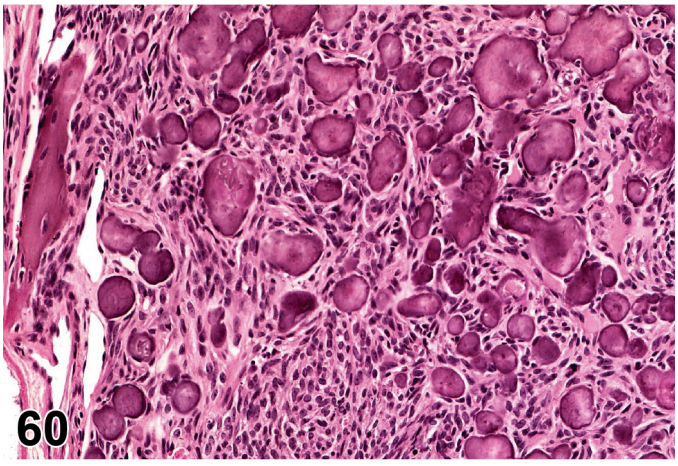

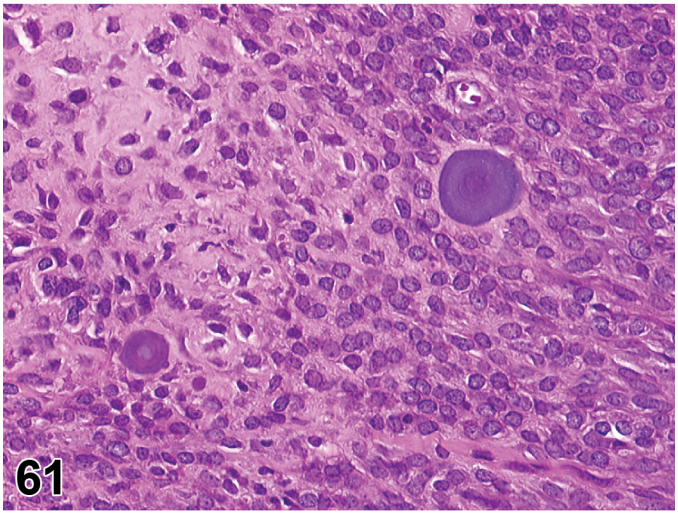

FIGURE 59. — Odontogenic fibroma, rat. This benign but locally expansile neoplasm is characterized by whorls of primitive-appearing, dental follicle-like mesenchyme separated by distinct areas of collagen formation. Decalcified tooth, H&E.

FIGURE 60. — Cementifying fibroma, mouse. This benign but locally expansile tumor features dense beds of neoplastic fibroblasts containing numerous cementicles (variably sized, irregular nodules of cementum). Decalcified tooth, H&E.

FIGURE 61. — Cementifying fibroma, mouse, higher magnification. Decalcified tooth, H&E.

References

Ahmad N, and Ruch JV. Comparison of growth and cell proliferation kinetics during mouse molar odontogenesis *in vivo* and *in vitro*. *Cell Tissue Kinet*. **20**: 319–329. 1987. [Medline]

Aigner T, Cook JL, Gerwin N, Glasson SS, Laverty S, Little CB, McIlwraith W, and Kraus VB. Histopathology atlas of animal model systems - overview of guiding principles. *Osteoarthritis Cartilage*. **18**(Suppl 3): S2–S6. 2010. [CrossRef] [Medline]

Albassam MA, Wojcinski ZW, Barsoum NJ, and Smith GS. Spontaneous fibro-osseous proliferative lesions in the sternums and femurs of B6C3F1 mice. *Vet Pathol*. **28**: 381–388. 1991. [CrossRef] [Medline]

Alvarez J, Horton J, Sohn P, and Serra R. The perichondrium plays an important role in mediating the effects of TGF-beta1 on endochondral bone formation. *Dev Dyn*. **221**: 311–321. 2001. [CrossRef] [Medline]

Andersen TL, Hauge EM, Rolighed L, Bollerslev J, Kjærsgaard-Andersen P, and Delaisse JM. Correlation between absence of bone remodeling compartment canopies, reversal phase arrest, and deficient bone formation in post-menopausal osteoporosis. *Am J Pathol*. **184**: 1142–1151. 2014. [CrossRef] [Medline]

Anderson HC, and Shapiro IM. The epiphyseal growth plate. In *Bone and development* (Bronner, F. ed.), pp. 39–64. Springer-Verlag, London. 2010.

Angevine DM, and Clemmons JJ. The occurrence of multiple fractures in suckling rats injected with beta-aminopropionitrile (Lathyrus factor). *Am J Pathol*. **33**: 175–187. 1957. [Medline]

Baden E, and Bouissou H. Experimental lathyrism: exostoses and aneurysmal-like bone cysts of the mandible in the rat. *Ann Pathol*. **7**: 297–303. 1987. [Medline]

Bahrami A, and Folpe AL. Adult-type fibrosarcoma: A reevaluation of 163 putative cases diagnosed at a single institution over a 48-year period. *Am J Surg Pathol*. **34**: 1504–1513. 2010. [CrossRef] [Medline]

Ballock RT, and O'Keefe RJ. Physiology and pathophysiology of the growth plate. *Birth Defects Res C Embryo Today*. **69**: 123–143. 2003; (Part C). [CrossRef] [Medline]

Banks WJ. *Applied Veterinary Histology,* Mosby-Year Book. 1993.

Barbolt TA, and Bhandari JC. Ameloblastic odontoma in a rat. *Lab Anim Sci*. **33**: 583–584. 1983. [Medline]

Bargman R, Huang A, Boskey AL, Raggio C, and Pleshko N. RANKL inhibition improves bone properties in a mouse model of osteogenesis imperfecta. *Connect Tissue Res*. **51**: 123–131. 2010. [CrossRef] [Medline]

Baron R, and Kneissel M. WNT signaling in bone homeostasis and disease: from human mutations to treatments. *Nat Med*. **19**: 179–192. 2013. [CrossRef] [Medline]

Bendele A, McComb J, Gould T, McAbee T, Sennello G, Chlipala E, and Guy M. Animal models of arthritis: relevance to human disease. *Toxicol Pathol*. **27**: 134–142. 1999. [CrossRef] [Medline]

Bendele AM. Animal models of osteoarthritis. *J Musculoskelet Neuronal Interact*. **1**: 363–376. 2001*a*. [Medline]

Bendele A. Animal models of rheumatoid arthritis. *J Musculoskelet Neuronal Interact*. **1**: 377–385. 2001*b*. [Medline]

Benke PJ, Fleshood HL, and Pitot HC. Osteoporotic bone disease in the pyridoxine-deficient rat. *Biochem Med*. **6**: 526–535. 1972. [CrossRef] [Medline]

Berman JJ, and Rice JM. Odontogenic tumours produced in Fischer rats by a single intraportal injection of methylnitrosourea. *Arch Oral Biol*. **25**: 213–220. 1980. [CrossRef] [Medline]

Blair HC, Zaidi M, and Schlesinger PH. Mechanisms balancing skeletal matrix synthesis and degradation. *Biochem J*. **364**: 329–341. 2002. [CrossRef] [Medline]

Bolon B, Morony S, Cheng Y, Hu YL, and Feige U. Osteoclast numbers in Lewis rats with adjuvant-induced arthritis: identification of preferred sites and parameters for rapid quantitative analysis. *Vet Pathol*. **41**: 30–36. 2004. [CrossRef] [Medline]

Bolon B, Grisanti M, Villasenor K, Morony S, Feige U, and Simonet WS. Generalized degenerataive joint disease in osteoprotegerin (*Opg*) null mutant mice. *Vet Pathol*. **52**: 873–882. 2015. [Medline]

Bolon B, Stolina M, King C, Middleton S, Gasser J, Zack D, and Feige U. Rodent preclinical models for developing novel antiarthritic molecules: comparative biology and preferred methods for evaluating efficacy. *J Biomed Biotechnol*. **2011**: 569068. 2011. [CrossRef] [Medline]

Bonewald LF, and Johnson ML. Osteocytes, mechanosensing and Wnt signaling. *Bone*. **42**: 606–615. 2008. [CrossRef] [Medline]

Bonewald LF, and Wacker MJ. FGF23 production by osteocytes. *Pediatr Nephrol*. **28**: 563–568. 2013. [CrossRef] [Medline]

Bonnet CS, and Walsh DA. Osteoarthritis, angiogenesis and inflammation. *Rheumatology (Oxford)*. **44**: 7–16. 2005. [CrossRef] [Medline]

Boorman GA, and Hollander CF. Spontaneous lesions in the female WAG-Rij (Wistar) rat. *J Gerontol*. **28**: 152–159. 1973. [CrossRef] [Medline]

Boss JH, and Misselevich I. Osteonecrosis of the femoral head of laboratory animals: the lessons learned from a comparative study of osteonecrosis in man and experimental animals. *Vet Pathol*. **40**: 345–354. 2003. [CrossRef] [Medline]

Bourrin S, Toromanoff A, Ammann P, Bonjour JP, and Rizzoli R. Dietary protein deficiency induces osteoporosis in aged male rats. *J Bone Miner Res*. **15**: 1555–1563. 2000. [CrossRef] [Medline]

Boyce RW, Paddock CL, Gleason JR, Sletsema WK, and Eriksen EF. The effects of risedronate on canine cancellous bone remodeling: three-dimensional kinetic reconstruction of the remodeling site. *J Bone Miner Res*. **10**: 211–221. 1995. [CrossRef] [Medline]

Boyce RW, and Weisbrode SE. Effect of dietary calcium on the response of bone to 1,25 (OH)2D3. *Lab Invest*. **48**: 683–689. 1983. [Medline]

Boyle WJ, Simonet WS, and Lacey DL. Osteoclast differentiation and activation. *Nature*. **423**: 337–342. 2003. [CrossRef] [Medline]

Brand DD. Rodent models of rheumatoid arthritis. *Comp Med*. **55**: 114–122. 2005. [Medline]

Bregman CL, Adler RR, Morton DG, Regan KS, Yano BL. Society of Toxicologic Pathology Recommended tissue list for histopathologic examination in repeat-dose toxicity and carcinogenicity studies: a proposal of the Society of Toxicologic Pathology (STP). *Toxicol Pathol*. **31**: 252–253. 2003. [Medline]

Brown AP, Courtney CL, King LM, Groom SC, and Graziano MJ. Cartilage dysplasia and tissue mineralization in the rat following administration of a FGF receptor tyrosine kinase inhibitor. *Toxicol Pathol*. **33**: 449–455. 2005. [CrossRef] [Medline]

Bucher JR, Hejtmancik MR, Toft JD 2nd, Persing RL, Eustis SL, and Haseman JK. Results and conclusions of the National Toxicology Program's rodent carcinogenicity studies with sodium fluoride. *Int J Cancer*. **48**: 733–737. 1991. [CrossRef] [Medline]

Carlton WW, Ernst H, Faccini JM, Greaves P, Krinke GJ, Long PH, Maekawa A, Newsholme SJ, and Weisse G. Soft tissue and musculoskeletal system In *International classification of rodent tumours. Part I: The rat.* (Mohr, U., Capen, C.C., Dungworth, D.L., Griesemer, R.A., Ito, N., Turusov, V.S. ed.), Vol. 122. IARC Scientific Publications, International Agency for Research on Cancer, Lyon, France. 1992.

Chai Y, Jiang X, Ito Y, Bringas P Jr, Han J, Rowitch DH, Soriano P, McMahon AP, and Sucov HM. Fate of the mammalian cranial neural crest during tooth and mandibular morphogenesis. *Development*. **127**: 1671–1679. 2000. [Medline]

Charles RT, and Turusov VS. Bone tumours in CF-1 mice. *Lab Anim*. **8**: 137–144. 1974. [CrossRef] [Medline]

Chow JW, Wilson AJ, Chambers TJ, and Fox SW. Mechanical loading stimulates bone formation by reactivation of bone lining cells in 13-week-old rats. *J Bone Miner Res*. **13**: 1760–1767. 1998. [CrossRef] [Medline]

Courtney CL, Kim SN, Walsh KM, Watkins JR, and Dominick MA. Proliferative bone lesions in rats given anticancer compounds. *Toxicol Pathol*. **19**: 184–188. 1991. [CrossRef] [Medline]

Coxon A, Bolon B, Estrada J, Kaufman S, Scully S, Rattan A, Duryea D, Hu YL, Rex K, Pacheco E, Van G, Zack D, and Feige U. Inhibition of interleukin-1 but not tumor necrosis factor suppresses neovascularization in rat models of corneal angiogenesis and adjuvant arthritis. *Arthritis Rheum*. **46**: 2604–2612. 2002. [CrossRef] [Medline]

Cullen JM, Ruebner BH, Hsieh DPH, and Burkes EJ Jr. Odontogenic tumors in Fischer rats. *J Oral Pathol*. **16**: 469–473. 1987. [CrossRef] [Medline]

Dallas SL, Prideaux M, and Bonewald LF. The osteocyte: an endocrine cell ... and more. *Endocr Rev*. **34**: 658–690. 2013. [CrossRef] [Medline]

Dawe CJ, Law LW, and Dunn TB. Studies of parotid-tumor agent in cultures of leukemic tissues of mice. *J Natl Cancer Inst*. **23**: 717–797. 1959. [Medline]

Dayan D, Waner T, Harmelin A, and Nyska A. Bilateral complex odontoma in a Swiss (CD-1) male mouse. *Lab Anim*. **28**: 90–92. 1994. [CrossRef] [Medline]

Delgado E, Rodríguez JI, Rodríguez JL, Miralles C, and Paniagua R. Osteochondroma induced by reflection of the perichondrial ring in young rat radii. *Calcif Tissue Int*. **40**: 85–90. 1987. [CrossRef] [Medline]

Delgado E, Rodriguez JI, Serrada A, Tellez M, and Paniagua R. Radiation-induced osteochondroma-like lesion in young rat radius. *Clin Orthop Relat Res*.: 251–258. 1985. [Medline]

Eisenberg E, Murthy AS, Vawter GF, and Krutchkoff DJ. Odontogenic neoplasms in Wistar rats treated with N-methylnitrosourea. *Oral Surg Oral Med Oral Pathol*. **55**: 481–486. 1983. [CrossRef] [Medline]

Ellis HA, and Peart KM. Dextran sulphate osteopathy in parathyroidectomized rats. *Br J Exp Pathol*. **52**: 684–695. 1971. [Medline]

EMEA. Guideline on the evaluation of medicinal products in the treatment of primary osteoporosis. European Medicines Agency Committee for Medicinal Products for Human Use (CHMP), London. 2006.

Erben RG. Trabecular and endocortical bone surfaces in the rat: modeling or remodeling? *Anat Rec*. **246**: 39–46. 1996. [CrossRef] [Medline]

Erben RG, and Glösmann M. Histomorphometry in rodents. *Methods Mol Biol*. **816**: 279–303. 2012. [CrossRef] [Medline]

Ernst H, and Mirea D. Ameloblastoma in a female Wistar rat. *Exp Toxicol Pathol*. **47**: 335–340. 1995. [CrossRef] [Medline]

Ernst H, and Mohr U. Ameloblastic odontoma of the mandible, rat. In *Monographs on pathology of laboratory animals.* Cardiovascular and musculoskeletal systems. (Jones, T.C., Mohr, U., Hunt, R.D. ed.), pp 218–224. Springer, Berlin, Heidelberg. 1991.

Ernst H, Scampini G, Durchfeld-Meyer B, Brander-Weber P, and Rittinghausen S. Odontogenic fibroma in Sprague-Dawley rats: a report of 2 cases. *Exp Toxicol Pathol*. **50**: 384–388. 1998. [CrossRef] [Medline]

Ernst H, Long PH, Wadsworth PF, Leininger JR, Reiland S, and Konishi Y. Skeletal system and teeth In *International classification of rodent tumours. Part II: The mouse* (Mohr, U., Capen, C.C., Dungworth, D.L., Griesemer, R.A., Ito, N., Turusov, V.S. ed.), pp. 389–415. Springer Verlag, Berlin, Heidelberg. 2001.

Faccini JM, Abbott DP, and Paulus GJJ. *Mouse histopathology. A glossary for use in toxicity and carcinogenicity studies.* Elsevier, Amsterdam, New York, Oxford. 1990.

Felix R, Hofstetter W, and Cecchini MG. Recent developments in the understanding of the pathophysiology of osteopetrosis. *Eur J Endocrinol*. **134**: 143–156. 1996. [CrossRef] [Medline]

Finkel MP, Lombard LS, Staffeldt EF, and Duffy PH. Odontomas in Peromyscus leucopus. *J Natl Cancer Inst*. **63**: 407–411. 1979. [Medline]

Fisher JE, Rodan GA, and Reszka AA. In vivo effects of bisphosphonates on the osteoclast mevalonate pathway. *Endocrinology*. **141**: 4793–4796. 2000. [CrossRef] [Medline]

Fitzgerald JE. Ameloblastic odontoma in the Wistar rat. *Toxicol Pathol*. **15**: 479–481. 1987. [CrossRef] [Medline]

Fondi C, and Franchi A. Definition of bone necrosis by the pathologist. *Clin Cases Miner Bone Metab*. **4**: 21–26. 2007. [Medline]

Franks LM, Rowlatt C, and Chesterman FC. Naturally occurring bone tumors in C57BL-Lcrf mice. *J Natl Cancer Inst*. **50**: 431–438. 1973. [Medline]

Frazier K, Thomas R, Scicchitano M, Mirabile R, Boyce R, Zimmerman D, Grygielko E, Nold J, DeGouville AC, Huet S, Laping N, and Gellibert F. Inhibition of ALK5 signaling induces physeal dysplasia in rats. *Toxicol Pathol*. **35**: 284–295. 2007. [CrossRef] [Medline]

Frith CH, Johnson BP, and Highman B. Osteosarcomas in BALB/c female mice. *Lab Anim Sci*. **32**: 60–63. 1982. [Medline]

Gerwin N, Bendele AM, Glasson S, and Carlson CS. The OARSI histopathology initiative - recommendations for histological assessments of osteoarthritis in the rat. *Osteoarthritis Cartilage*. **18**(Suppl 3): S24–S34. 2010. [CrossRef] [Medline]

Ghoreschi K, Jesson MI, Li X, Lee JL, Ghosh S, Alsup JW, Warner JD, Tanaka M, Steward-Tharp SM, Gadina M, Thomas CJ, Minnerly JC, Storer CE, LaBranche TP, Radi ZA, Dowty ME, Head RD, Meyer DM, Kishore N, and O'Shea JJ. Modulation of innate and adaptive immune responses by tofacitinib (CP-690,550). *J Immunol*. **186**: 4234–4243. 2011. [CrossRef] [Medline]

Gibson CW, Lally E, Herold RC, Decker S, Brinster RL, and Sandgren EP. Odontogenic tumors in mice carrying albumin-myc and albumin-rats transgenes. *Calcif Tissue Int*. **51**: 162–167. 1992. [CrossRef] [Medline]

Gimbel W, Schmidt J, Brack-Werner R, Luz A, Strauss PG, Erfle V, and Werner T. Molecular and pathogenic characterization of the RFB osteoma virus: lack of oncogene and induction of osteoma, osteopetrosis, and lymphoma. *Virology*. **224**: 533–538. 1996. [CrossRef] [Medline]

Glasson SS, Chambers MG, Van Den Berg WB, and Little CB. The OARSI histopathology initiative - recommendations for histological assessments of osteoarthritis in the mouse. *Osteoarthritis Cartilage*. **18**(Suppl 3): S17–S23. 2010. [CrossRef] [Medline]

Glasson SS. *In vivo* osteoarthritis target validation utilizing genetically-modified mice. *Curr Drug Targets*. **8**: 367–376. 2007. [CrossRef] [Medline]

Goessner W, and Luz A. Tumours of the jaws. In: *Pathology of tumours in laboratory animals. Vol 2. Tumours of the mouse*, 2nd edition. (Turusov, V.S., Mohr, U. ed.), pp 141–165. IARC Scientific Publications No. 111, Lyon. 1994.

Gollard RP, Slavkin HC, and Snead ML. Polyoma virus-induced murine odontogenic tumors. *Oral Surg Oral Med Oral Pathol*. **74**: 761–767. 1992. [CrossRef] [Medline]

Greaves P. Musculoskeletal system In *Histopathology of preclinical toxicity studies: Interpretation and relevance in drug safety studies*, Vol. 2, pp 166–167. Elsevier. 2000.

Greaves P. Musculoskeletal system. In: *Histopathology of preclinical toxicity studies,* 4th ed. (Greaves, P., ed.), pp 157–206. Academic Press, San Diego, CA. 2012.

Greene GW Jr, Collins DA, and Bernier JL. Response of embryonal odontogenic epithelium in the lower incisor of the mouse to 3-methylcholanthrene. *Arch Oral Biol*. **1**: 325–332. 1960. [CrossRef] [Medline]

Gregson RL, and Offer JM. Metastasizing chondrosarcoma in laboratory rats. *J Comp Pathol*. **91**: 409–413. 1981. [CrossRef] [Medline]

Gunson D, Gropp KE, and Varela A. Bones and joints In *Haschek and Rousseaux's Handbook of toxicologic pathology*, Vol. 2 (Haschek, W.M., Rousseaux, C. G., and Wallig, M. A. ed.), pp 2761–2858. Academic Press, San Diego. 2013.

Hähnel H, Módis L, and Lévai G. Histological and histochemical investigations of the epiphyseal cartilage in rats after administration of heparin, coumarin as well as coumarin and diphosphonate (EHDP). *Exp Pathol (Jena)*. **15**: 196–207. 1978. [Medline]

Haldar M, Hedberg ML, Hockin MF, and Capecchi MR. A CreER-based random induction strategy for modeling translocation-associated sarcomas in mice. *Cancer Res*. **69**: 3657–3664. 2009. [CrossRef] [Medline]

Hall AP, Westwood FR, and Wadsworth PF. Review of the effects of anti-angiogenic compounds on the epiphyseal growth plate. *Toxicol Pathol*. **34**: 131–147. 2006. [CrossRef] [Medline]

Hartke J. "Have you seen this?" Bone anti-resorptive properties of bisphosphonates. *Toxicol Pathol*. **24**: 799–800. 1996. [CrossRef] [Medline]

Hashimoto K. The effect of colchicine on the pigmentation of the enamel surface in rat incisors. *Bull Tokyo Med Dent Univ*. **31**: 115–126. 1984. [Medline]

Hay MF. The development *in vivo* and *in vitro* of the lower incisor and molars of the mouse. *Arch Oral Biol*. **3**: 86–109. 1961. [CrossRef] [Medline]

Highman B, Roth SI, and Greenman DL. Osseous changes and osteosacomas in mice continuously fed diets containing diethylstilbestrol or 17 beta-estradiol. *J Natl Cancer Inst*. **67**: 653–662. 1981. [Medline]

Hirano T, Iwasaki K, Sagara K, Nishimura Y, and Kumashiro T. Necrosis of the femoral head in growing rats. Occlusion of lateral epiphyseal vessels. *Acta Orthop Scand*. **60**: 407–410. 1989. [CrossRef] [Medline]

Höger H, Gialamas J, and Jelinek F. Multiple osteomas in mice. *Vet Pathol*. **31**: 429–434. 1994. [CrossRef] [Medline]

Horne WC, Neff L, Chatterjee D, Lomri A, Levy JB, and Baron R. Osteo-

clasts express high levels of pp60c-src in association with intracellular membranes. *J Cell Biol*. **119**: 1003–1013. 1992. [CrossRef] [Medline]

Humphreys ER, Robins MW, and Stones VA. Age-related and 224Ra-induced abnormalities in the teeth of male mice. *Arch Oral Biol*. **30**: 55–64. 1985. [CrossRef] [Medline]

Jee WS, and Yao W. Overview: animal models of osteopenia and osteoporosis. *J Musculoskelet Neuronal Interact*. **1**: 193–207. 2001. [Medline]

Jolette J, Wilker CE, Smith SY, Doyle N, Hardisty JF, Metcalfe AJ, Marriott TB, Fox J, and Wells DS. Defining a noncarcinogenic dose of recombinant human parathyroid hormone 1-84 in a 2-year study in Fischer 344 rats. *Toxicol Pathol*. **34**: 929–940. 2006. [CrossRef] [Medline]

Kavirayani AM, Sundberg JP, and Foreman O. Primary neoplasms of bones in mice: retrospective study and review of literature. *Vet Pathol*. **49**: 182–205. 2012. [CrossRef] [Medline]

Kharode YP, Sharp MC, and Bodine PV. Utility of the ovariectomized rat as a model for human osteoporosis in drug discovery. *Methods Mol Biol*. **455**: 111–124. 2008. [CrossRef] [Medline]

Kiebzak GM, Smith R, Gundberg CC, Howe JC, and Sacktor B. Bone status of senescent male rats: chemical, morphometric, and mechanical analysis. *J Bone Miner Res*. **3**: 37–45. 1988*a*. [CrossRef] [Medline]

Kiebzak GM, Smith R, Howe JC, Gundberg CM, and Sacktor B. Bone status of senescent female rats: chemical, morphometric, and biomechanical analyses. *J Bone Miner Res*. **3**: 439–446. 1988*b*. [CrossRef] [Medline]

Kilborn SH, Trudel G, and Uhthoff H. Review of growth plate closure compared with age at sexual maturity and lifespan in laboratory animals. *Contemp Top Lab Anim Sci*. **41**: 21–26. 2002. [Medline]

Kimura A, Yoshizawa K, Sasaki T, Uehara N, Kinoshita Y, Miki H, Yuri T, Uchida T, and Tsubura A. N-methyl-N-nitrosourea-induced changes in epithelial rests of Malassez and the development of odontomas in rats. *Exp Ther Med*. **4**: 15–20. 2012. [Medline]

Komori T, Yagi H, Nomura S, Yamaguchi A, Sasaki K, Deguchi K, Shimizu Y, Bronson RT, Gao YH, Inada M, Sato M, Okamoto R, Kitamura Y, Yoshiki S, and Kishimoto T. Targeted disruption of Cbfa1 results in a complete lack of bone formation owing to maturational arrest of osteoblasts. *Cell*. **89**: 755–764. 1997. [CrossRef] [Medline]

Kronenberg HM. Developmental regulation of the growth plate. *Nature*. **423**: 332–336. 2003. [CrossRef] [Medline]

Kubicky RA, Wu S, Kharitonenkov A, and De Luca F. Role of fibroblast growth factor 21 (FGF21) in undernutrition-related attenuation of growth in mice. *Endocrinology*. **153**: 2287–2295. 2012. [CrossRef] [Medline]

Kuijpers MHM, van de Kooij AJ, and Slootweg PJ. Review article. The rat incisor in toxicologic pathology. *Toxicol Pathol*. **24**: 346–360. 1996. [CrossRef] [Medline]

LaBranche TP, Hickman-Brecks CL, Meyer DM, Storer CE, Jesson MI, Shevlin KM, Happa FA, Barve RA, Weiss DJ, Minnerly JC, Racz JL, and Allen PM. Characterization of the KRN cell transfer model of rheumatoid arthritis (KRN-CTM), a chronic yet synchronized version of the K/BxN mouse. *Am J Pathol*. **177**: 1388–1396. 2010. [CrossRef] [Medline]

LaBranche TP, Jesson MI, Radi ZA, Storer CE, Guzova JA, Bonar SL, Thompson JM, Happa FA, Stewart ZS, Zhan Y, Bollinger CS, Bansal PN, Wellen JW, Wilkie DP, Bailey SA, Symanowicz PT, Hegen M, Head RD, Kishore N, Mbalaviele G, and Meyer DM. JAK inhibition with tofacitinib suppresses arthritic joint structural damage through decreased RANKL production. *Arthritis Rheum*. **64**: 3531–3542. 2012. [CrossRef] [Medline]

Leininger JR, and Riley MGI. Bones, joints, and synovia. In *Pathology of the Fischer rat: Reference and atlas*. (Boorman, G.A., Eustis, S.L., Elwell, M.R., Montgomery, C.A., MacKenzie, W.F. ed.), pp 209–226. Academic Press, San Diego, CA. 1990.

Lelovas PP, Xanthos TT, Thoma SE, Lyritis GP, and Dontas IA. The laboratory rat as an animal model for osteoporosis research. *Comp Med*. **58**: 424–430. 2008. [Medline]

Lewis DJ, Cherry CP, and Gibson WA. Ameloblastoma (adamantinoma) of the mandible in the rat. *J Comp Pathol*. **90**: 379–384. 1980. [CrossRef] [Medline]

Li X, Ominsky MS, Warmington KS, Morony S, Gong J, Cao J, Gao Y, Shalhoub V, Tipton B, Haldankar R, Chen Q, Winters A, Boone T, Geng Z, Niu QT, Ke HZ, Kostenuik PJ, Simonet WS, Lacey DL, and Paszty C. Sclerostin antibody treatment increases bone formation, bone mass, and bone strength in a rat model of postmenopausal osteoporosis. *J Bone Miner Res*. **24**: 578–588. 2009. [CrossRef] [Medline]

Lindemann G, and Nylen MU. Calcium fluoride containing granules produced in vitro in rat bones. *Scand J Dent Res*. **87**: 381–389. 1979. [Medline]

Liu HH. Safety profile of the fluoroquinolones: focus on levofloxacin. *Drug Saf*. **33**: 353–369. 2010. [CrossRef] [Medline]

Long PH, and Herbert RA. Epithelial-induced intrapulpal denticles in B6C3F1 mice. *Toxicol Pathol*. **30**: 744–748. 2002. [CrossRef] [Medline]

Long PH, Herbert RA, and Nyska A. Hexachlorobenzene-induced incisor degeneration in Sprague-Dawley rats. *Toxicol Pathol*. **32**: 35–40. 2004. [CrossRef] [Medline]

Long PH, and Leininger JR. Teeth. In *Pathology of the mouse. Reference and atlas*. (Maronpot, R.R., Boorman, G.A., Gaul, B.W. ed.), pp 13–28. Cache River Press, Vienna. 1999a.

Long PH, and Leininger JR. Bones, joints, and synovia. In *Pathology of the mouse. Reference and atlas* (Maronpot, R.R., Boorman, G. A., and Gaul, B. W. ed.), pp 645–678. Cache River Press, Vienna. 1999b.

Long PH, Leininger JR, and Ernst H. Non-proliferative lesions of bone, cartilage, tooth, and synovium in rats, MST-2. In *Guides for toxicologic pathology*. STP/ARP/AFIP, Washington, D.C. 1996.

Long PH, Leininger JR, Nold JB, and Lieuallen WG. Proliferative lesions of bone, cartilage, tooth, and synovium in rats, MST-2. In *Guides for toxicologic pathology*. STP/ARP/AFIP, Washington, D.C. 1993.

Long PH, Maronpot RR, Ghanayem BI, Roycroft JH, and Nyska A. Dental pulp infarction in female rats following inhalation exposure to 2-butoxyethanol. *Toxicol Pathol*. **28**: 246–252. 2000. [CrossRef] [Medline]

Losco PE. Dental dysplasia in rats and mice. *Toxicol Pathol*. **23**: 677–688. 1995. [CrossRef] [Medline]

Lotinun S, Sibonga JD, and Turner RT. Evidence that the cells responsible for marrow fibrosis in a rat model for hyperparathyroidism are preosteoblasts. *Endocrinology*. **146**: 4074–4081. 2005. [CrossRef] [Medline]

Luz A, Goessner W, and Murray AB. Osteosarcoma, spontaneous and radiation-induced, mouse. In *Monographs on pathology of laboratory animals*. Cardiovascular and musculoskeletal systems (Jones, T.C., Mohr, U., Hunt, R.D. ed.), pp 202–213. Springer, Berlin Heidelberg New York Tokyo. 1991a.

Luz A, Goessner W, and Murray AB. Ossifying fibroma, mouse. In *Monographs on pathology of laboratory animals*. Cardiovascular and musculoskeletal systems (Jones, T.C., Mohr, U., Hunt, R.D. ed.), pp 228–232. Springer, Berlin Heidelberg New York Tokyo. 1991b.

Machado EA, and Beauchene RE. Spontaneous osteogenic sarcoma in the WI/Ten rat: a case report. *Lab Anim Sci*. **26**: 98–100. 1976. [Medline]

Maekawa A, Onodera H, Tanigawa H, Furuta K, Takahashi M, Kurokawa Y, Kokubo T, Ogiu T, Uchida O, Kobayashi K, *et al* Spontaneous tumors of the nervous system and associated organs and/or tissues in rats. *Gan*. **75**: 784–791. 1984. [Medline]

Malluche HH. Aluminium and bone disease in chronic renal failure. *Nephrol Dial Transplant*. **17**(Suppl 2): 21–24. 2002. [CrossRef] [Medline]

Marsell R, and Einhorn TA. The biology of fracture healing. *Injury*. **42**: 551–555. 2011. [CrossRef] [Medline]

Matyas JR, Sandell LJ, and Adams ME. Gene expression of type II collagens in chondro-osteophytes in experimental osteoarthritis. *Osteoarthritis Cartilage*. **5**: 99–105. 1997. [CrossRef] [Medline]

Maurer JK, Cheng MC, Boysen BG, and Anderson RL. Two-year carcinogenicity study of sodium fluoride in rats. *J Natl Cancer Inst*. **82**: 1118–1126. 1990. [CrossRef] [Medline]

Maurer JK, Cheng MC, Boysen BG, Squire RA, Strandberg JD, Weisbrode SE, Seymour JL, and Anderson RL. Confounded carcinogenicity study of sodium fluoride in CD-1 mice. *Regul Toxicol Pharmacol*. **18**: 154–168. 1993. [CrossRef] [Medline]

Mazurek SG, Li J, Nabozny GH, Reinhart GA, Muthukumarana AC, Harrison PC, and Fryer RM. Functional biomarkers of musculoskeletal syndrome (MSS) for early in vivo screening of selective MMP-13 inhibitors. *J Pharmacol Toxicol Methods*. **64**: 89–96. 2011. [CrossRef] [Medline]

Melhus A. Fluoroquinolones and tendon disorders. *Expert Opin Drug Saf*. **4**: 299–309. 2005. [CrossRef] [Medline]

Mii Y, Tsutsumi M, Shiraiwa K, Miyauchi Y, Hohnoki K, Maruyama H, Ogushi H, Masuhara K, and Konishi Y. Transplantable osteosarcomas with high lung metastatic potential in Fischer 344 rats. *Jpn J Cancer Res*. **79**: 589–592. 1988. [CrossRef] [Medline]

Minato Y, Yamamura T, Takada H, Kojima A, Imaizumi K, Wada I, Takeshita M, and Okaniwa A. An extraskeletal osteosarcoma in an aged rat. *Nippon Juigaku Zasshi*. **50**: 259–261. 1988. [CrossRef] [Medline]

Mouse Tumor Biology Database (MTB), Mouse Genome Informatics (MGI), The Jackson Laboratory, Bar Harbor, ME (http://www.informatics.jax.org/). (Accessed May, 2011).

Mullender MG, and Huiskes R. Osteocytes and bone lining cells: which are the best candidates for mechano-sensors in cancellous bone? *Bone*. **20**: 527–532. 1997. [CrossRef] [Medline]

Nakashima T, Hayashi M, Fukunaga T, Kurata K, Oh-Hora M, Feng JQ, Bonewald LF, Kodama T, Wutz A, Wagner EF, Penninger JM, and Takayanagi H. Evidence for osteocyte regulation of bone homeostasis through RANKL expression. *Nat Med*. **17**: 1231–1234. 2011. [CrossRef] [Medline]

Nilsson A, and Stanton MF. Tumours of the bone. In *Pathology of tumours in laboratory animals. Vol 2. Tumours of the mouse*, 2nd edition (Turusov, V.S., Mohr, U. ed.), pp 681–729. IARC Scientific Publications No. 111, Lyon. 1994.

Noden DM, and De Lahunta A. Trunk Muscles and Connective Tissues In *The embryology of domestic animals: Developmental mechanisms and malformations*, pp. 140. Lippincott Williams & Wilkins, Baltimore. 1985.

Noguchi C, Miyata H, Sato Y, Iwaki Y, and Okuyama S. Evaluation of bone toxicity in various bones of aged rats. *J Toxicol Pathol*. **24**: 41–48. 2011. [CrossRef] [Medline]

Nozue T, and Kayano T. Effects of mitomycin C in postnatal tooth development in mice with special reference to neural crest cells. *Acta Anat (Basel)*. **100**: 85–94. 1978. [CrossRef] [Medline]

NTP (April 2011). TDMS Study Data Search In *http://ntp.niehs.nih.gov*.

Olson HM, and Capen CC. Virus-induced animal model of osteosarcoma in the rat: Morphologic and biochemical studies. *Am J Pathol*. **86**: 437–458. 1977. [Medline]

Ominsky MS, Niu Q-T, Li C, Li X, and Ke HZ. Tissue-level mechanisms responsible for the increase in bone formation and bone volume by sclerostin antibody. *J Bone Miner Res*. **29**: 1424–1430. 2014. [CrossRef] [Medline]

Palmer AW, Guldberg RE, and Levenston ME. Analysis of cartilage matrix fixed charge density and three-dimensional morphology via contrast-enhanced microcomputed tomography. *Proc Natl Acad Sci USA*. **103**: 19255–19260. 2006. [CrossRef] [Medline]

Pastoureau PC, Hunziker EB, and Pelletier J-P. Cartilage, bone and synovial histomorphometry in animal models of osteoarthritis. *Osteoarthritis Cartilage*. **18**(Suppl 3): S106–S112. 2010. [CrossRef] [Medline]

Patyna S, Arrigoni C, Terron A, Kim TW, Heward JK, Vonderfecht SL, Denlinger R, Turnquist SE, and Evering W. Nonclinical safety evaluation of sunitinib: a potent inhibitor of VEGF, PDGF, KIT, FLT3, and RET receptors. *Toxicol Pathol*. **36**: 905–916. 2008. [CrossRef] [Medline]

Pearl GS, and Takei Y. Transplacental induction of ameloblastoma in rat using ethylnitrosourea (ENU). *J Oral Pathol*. **10**: 60–62. 1981. [CrossRef]

Pelfrene A, Mirvish SS, and Gold B. Induction of malignant bone tumors in rats by 1-(2-hydroxyethyl)-1-nitrosourea. *J Natl Cancer Inst*. **56**: 445–446. 1976. [Medline]

Price PA, Williamson MK, Haba T, Dell RB, and Jee WS. Excessive mineralization with growth plate closure in rats on chronic warfarin treatment. *Proc Natl Acad Sci USA*. **79**: 7734–7738. 1982. [CrossRef] [Medline]

Pritzker KP. Animal models for osteoarthritis: processes, problems and prospects. *Ann Rheum Dis*. **53**: 406–420. 1994. [CrossRef] [Medline]

Pybus FC, and Miller EW. Hereditary Bone Tumours in Mice. *BMJ*. **1**: 1300–1322.1, 1, 1. 1938. [CrossRef] [Medline]

Qi H, Li M, and Wronski TJ. A comparison of the anabolic effects of parathyroid hormone at skeletal sites with moderate and severe osteopenia in aged ovariectomized rats. *J Bone Miner Res*. **10**: 948–955. 1995. [CrossRef] [Medline]

Renkiewicz R, Qiu L, Lesch C, Sun X, Devalaraja R, Cody T, Kaldjian E, Welgus H, and Baragi V. Broad-spectrum matrix metalloproteinase inhibitor marimastat-induced musculoskeletal side effects in rats. *Arthritis Rheum*. **48**: 1742–1749. 2003. [CrossRef] [Medline]

Reuber MD, and Reznik-Schüller HM. Benign chordoma (sacrococcygeal) in the rat: a light and electron microscopic study. *Vet Pathol*. **21**: 536–538. 1984. [Medline]

Reznik G, and Russfield A. Chordoma of the spinal cord in a F344 rat. *Pathol Res Pract*. **172**: 191–195. 1981. [CrossRef] [Medline]

Riminucci M, Fisher LW, Shenker A, Spiegel AM, Bianco P, and Gehron Robey P. Fibrous dysplasia of bone in the McCune-Albright syndrome: abnormalities in bone formation. *Am J Pathol*. **151**: 1587–1600. 1997. [Medline]

Rivenson A, Mu B, Silverman J, and Williams GM. Chemically induced rat odontomas: morphogenetic considerations. *Cancer Detect Prev*. **7**: 293–298. 1984. [Medline]

Roach HI, Mehta G, Oreffo RO, Clarke NM, and Cooper C. Temporal analysis of rat growth plates: cessation of growth with age despite presence of a physis. *J Histochem Cytochem*. **51**: 373–383. 2003. [CrossRef] [Medline]

Robins MW, and Rowlatt C. Dental abnormalities in aged mice. *Gerontologia*. **17**: 261–272. 1971. [CrossRef] [Medline]

Rosenberg AE. Bones, joints, and soft-tissue tumors. In *Robbins and Cotran pathologic basis of disease,* 8th ed (Kumar, V., Abbas, A.K., Fausto, N., Aster, J.C., ed.), pp 1205–1256. Saunders Elsevier, Philadelphia, PA. 2010.

Rothenberg AB, Berdon WE, Woodard JC, and Cowles RA. Hypervitaminosis A-induced premature closure of epiphyses (physeal obliteration) in humans and calves (hyena disease): a historical review of the human and veterinary literature. *Pediatr Radiol*. **37**: 1264–1267. 2007. [CrossRef] [Medline]

Säämänen A-M, Hyttinen M, and Vuorio E. Analysis of arthritic lesions in the Del1 mouse: a model for osteoarthritis. *Methods Mol Med*. **136**: 283–302. 2007. [CrossRef] [Medline]

Sakura Y. Periodontal inflammatory and cystlike lesions in BDF1 and B6C3F1 mice. *Vet Pathol*. **34**: 460–463. 1997. [CrossRef] [Medline]

Sass B, and Montali RJ. Spontaneous fibro-osseous lesions in aging female mice. *Lab Anim Sci*. **30**: 907–909. 1980. [Medline]

Schell H, Lienau J, Epari DR, Seebeck P, Exner C, Muchow S, Bragulla H, Haas NP, and Duda GN. Osteoclastic activity begins early and increases over the course of bone healing. *Bone*. **38**: 547–554. 2006. [CrossRef] [Medline]

Schenk R, Eggli P, Fleisch H, and Rosini S. Quantitative morphometric evaluation of the inhibitory activity of new aminobisphosphonates on bone resorption in the rat. *Calcif Tissue Int*. **38**: 342–349. 1986. [CrossRef] [Medline]

Schenk R, Merz WA, Mühlbauer R, Russell RG, and Fleisch H. Effect of ethane-1-hydroxy-1,1-diphosphonate (EHDP) and dichloromethylene diphosphonate (Cl 2 MDP) on the calcification and resorption of cartilage and bone in the tibial epiphysis and metaphysis of rats. *Calcif Tissue Res*. **11**: 196–214. 1973. [CrossRef] [Medline]

Sims NA, and Gooi JH. Bone remodeling: Multiple cellular interactions required for coupling of bone formation and resorption. *Semin Cell Dev Biol*. **19**: 444–451. 2008. [CrossRef] [Medline]

Smulow JB, Konstantinidis A, and Sonnenschein C. Age-dependent odontogenic lesions in rats after a single i.p. injection of N-nitroso-N-methylurea. *Carcinogenesis*. **4**: 1085–1088. 1983. [CrossRef] [Medline]

Sokoloff L, and Zipkin I. Odontogenic hamartomas in an inbred strain of mouse (STR-1N). *Proc Soc Exp Biol Med*. **124**: 147–149. 1967. [CrossRef] [Medline]

Standeven AM, Davies PJ, Chandraratna RA, Mader DR, Johnson AT, and Thomazy VA. Retinoid-induced epiphyseal plate closure in guinea pigs. *Fundam Appl Toxicol*. **34**: 91–98. 1996. [CrossRef] [Medline]

Stanley HR, Baer PN, and Kilham L. Oral tissue alterations in mice inoculated with the Rowe substrain of polyoma virus. *Periodontics*. **3**: 178–183. 1965. [Medline]

Stanley HR, Dawe CJ, and Law LW. Oral tumors induced by polyoma virus in mice. *Oral Surg Oral Med Oral Pathol*. **17**: 547–558. 1964. [CrossRef] [Medline]

Stanton MF. Tumours of the bone. *IARC Sci Publ*. **23**: 577–609. 1979. [Medline]

Stefanski SA, Elwell MR, Mitsumori K, Yoshitomi K, Dittrich K, and Giles HD. Chordomas in Fischer 344 rats. *Vet Pathol*. **25**: 42–47. 1988. [CrossRef] [Medline]

Stinson SF. Spontaneous tumors in Fischer rats. In *Atlas of tumor pathology of the Fischer rat* (Stinson, S.F., Schuller, H.M., Reznik, G., ed.), pp 1–18. CRC Press, Boca Raton, FL. 1990.

Stoica G, and Koestner A. Diverse spectrum of tumors in male Sprague-Dawley rats following single high doses of N-ethyl-N-nitrosourea (ENU). *Am J Pathol*. **116**: 319–326. 1984. [Medline]

Stromberg PC, and Vogtsberger LM. Pathology of the mononuclear cell leukemia of Fischer rats. I. Morphologic studies. *Vet Pathol*. **20**: 698–708. 1983. [CrossRef] [Medline]

Takahashi M, Yoshida M, Inoue K, Morikawa T, and Nishikawa A. Age-related susceptibility to induction of osteochondral and vascular lesions by semicarbazide hydrochloride in rats. *Toxicol Pathol*. **38**: 598–605. 2010. [CrossRef] [Medline]

Tanas MR, Rubin BP, Tubbs RR, Billings SD, Downs-Kelly E, and Goldblum JR. Utilization of fluorescence *in situ* hybridization in the diagnosis of 230 mesenchymal neoplasms: an institutional experience. *Arch Pathol Lab Med*. **134**: 1797–1803. 2010. [Medline]

Thompson Jr RC. Heparin osteoporosis. An experimental model using rats. *J Bone Joint Surg Am*. **55**: 606–612. 1973. [Medline]

Tucker MJ. A survey of bone disease in the Alpk/AP rat. *J Comp Pathol*. **96**: 197–203. 1986. [CrossRef] [Medline]

Vahle JL, Sato M, Long GG, Young JK, Francis PC, Engelhardt JA, Westmore MS, Linda Y, and Nold JB. Skeletal changes in rats given daily subcutaneous injections of recombinant human parathyroid hormone (1-34) for 2 years and relevance to human safety. *Toxicol Pathol*. **30**: 312–321. 2002. [CrossRef] [Medline]

van der Kraan PM, and van den Berg WB. Osteophytes: relevance and biology. *Osteoarthritis Cartilage*. **15**: 237–244. 2007. [CrossRef] [Medline]

Van Rijssel TG, and Mühlbock O. Intramandibular tumors in mice. *J Natl Cancer Inst*. **16**: 659–689. 1955. [Medline]

Viola PL, Bigotti A, and Caputo A. Oncogenic response of rat skin, lungs, and bones to vinyl chloride. *Cancer Res*. **31**: 516–522. 1971. [Medline]

Wachsmann D, and Sibilia J. Survival in the rheumatoid synovium. *Joint Bone Spine*. **78**: 435–437. 2011. [CrossRef] [Medline]

Wadsworth PF. Tumours of the bone in C57BL/10J mice. *Lab Anim*. **23**: 324–327. 1989. [CrossRef] [Medline]

Wancket LM, Devor-Henneman D, and Ward JM. Fibro-osseous (FOL) and degenerative joint lesions in female outbred NIH Black Swiss mice. *Toxicol Pathol*. **36**: 362–365. 2008. [CrossRef] [Medline]

Wang H, Terashi S, and Fukunishi R. Ameloblastic odontoma in rats induced by N-butylnitrosourea. *Gan*. **66**: 319–321. 1975. [Medline]

Weinstock A. Cytotoxic effects of puromycin on the Golgi apparatus of pancreatic acinar cells, hepatocytes and ameloblasts. *J Histochem Cytochem*. **18**: 875–886. 1970. [CrossRef] [Medline]

Weise M, De-Levi S, Barnes KM, Gafni RI, Abad V, and Baron J. Effects of estrogen on growth plate senescence and epiphyseal fusion. *Proc Natl Acad Sci USA*. **98**: 6871–6876. 2001. [CrossRef] [Medline]

Westergaard J. Structural changes induced by tetracycline in secretory ameloblasts in young rats. *Scand J Dent Res*. **88**: 481–495. 1980. [Medline]

Wieland HA, Michaelis M, Kirschbaum BJ, and Rudolphi KA. Osteoarthritis - an untreatable disease? *Nat Rev Drug Discov*. **4**: 331–344. 2005. [CrossRef] [Medline]

Wilson JT, Hauser RE, and Ryffel B. Osteomas in OF-1 mice: no alteration in biologic behavior during long-term treatment with cyclosporine. *J Natl Cancer Inst*. **75**: 897–903. 1985. [Medline]

Wimberly HC. Vascular embolization of a vertebral chordoma in a Fischer 344 rat. *Lab Anim Sci*. **38**: 614–615. 1988. [Medline]

Wong J, Bennett W, Ferguson MWJ, and McGrouther DA. Microscopic and histological examination of the mouse hindpaw digit and flexor tendon arrangement with 3D reconstruction. *J Anat*. **209**: 533–545. 2006. [CrossRef] [Medline]

Woodard JC, Burkhardt JE, and Jee W. Bones and joints. In *Handbook of toxicologic pathology,* Vol 2, 2nd ed (Haschek, W.M., Rousseaux, C.G., Wallig, M.A., ed). pp 457–508. Academic Press, San Diego, CA. 2002.

Wronski TJ, Dann LM, Scott KS, and Cintrón M. Long-term effects of ovariectomy and aging on the rat skeleton. *Calcif Tissue Int*. **45**: 360–366. 1989. [CrossRef] [Medline]

Wu S, Levenson A, Kharitonenkov A, and De Luca F. Fibroblast growth factor 21 (FGF21) inhibits chondrocyte function and growth hormone action directly at the growth plate. *J Biol Chem*. **287**: 26060–26067. 2012. [CrossRef] [Medline]

Yakar S, Rosen CJ, Beamer WG, Ackert-Bicknell CL, Wu Y, Liu JL, Ooi GT, Setser J, Frystyk J, Boisclair YR, and LeRoith D. Circulating levels of IGF-1 directly regulate bone growth and density. *J Clin Invest*. **110**: 771–781. 2002. [CrossRef] [Medline]

Yamaguchi A, Komori T, and Suda T. Regulation of osteoblast differentiation mediated by bone morphogenetic proteins, hedgehogs, and Cbfa1. *Endocr Rev*. **21**: 393–411. 2000. [CrossRef] [Medline]

Yoshiki S, Ueno T, Akita T, and Yamanouchi M. Improved procedure for histological identification of osteoid matrix in decalcified bone. *Stain Technol*. **58**: 85–89. 1983. [CrossRef] [Medline]

Zaidi M, Blair HC, Moonga BS, Abe E, and Huang CL. Osteoclastogenesis, bone resorption, and osteoclast-based therapeutics. *J Bone Miner Res*. **18**: 599–609. 2003. [CrossRef] [Medline]

Zegarelli EV. Adamantoblastomas in the Slye stock of mice. *Am J Pathol*. **20**: 23–87. 1944. [Medline]

Zuo C, Huang Y, Bajis R, Sahih M, Li YP, Dai K, and Zhang X. Osteoblastogenesis regulation signals in bone remodeling. *Osteoporos Int*. **23**: 1653–1663. 2012. [CrossRef] [Medline]

Zwicker GM, and Eyster RC. Chordoma in a Sprague-Dawley rat. *Toxicol Pathol*. **19**: 607–609. 1991. [CrossRef] [Medline]